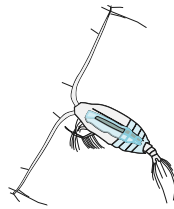


Pelagic community responses
to changes in N:P stoichiometry
in the Eastern Tropical Atlantic and Pacific



Dissertation
zur Erlangung des Doktorgrades
der Mathematisch-Naturwissenschaftlichen Fakultät
der Christian-Albrechts-Universität zu Kiel

vorgelegt von
Helena Hauss
Kiel, März 2012

Referent: Prof. Dr. Ulrich Sommer

Korreferent: Prof. Dr. Monika Winder

Datum der mündlichen Prüfung: 03.05.2012

zum Druck genehmigt: 03.05.2012

ZUSAMMENFASSUNG	2
SUMMARY	4
INTRODUCTION	7
Eastern Boundary Current Systems	7
Oxygen Minimum Zones	9
Redox-dependent nutrient stoichiometry and implications for primary producers	13
Nutrient stoichiometry and food quality: implications for consumers	16
Objectives	19
CHAPTER I: Changes in N:P stoichiometry influence taxonomic composition and nutritional quality of phytoplankton in the Peruvian Upwelling	21
CHAPTER II: Impact of changes in dissolved N:P on phytoplankton biomass, functional and elemental composition and resulting effects on zooplankton in the Eastern Tropical North Atlantic	47
CHAPTER III: Can tropical marine zooplankton excretion exacerbate dissolved nutrient imbalances?	71
CHAPTER IV: Relative contribution of upwelled and atmospheric nitrogen to the eastern tropical North Atlantic food web: Spatial distribution of $\delta^{15}\text{N}$ in mesozooplankton biomass and relation to dissolved nutrient dynamics	85
CONCLUSIONS AND PERSPECTIVES	104
Pacific-Atlantic comparison: Nutrient limitation	104
Pacific-Atlantic comparison: N_2 -fixation	108
Limitations to zooplankton production: Food quality or quantity?	110
REFERENCES	115
CONTRIBUTIONS OF AUTHORS	128
ACKNOWLEDGEMENTS	130
<i>CURRICULUM VITAE</i>	131
EIDESSTATTLICHE ERKLÄRUNG	133

Zusammenfassung

Aktuelle Studien weisen darauf hin, daß der Sauerstoffgehalt im tropischen Ozean abnimmt. Dies ist in der Nähe von tropischen Auftriebsgebieten besonders kritisch, da die hohe Produktivität dieser Systeme ohnehin mit Sauerstoffminimumzonen (OMZs) in der Tiefe unter der photischen Zone einhergeht. Das Ausmaß der Wassermassen mit geringem Sauerstoffgehalt hat einen Einfluß auf den Bestand gelöster Nährstoffe, weil sauerstoffsensitive Stickstoff(N)-Senken wie Denitrifizierung und Anammox verstärkt auftreten und gleichzeitig Phosphor (P) aus den Sedimenten remobilisiert wird. Beides führt zu sehr niedrigen N:P Verhältnissen im auftreibenden Wasser, insbesondere im östlichen Pazifik. Die vorliegende Studie hatte das Ziel, den Einfluß sich ändernder N- und P-Konzentrationen auf Primärproduzenten und Konsumenten im Epipelagial zu untersuchen. In neu entwickelten schiffsbasierten Mesokosmen wurden Nährstoffmanipulationsexperimente im östlichen tropischen Pazifik und Atlantik durchgeführt (Kapitel I und II). Die Ergebnisse weisen darauf hin, daß in diesen Gebieten, in denen das N:P-Verhältnis der gelösten anorganischen Nährstoffe generell unter dem Redfield-Verhältnis von 16:1 liegt, N der Hauptkontrollfaktor der Biomasseproduktion ist, unabhängig von der zugeführten P-Menge. Dies war besonders deutlich für blütenformende Diatomeen sowie Mikrozooplankton (Ciliaten). Allerdings waren die artspezifischen Effekte sowie die Änderungen in der elementaren Zusammensetzung des organischen Materials differenzierter. Beispielsweise profitierten *Phaeocystis globosa* und *Heterosigma* sp. deutlich von hohen P-Mengen (Kapitel I). Die Nahrungsqualität dieser beiden Algengruppen für Zooplankton wird generell geringer eingeschätzt als die diatomeendominierter Gemeinschaften. So war der Anteil ungesättigter Fettsäuren im partikulären Material am Ende des Experiments positiv korreliert mit der maximalen Diatomeenbiomasse zum Blütezeitpunkt (Kapitel I). Die Ergebnisse der Nährstoffmanipulationsexperimente im Auftriebsgebiet vor Peru und vor der westafrikanischen Küste waren überraschend ähnlich, obwohl das nordatlantische Becken durch den hohen Anteil an Stickstofffixierung (begünstigt durch den hohen Staubeintrag) und das Fehlen von suboxischen Bedingungen einen N-Überschuss im Tiefenwasser aufweist. Darüber hinaus weist die Zunahme von cyanobakterienspezifischen Pigmenten darauf hin, daß gerade in jenen Mesokosmen, in die zu Beginn der Experimente eine hohe N-Menge zugegeben wurde, nach Aufzehrung der gelösten Nährstoffe diazotrophe Primärproduzenten auftraten (Kapitel I und II). Das N:P-Verhältnis in der Exkretion von omnivoren Copepoden (*Undinula vulgaris*), die mit der sich in den Mesokosmen entwickelnden Planktongemeinschaft gefüttert wurden, war vom N:P-Verhältnis des organischen Materials beeinflusst, welches sich seinerseits in den

verschiedenen N:P-Manipulationsansätzen unterschied (Kapitel II). Um die natürlich auftretende Variabilität der N- und P-Exkretion von Zooplankton im tropischen Ostatlantik zu untersuchen, wurden an mehreren Stationen Inkubationen von drei epipelagischen Copepodenarten durchgeführt (Kapitel III). Innerhalb der untersuchten Arten war das N:P-Verhältnis der Exkretion beeinflusst vom N:P des partikulären organischen Materials in der Wassersäule (PON:POP). Zwischen den untersuchten Arten bestanden ebenfalls Unterschiede; so war das N:P-Verhältnis der Exkretion bei der carnivoren Art *Euchaeta marina* stets höher als bei den beiden omnivoren Arten *U. vulgaris* und *Scolecithrix danae*. Dies ist dem höheren N:P der Beutetiere von *E. marina*, verglichen mit dem eher variablen N:P der Futterorganismen (phototrophe und heterotrophe Protisten) der beiden anderen Arten, geschuldet.

Eine weitere Fragestellung der vorliegenden Arbeit war, inwieweit atmosphärische N-Quellen wie Staubeintrag und Stickstofffixierung zur Biomasse von epipelagischem Zooplankton im tropischen Nordostatlantik beitragen, und wie dieser Beitrag in Abhängigkeit vom vertikalen Fluß gelösten Stickstoffs steht (Kapitel IV). Dies wurde anhand der Isotopensignatur ($\delta^{15}\text{N}$) im Zooplankton in Relation zur Vertikalverteilung gelöster Nährstoffe ermittelt und reicht von <20% nahe der westafrikanischen Küste bis zu ca. 60% im offenen Ozean (Guinea Dome).

Summary

Recent studies indicate that the tropical ocean is losing oxygen. This becomes crucial in regions adjacent to eastern boundary currents, as the productivity of these systems is already accompanied by oxygen minimum zones (OMZ) at depth below the photic zone. The extent of low oxygen water masses influences dissolved nutrient inventories, as oxygen-sensitive nitrogen (N) loss processes such as denitrification and anammox are enhanced and inorganic phosphorus is remobilized from sediments, resulting in low N:P of upwelled waters, especially in the East Pacific. The present study aimed to investigate the impact of changing N and P supply on the pelagic primary producers and consumers in the photic zone. To achieve this, nutrient manipulation experiments were conducted in the eastern tropical Pacific and Atlantic Ocean using a newly designed shipboard mesocosm setup. Results demonstrated that in these regions, where N:P is generally below the canonical Redfield ratio of 16, inorganic N is the key control of bulk productivity regardless of the amount of P added, especially of bloom-forming diatom species and ciliate consumers (chapter I and II). However, the response of individual species and pools of organic matter was found to be more complex. For example, *Phaeocystis globosa* and *Heterosigma* sp. clearly benefitted from high P-levels (chapter I). Both algal groups are considered of inferior quality to mesozooplankton consumers compared to diatom-dominated assemblages. The observation that the relative content of unsaturated fatty acids in the particulate matter was positively related to diatom biomass (chapter I) is a second clue that decreasing N-flux to the surface ocean impacts food web productivity. However, the RNA/DNA ratio, as a proxy for nutritional condition, did not change in the copepod *Undinula vulgaris* when fed on the manipulated mesocosm community over a period of three days (chapter II). The results of the nutrient manipulation experiments off Peru and West Africa were surprisingly similar, despite the fact that the North Atlantic features excess N at depth due to N₂-fixation and the lack of suboxic conditions that would promote N-loss processes. Furthermore, pigments characteristic for cyanobacteria indicated that diazotrophs were increasing in those mesocosms that had received a higher initial N load (chapter I and II), which contradicts the common understanding that diazotrophs would benefit from excess P.

In addition, we observed that the N:P excretion ratio of copepods (*U. vulgaris*) feeding on the manipulated mesocosm assemblage was influenced by the N:P of bulk particulate organic matter (PON:POP), which in turn responded directly to the manipulation ratios (chapter II). In order to survey the natural variability in N and P excretion rates in the Eastern Tropical North Atlantic, measurements were conducted in shipboard incubations at several stations on three epipelagic

copepod species (chapter III). Within species, excretion N:P was positively related to PON:POP at the respective station; however, the low number of stations sampled and the variability of PON:POP within the upper 150 m hampered the establishment of a functional relationship. The N:P excretion ratio was consistently higher in the carnivorous *Euchaeta marina* compared to the omnivorous *U. vulgaris* and *Scolecithrix danae*. This can be attributed to the rather rigid N:P stoichiometry of zooplanktonic prey items of *E. marina* in contrast to the unicellular food items of the other two species (such as diatoms, dinoflagellates and heterotrophic protists) with more variable N:P.

A further question addressed in this study was to what extent atmospheric N sources (N_2 -fixation and dust) are contributing to secondary production in the Eastern Tropical North Atlantic, and how this contribution is related to the vertical flux of dissolved inorganic nitrogen (chapter IV). We used zooplankton stable nitrogen isotopes ($\delta^{15}\text{N}$) to estimate the relative contribution of atmospheric N sources and found that it ranged from less than 20% off the West African coast to 60% in the open ocean (Guinea Dome region), and was positively related to the depth of the nitracline.

Introduction

Eastern Boundary Current Systems

Coastal upwelling is generated by atmospheric forcing, when prevailing wind directions are offshore or alongshore. In lower latitudes, the trade winds provide steady equatorward forcing throughout the year that, in concert with the Coriolis force, creates Ekman transport. The surface water masses that are thus driven offshore are replaced by upwelled, cold and nutrient-rich deep waters (Barber & Smith 1981). This creates the large, productive ecosystems of the eastern boundary currents at the eastern margins of the oceanic gyres (Fig. 1). In the Atlantic, these are the Canary Current and Mauritanian Upwelling systems in the northern, and the Benguela Current in the southern hemisphere, with their Pacific counterparts being the California Current in the northern and the Humboldt current in the southern hemisphere. In all these large marine ecosystems, both the latitudinal extent and the intensity of upwelling vary seasonally with the shift of the inner tropic convergence zone, but centers of year-round productivity remain, in contrast to seasonally restricted events such as the monsoonal upwelling in the Arabian Sea. In a comparison of these four eastern boundary current systems, Chavez & Messié (2009) provided a summarized overview of physical forcing, chemical properties, and biological production. A common feature of eastern boundary current systems is the comparatively high nutrient load and high turbulence. According to Margalef (1978), these two factors combined result in dominance of *r*-selected phytoplankton, thus supporting the classic diatom-copepod-fish link. In spite of the significantly lower average wind speed in the Peru system compared to the other areas, total upwelled volume is largest due to the latitude-dependence of the Coriolis parameter. Chavez & Messié (2009) note that the annual mean primary productivity is similar in all areas, while the annual fish catches off Peru exceed those in the other areas by an order of magnitude. However, primary production estimates in this study are based on SeaWiFS chlorophyll (Carr 2001), not on direct measurements of photosynthetic rates. While chl-*a* standing stock and primary production are tightly coupled on a global average (Behrenfeld & Falkowski 1997), high grazing pressure by herbivorous zooplankton and small pelagic fishes (e.g. Peruvian anchoveta, *Engraulis ringens*) can lead to a considerable underestimation of primary production. Nevertheless, the unique productivity of the Peruvian Ecosystem in terms of fish catches remains intriguing. To some extent, this remarkable difference to other regions is due to the mere catchability of small

pelagics due to oxygen-based habitat compression at the surface (see below), increasing the catch per unit effort and the profitability of the fishery as such. In addition, it is suggested that the combination of low latitude/low wind stress causes little turbulence at high upwelling rates and comparatively long residence time of coastal surface waters, generating optimal feeding and growth conditions for larval fish (Bakun & Weeks 2008). Furthermore, El Niño events may act as a periodic “reset” of the pelagic system, favouring *r*-selection and maintaining the dominance of diatoms, euphausiids and anchoveta as predatory top-down control is restricted (Bakun & Weeks 2008; Chavez & Messié 2009).

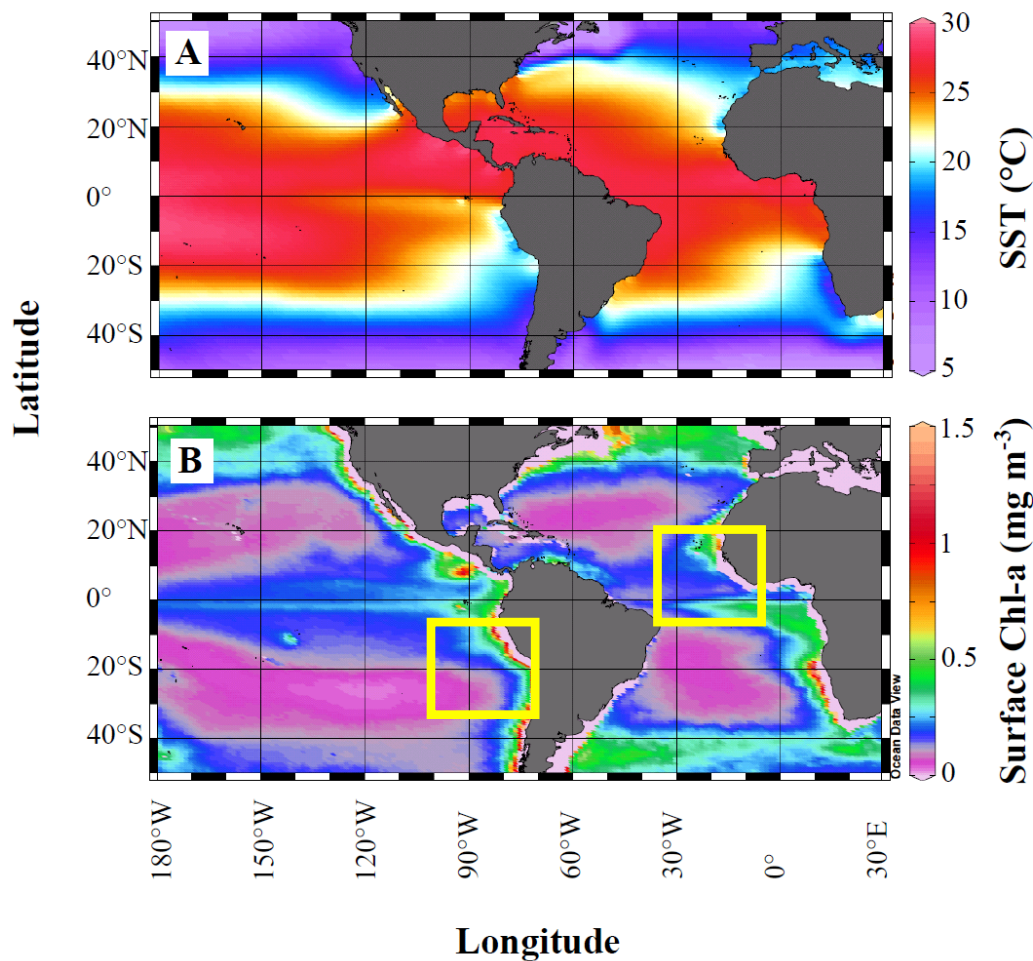


Figure 1: Sea surface temperature SST (°C, panel A) and surface chlorophyll-*a* (mg m⁻³, panel B) distribution in the Pacific and Atlantic Ocean. Temperature data are from World Ocean Atlas 2009 (NOAA). Chl-*a* data are five year (2000-2005) mean predictions from the NASA Ocean Biogeochemical Model (NOBM). Yellow boxes indicate the two areas investigated in the present study in the Eastern Tropical South Pacific and North Atlantic.

Oxygen Minimum Zones

As tropical upwelling systems are immensely productive, they are not very efficient in terms of energy and carbon fluxes in the pelagic food web. Microplankton (size range 20-200 μm), and in particular diatoms, contribute the majority of total primary production (up to 70%, as opposed to <20% in oligotrophic oceanic gyres, Uitz et al. 2010). Also, diatoms mainly use new nitrogen (upwelled nitrate) and thus are important in determining levels of new production (Dugdale 1985) and the f -ratio (Eppley & Peterson 1979). Due to their large size, built-in silica ballast and rapid aggregation (especially in chain-forming species and those with long setae), diatoms are key vectors of particulate organic carbon (POC) export flux to the deep ocean. A substantial part of the large phytoplankton sinks out of the photic zone before it can be consumed, and sloppy feeding and faeces of zooplankton and fish add on to the particulate organic matter (POM) that is being remineralized at depth. Since this involves largely respiratory processes, oxygen minimum zones (OMZ) are formed below upwelling systems, often reaching far offshore (Keeling et al. 2010). Since the two Pacific Systems are more productive than the Atlantic ones, the OMZs associated to them are also more extreme in their extent and in their absolute O_2 concentrations (Fig. 2 A), with large parts of the water column being completely anoxic (Karstensen et al. 2008).

In one of the first studies addressing the global distribution of oceanic dissolved oxygen and its relationship with ocean circulation, Wyrski (1962) noted that oxygen minima exist at intermediate depths below the mixed layer, and concluded that while biochemical processes are responsible for their existence, circulation determines their position, as layers of low oxygen can persist in layers of low advective circulation. Similarly, Deutsch et al. (2011) concluded from a biogeochemical model that was forced with observed atmospheric data and tuned to observed surface nutrient concentrations, that the depth of the tropical and subtropical thermocline is the key modulator of suboxic volume. Its shoaling enhances both the upward flux of dissolved inorganic nutrients into the photic zone (enhancing productivity), and the fraction of sinking organic matter that is remineralized at already low O_2 conditions. In the results of their model, they determined that the upper OMZ boundary plunges and shoals in concert with the thermocline, but with a fivefold amplification due to the multiplicative effect of the two aforementioned mechanisms.

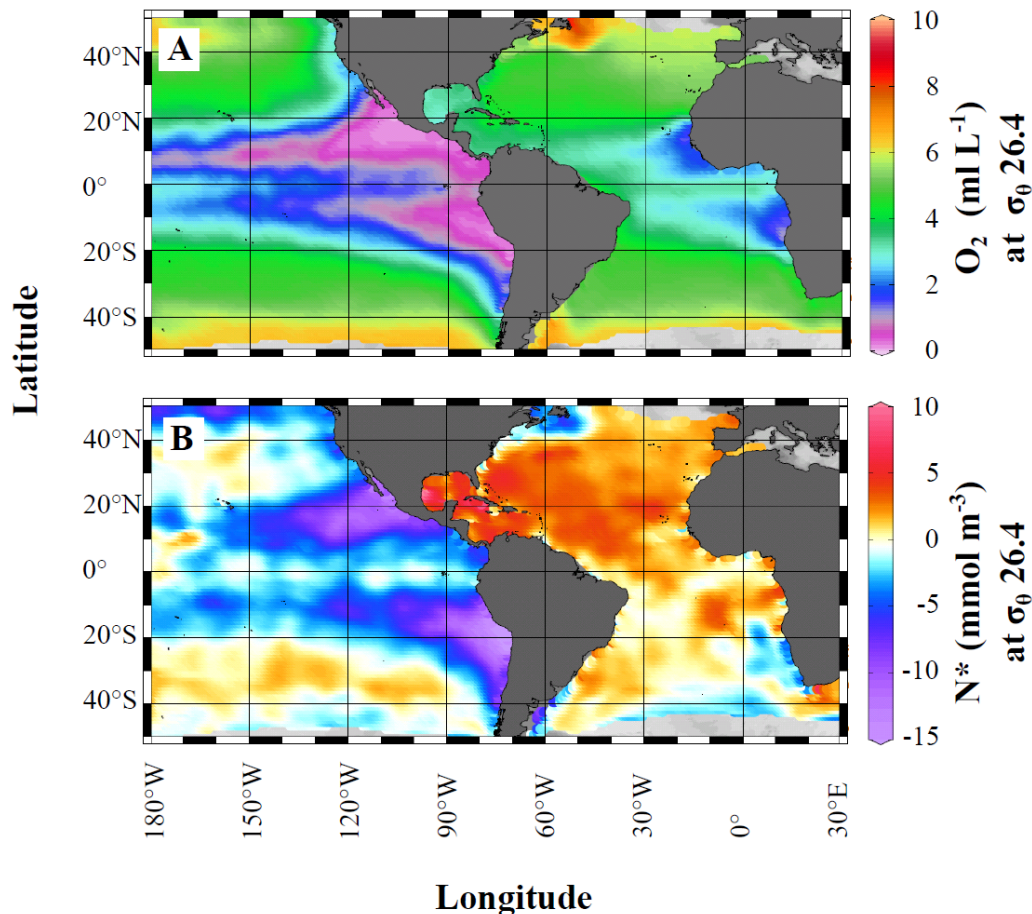


Figure 2: Dissolved oxygen ($ml L^{-1}$, panel A) and deficit/excess of nitrate relative to phosphate N^* ($mmol m^{-3}$, panel B) distribution on the potential density surface $\sigma_0 = 26.4$ in the Pacific and Atlantic Ocean. Data are from World Ocean Atlas 2009 (NOAA), N^* was computed using the empirical relationship presented in Gruber & Sarmiento (1997).

It has been observed that tropical oceanic OMZs in the Eastern North Pacific (Bograd et al. 2008) as well as in the Indian Ocean, the Eastern Tropical South Pacific and the Eastern Tropical North Atlantic (Stramma et al. 2008) are expanding in the course of the last decades, both in their vertical extent and in the area covered. Although OMZ research is now focused towards these tropical and subtropical areas due to their already extremely low O_2 concentrations at the OMZ core and evident implications for “tipping points” in marine biogeochemistry and ecology, O_2 loss from the oceans is a global phenomenon and has also been observed in the subarctic ocean (e.g. Whitney et al. 2007). Its three main causes are closely interlinked and driven by global climate change: first, warming results in lower solubility of gases in seawater; second, rising pCO_2 due to anthropogenic emissions enhances primary productivity in surface waters, thus increasing the amount of organic matter that is respired at depth (Oschlies et al. 2008); third, warming also causes increased stratification, which in turn reduces ventilation of the ocean interior. The latter, however, also strongly influences export production negatively, as it

decreases the vertical flux of nutrients across density layers (Bopp et al. 2001), and may therefore to some extent counteract oxygen loss.

The direct implications of oxygen loss for marine life appear to be evident: Metazoan animals cannot exist for prolonged periods of time within an anoxic or hypoxic environment. In a meta-analysis of experimental studies on benthic organisms, Vaquer-Sunyer & Duarte (2008) identified marked taxon-specific differences in oxygen sensitivity, with crustaceans and fish being most sensitive than mollusks, echinoderms and cnidarians, both in terms of lethal concentration and lethal exposure time. Up to now, there is no comparably comprehensive study on oxygen-dependent mortality of pelagic species, mainly due to the scarcity of experimental data. Because both feeding and metabolic demands have to be met in all animals, the distribution of biomass, temperature and oxygen in the water column creates distinctly vertically variable habitats. Studies addressing the vertical distribution of zooplankton in the Peruvian upwelling system demonstrated that the upper boundary of the oxycline is the single most critical factor structuring the habitat of most organisms (Semenova et al. 1982; Escribano et al. 2009). Most species did not occur below the 0.1 ml isopleth (Judkins 1980). However, some species have adapted their metabolism to allow them to actively migrate in and out of the OMZ. In a study by Semenova et al. (1982) covering transects between 7° and 15°S, two out of 37 species were found to inhabit the OMZ: the calanoid copepod *Eucalanus inermis* (permanently) and the euphausiid *Euphausia mucronata* (temporarily). In the former, adaptations of both body composition and physiological rates were found to be remarkably different from *Calanus*-species inhabiting surface waters of the same area (Flint et al. 1991), leading the authors to figuratively name the eucalanids “jelly-body copepods”. Daytime excursions into OMZ waters are thought to be a strategy of predator avoidance in zooplankton (Escribano et al. 2009), as most zooplanktivorous fishes as well as their predators have higher respiratory demands. For the latter, a notable exception appears to be the Humboldt squid *Dosidicus gigas*, a characteristic fast-growing predator of the Eastern Pacific. Contrary to most predatory fish species, this cephalopod routinely migrates into the OMZ at daytime, where its motion becomes sluggish and weight-specific respiration is reduced to less than one fifth of surface values (Rosa & Seibel 2009). It is hypothesized that this strategy of deliberate metabolic suppression saves energy and discloses a large foraging environment uninhabitable for their competitors (Seibel 2011).

Onshore shoaling of the oxycline thus results in surface accumulation relative to offshore waters, which creates high prey densities for planktivorous small pelagic fishes that (along with their large and active predators) are also confined to oxygenated surface waters (Stramma et al. 2010). It has been observed that the upper limit of the OMZ can be mapped accurately by means of

hydroacoustics reflecting the vertical distribution of Peruvian anchovy (Bertrand et al. 2010). Thus, habitat compression may also facilitate exploitation of this species, at the same time skewing stock estimates that rely on catch per unit effort data. Although predatory fishes may also benefit from densely aggregated prey, their habitat is likewise compressed, making them more vulnerable to surface fishing gears (Prince & Goodyear 2006). Noteworthy, it could be demonstrated that even the comparably moderate OMZ of the tropical Atlantic is avoided by billfishes whose high metabolic rates demand high oxygen waters (Prince et al. 2010). The CalCOFI ichthyoplankton time series provides fishery-independent insight to the stock dynamics of a number of epipelagic and mesopelagic fish species along with environmental variables since 1951, enabling the investigation of the response of fish stocks to oxygen itself. Koslow et al. (2011) were able to ascribe observed declines in the mesopelagic fishes of the southern California Current to periods of low oxygen. The authors argue that the observed shoaling of the hypoxic boundary layer of only a few meters involves a two- to sevenfold increase in light levels, rendering its inhabitants much more vulnerable to visual predation which supposedly has a larger impact than the metabolic requirements of reduced O₂ concentrations. Thus, even seemingly subtle changes in oxycline depth may have large impacts on the marine ecosystem.

Redox-dependent nutrient stoichiometry and implications for primary producers

Dissolved oxygen concentrations not only affect metazoan animals, but also biogeochemical cycles by acting as a switch for microbial processes and water chemistry (Fig. 3). At the sediment-water column interface, O₂ conditions govern the dissolution of redox sensitive trace metals and phosphorus, which is released from terrigenous or biogenic sediments where it is bound in iron oxides, organic material or apatite from fish debris (Ingall & Jahnke 1994) and enters the upwelled waters as biologically available dissolved inorganic phosphorus (DIP). On the other hand, nitrogen (N) loss processes occurring in both the sediment and the water column are highly sensitive to dissolved oxygen concentrations (Fig. 3). Heterotrophic denitrification, which was assumed to be the major N loss mechanism in the ocean until the 1990s, requires oxygen depletion and supply of organic material. More recently, evidence is growing that anaerobic ammonium oxidation (anammox) is also a major pathway to remove fixed inorganic N. In the OMZs off Namibia (Kuypers et al. 2005), Chile (Thamdrup et al. 2006), and Peru (Hamersley et al. 2007), anammox was found to be the dominant N loss process compared to denitrification. In the eastern tropical Atlantic, the presence of ammonium-oxidizing bacteria in the sediments of NW Africa has been detected (Jaeschke et al. 2010) but rate estimates are still lacking. Generally, O₂ concentrations in the Eastern Tropical North Atlantic OMZ core are too high (40-50 $\mu\text{mol kg}^{-1}$ as opposed to the assumed 5 $\mu\text{mol kg}^{-1}$ “switch”) to efficiently promote water column N loss processes (Karstensen et al. 2008). However, this generalization might not hold true on smaller spatial and temporal scales: in the core of spin-off eddies passing the northern side of the Cape Verde archipelago, O₂ concentrations reaching almost zero have been documented by moored sensors (Karstensen, pers. comm.).

In summary, low oxygen conditions promote N loss processes and provide a P source, thus, dissolved N:P stoichiometry in upwelled waters is very low (Fig. 2 B). The term “stoichiometry” refers to quantitative proportions of constituents (usually expressed as molar ratios of elements) in a composite substance. In ecological theory, stoichiometry considers elemental balances in the environment and in organisms, and the interactions between the two. Since Liebig’s Law of the Minimum, the concept of productivity limitation by the nutrient in shortest supply has been widely adopted. In the ocean, it has been observed that the abundance of the three major elements in the ocean (carbon, nitrogen, and phosphorus) relative to each other remains on average fairly constant. This empirical relationship of 106:16:1, which was first described by Redfield (1934) and therefore later dubbed the “Redfield ratio”, applies both for dissolved

nutrient concentrations and for particulate organic matter. Redfield later proposed the idea of a biological control of chemical constituents in the ocean (Redfield 1958) to explain this match. While bulk phytoplankton biomass tends to be close to the Redfield ratio under optimal growth conditions, nutrient limitation causes primary producers to fix more carbon relative to the limiting nutrient. Likewise, the N:P ratio is quite variable among primary producers (Geider & LaRoche 2002), depending on the nutrient availability in the environment and the growth strategy of the species. While enzymes and pigments have a high N content, nucleic acids (e.g. rRNA) are rich in P. Different physiological strategies in phytoplankton (energy vs. growth metabolism) therefore result in different overall stoichiometry (Arrigo 2005). As an example, oceanic picophytoplankton residing in the deep chl-*a* maximum under low nutrient and light conditions require extensive cellular resource acquisition machinery (such as enzymes and pigments) and only relatively little assembly machinery (such as nucleic acids). This means that their cellular N:P is greatly in excess of the canonical Redfield ratio. Because of these requirements, they can be N limited even when deep water N:P supply exceeds 16 (Klausmeier et al. 2004). Still, the robustness of the “Redfield ratio” has puzzled researchers for decades. Based upon a modeling approach, Loladze & Elser (2011) argue that the balance between two fundamental processes, protein and rRNA synthesis, results in a homeostatically stable protein/rRNA (and thus N:P) ratio. Due to the different requirements of various functional groups of microalgae, changes in dissolved N:P stoichiometry not only influence overall productivity, but also competitive interactions among primary producers (Grover 1997). In seasonal observations off northern Chile, Herrera & Escribano (2006) found that changes in phytoplankton community structure were closely correlated with OMZ depth. Although they could not establish a causal relationship, they hypothesized that nutrient limitation plays a major role, causing the disappearance of chain-forming diatoms that are usually present in upwelling conditions. Nutrient enrichment experiments are a widespread approach to identify the proximate limiting nutrient, or interactions among several key nutrients (see e.g. Hecky & Kilham 1988; Downing et al. 1999; Elser et al. 2007 and references therein). However, most bioassay and enrichment experiments were conducted focusing solely on the identification of certain biomass (e.g. POC accumulation) or rate (primary production, N₂-fixation) parameters, rather than aiming to identify community responses that can be important in the further cycling of nutrients and organic matter.

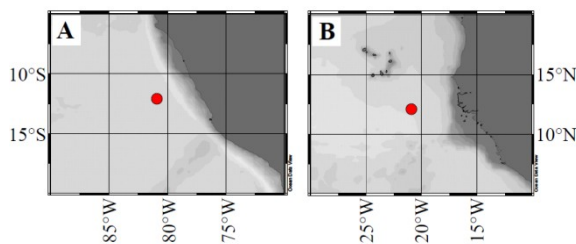
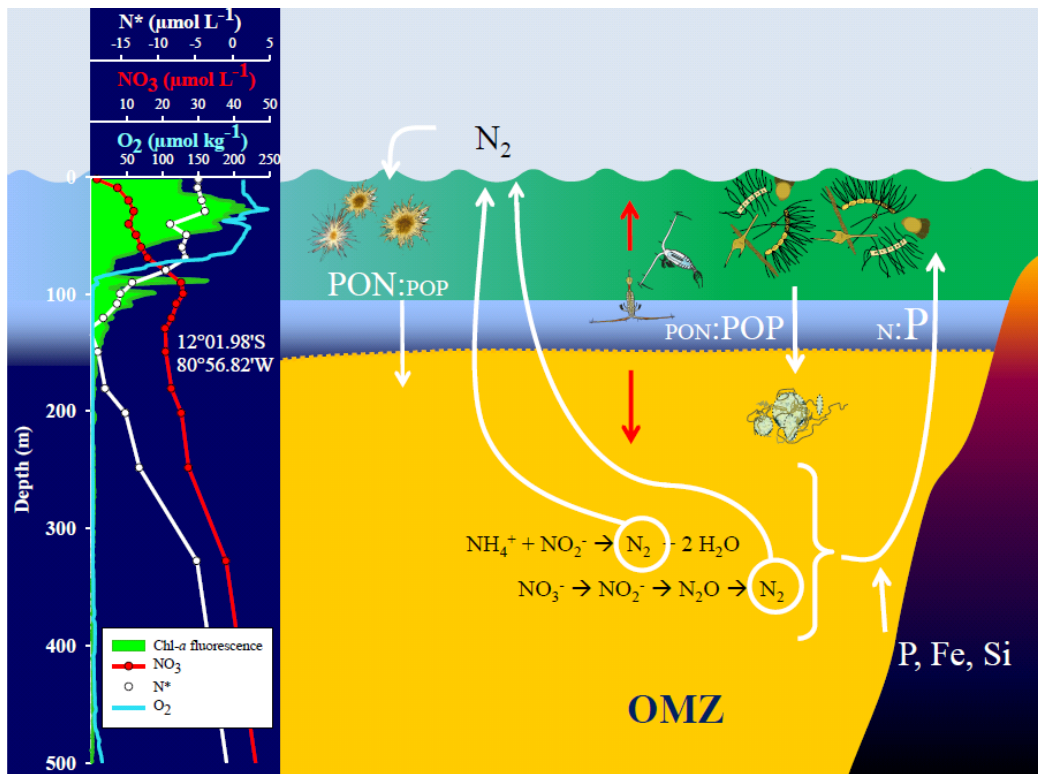
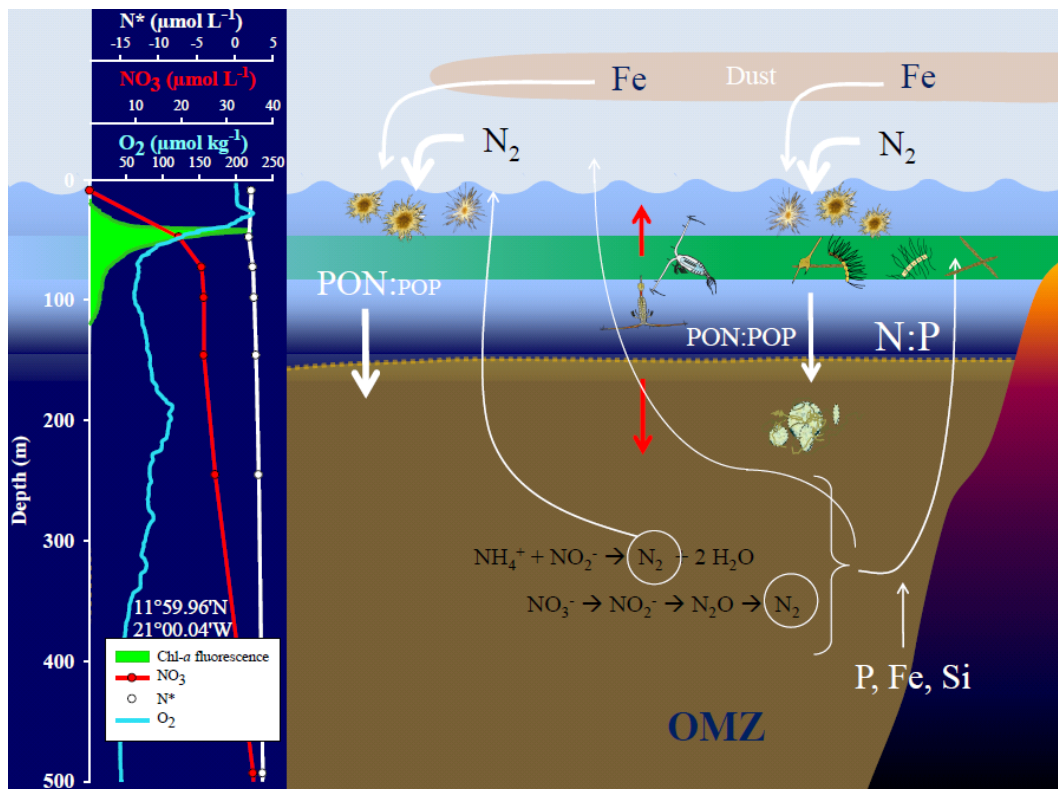


Figure 3: Conceptual sketch of N and P fluxes along with example profiles (O_2 , NO_3^- , N^* , chl- a) in the Eastern Tropical Pacific (top, station A) and Atlantic (bottom, station B).



Nutrient stoichiometry and food quality: implications for consumers

The nutritional quality of a particular diet is caused by various physical and biochemical characteristics of the prey organisms involved. Most obvious is the palatability of a food item, which is determined by its size, shape (spines etc.) and physical defense mechanisms such as mucus production. If a food item is readily ingested but results in decreased growth or reproductive rates, this may either be due to some component that inhibits growth being present or to some component essential for growth being too scarce or absent. The first category comprises phytoplankton grazing protection such as aldehydes produced by some diatom species (Ianora et al. 2004). The second category can be divided into the elemental stoichiometry and the biochemical makeup of the producer relative to the requirements of the consumer.

Elemental imbalance is a measure of the dissimilarity in composition between a consumer and its resource. This dissimilarity of various degrees can often be observed in aquatic food webs, because the elemental composition of metazoans is rather rigid compared to the plasticity of microalgal cellular composition (Sterner & Elser 2002). The vast majority of field and laboratory studies as well as theoretical considerations are based on freshwater systems. A fundamental difference between limnic and marine systems concerning these imbalances is the difference in N:P. In a comparison of several marine and freshwater sites, Elser & Hassett (1994) pointed out that, while the average seston N:P is much lower in the sea than in lakes, the zooplankton N:P in the marine environment exceeds that in freshwater, often ranging between 25 and 30. As a consequence, the elemental imbalance ($N:P_I = N:P_{\text{seston}} - N:P_{\text{consumer}}$) tends to be positive in lakes and negative in the sea. A strong imbalance between producer and consumer elemental composition can negatively influence zooplankton dynamics and secondary production (Elser et al. 1998). Since the contrast between freshwater phytoplankton and zooplankton C:N:P is mainly due to reduced P availability, deleterious effects of low food quality have been largely assigned to a shortage in P (Gulati & Demott 1997). Compared to the extensive research of this concept in freshwater ecosystems, remarkably little experimental evidence exists for food quality impacts in terms of low N:P stoichiometry on marine zooplankton. As a feedback to the elemental composition of phytoplankton, changes in the relative dominance of these zooplankton species can alter internal nutrient cycling in pelagic food webs (Elser & Urabe 1999). Due to the mean N:P of marine mesozooplankton (e.g. copepods) being substantially higher than the average phytoplankton N:P (Elser & Hassett 1994), zooplankton can influence mineral recycling by differential excretion as they preferentially retain N and recycle P, and potentially alter dissolved nutrient inventories (Liu et al. 2006).

Within the biochemical make-up of primary producers, the fatty acid (FA) composition is recognized as one of the key factors of food quality. Especially long-chained polyunsaturated fatty acids (PUFAs), such as eicosapentaenoic acid (EPA; 20:5n-3) and docosahexaenoic acid (DHA; 22:6n-3) are considered essential to metazoan consumers as these usually are unable to synthesize them *de novo* and thus have to ingest adequate amounts with their diet. A large part of the current knowledge stems from aquaculture research, because the rearing of marine fish larvae continues to be a bottleneck in the large-scale production, and among the nutritional requirements for first-feeding larvae the demand for suitable amounts of certain FAs has to be met (see e.g. Sargent et al. 1997 and references therein). In natural food webs, these components influence the growth and reproduction of zooplankton as well as trophic transfer efficiency (Brett & Müller-Navarra 1997; Müller-Navarra et al. 2000; Kainz et al. 2004). In several freshwater studies, PUFA content in the particulate matter was positively related to the P supply and predicted production of higher trophic levels (Müller-Navarra et al. 2004; Gulati & DeMott 1997). That P starvation causes a decrease in long chained PUFAs is likely due to their role in the phospholipids of cell membranes. However, N limitation can also have a negative effect on relative PUFA content, as shown by Klein Breteler et al. (2005). In their laboratory setup, development of copepods (*Temora longicornis* and *Pseudocalanus elongatus*) was retarded when feeding on either N- or P-limited diatoms (*Thalassiosira weissflogii*) that contained significantly less EPA than nutrient-replete cultures. While carbon accumulation in nutrient-limited phytoplankton leads to cells being rich in storage lipids (e.g. Parrish & Wangersky 1990), this increase in total FA is primarily due to increasing amounts of saturated FAs, with PUFA content tending to decrease in nutrient-limited algae (Dunstan et al. 1993; Müller-Navarra 1995). However, some exceptions from this pattern have been observed. In the cryptophytes *Rhodomonas salina*, nutrient limited cultures were found to be higher not only in total lipids, but also in n-3 and n-6 fatty acids, suggesting that both N and P limited *R. salina* are superior to unlimited cultures in terms of food quality (Malzahn et al. 2010). The somewhat contradictory observations in laboratory monoculture experiments adumbrate that the impact of nutrient limitation on the nutritional quality of a mixed phytoplankton assemblage in the natural environment still remains poorly understood.

Besides direct and indirect effects on the growth of consumers, dissolved N:P inventories (and, hence, supply ratios to the euphotic zone) can also indirectly affect trophic transfer and cycling of N. At low N:P ratios, phytoplankton with the ability to fix atmospheric N₂ have a competitive advantage over non-diazotrophs. Because the $\delta^{15}\text{N}$ signature of atmospheric N is zero, and thus much lower than that of upwelled NO₃⁻, their relative contribution to the foodweb can be tracked

using the $\delta^{15}\text{N}$ signature of the various foodweb components (Montoya 2008). Because the mass difference of the heavy and light isotope of a covalent-bond forming element influences its rate of chemical reactions, trophic fractionation occurs, i.e. enrichment of the heavier isotope in higher trophic levels, and depletion of the heavy isotope in excretion products (Fig. 4). Thus, $\delta^{15}\text{N}$ in zooplankton biomass exceeds that of suspended particulate matter, while $\delta^{15}\text{N}$ in zooplankton excretion is lower than in zooplankton biomass, and $\delta^{15}\text{N}$ in fecal pellets slightly higher (Checkley & Entzeroth 1985).

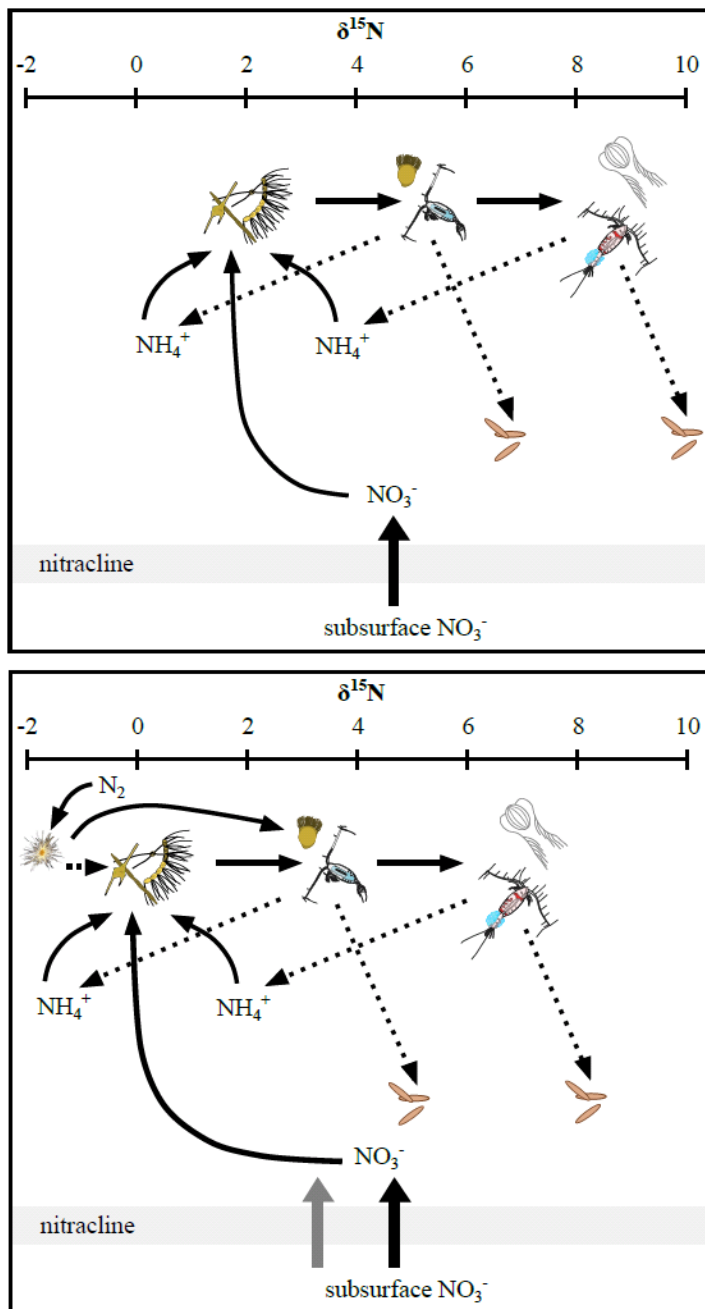


Figure 4: Schematic overview of the major processes controlling the $\delta^{15}\text{N}$ signature in organic and inorganic N pools, under absence (top) and presence (bottom) of nitrogen fixation. Solid arrows represent consumption and trophic transfer of N, and broken arrows denote excretion and egestion processes leading to remineralization of inorganic N. Note the general shift in all foodweb components (i.e. primary producers, primary and secondary consumers), and that this shift is depending on the relative contribution of surface diazotroph N and the vertical flux of NO_3^- . Figure modified after Montoya et al. 2002.

Objectives

The present study aimed to elucidate the effect of N and P concentrations as well as their supply ratios on natural phytoplankton in Eastern Boundary Current Systems in the Pacific and Atlantic Ocean, which was approached by nutrient manipulation experiments in shipboard mesocosms off Peru and West Africa (Chapter I and II). Further, it was aimed to track potential transmission on zooplankton nutritional condition and growth as well as excretion of inorganic N and P, providing a feedback to primary producers, which was tackled by feeding experiments associated to the mesocosm setup as well as field sampling (Chapter II and III). In the Eastern Tropical North Atlantic, the differential importance of upwelled and atmospheric nitrogen sources on primary productivity and its respective transfer was quantified using stable N isotopes in zooplankton (Chapter IV).

Chapter I

Changes in N:P stoichiometry influence taxonomic composition and nutritional quality of phytoplankton in the Peruvian upwelling

Helena M. Hauss, Jasmin Franz and Ulrich Sommer

Abstract

Inorganic dissolved macronutrient (nitrogen, N, and phosphorus, P) supply to surface waters in the eastern tropical South Pacific is influenced by expanding oxygen minimum zones, since N loss occurs due to microbial processes under anoxic conditions while P is increasingly released from the shelf sediments. To investigate the impact of decreasing N:P supply ratios in the Peruvian Upwelling, we conducted nutrient manipulation experiments using a shipboard mesocosm setup with a natural phytoplankton community. In a first experiment, either N or P or no nutrients were added with mesozooplankton present or absent. In a second experiment, initial nutrient concentrations were adjusted to four N:P ratios ranging from 2.5 to 16 using two “high N” and two “high P” levels in combination (i.e., +N, +P, +N and P, no addition). Over six and seven days, respectively, microalgal biomass development as well as nutrient uptake was monitored. Phytoplankton biomass strongly responded to N addition, in both mesozooplankton-grazed and not grazed treatments. The developing diatom bloom in the “high N” exceeded that in the “low N” treatments by a factor of two. No modulation of the total biomass by P-addition was observed, however, species-specific responses were more variable. Notably, some organisms were able to benefit from low N:P fertilization ratios, especially *Heterosigma* sp. and *Phaeocystis globosa* which are notorious for forming blooms that are toxic or inadequate for mesozooplankton nutrition. After the decline of the diatom bloom, the relative contribution of unsaturated fatty acid to the lipid content of seston was positively correlated to diatom biomass in the peak bloom, indicating that positive effects of diatom blooms on food quality of the protist community to higher trophic levels remain even after the phytoplankton biomass was incorporated by grazers. Our results indicate an overall N-limitation of the system, especially in the case of dominating diatoms, which were able to immediately utilize the available nitrate (within two days) and develop a biomass maximum within three days of incubation. After the decline of diatom biomass, detection of the cyanobacterial marker pigment aphanizophyll indicated the occurrence of diazotrophs, especially in those enclosures initially provided with high N supply. This was surprising, as diazotrophs are thought to play a role in compensating to some extent the N deficit above OMZs in the succession of phytoplankton after an upwelling event.

I. 1 Introduction

Coastal upwelling systems are immensely productive, contributing an estimated 11% to the annual new production while covering only 1% of the world's oceans (Chavez & Toggweiler 1995; Pennington et al. 2006). In the eastern tropical South Pacific, the high productivity in the photic zone leads to an extensive oxygen minimum zone (OMZ) at depth, reaching suboxic and in some regions anoxic oxygen (O_2) levels (Fiedler & Talley 2006). Recent observations indicate that this OMZ is expanding in the course of global climate change (Stramma et al. 2008). Besides direct effects of low O_2 concentrations on metazoan life (Vaquer-Sunyer & Duarte 2008), the biogeochemistry of both water column and sediments are highly influenced by concentrations of dissolved O_2 : under anaerobic conditions, massive losses of dissolved inorganic nitrogen (N) occur through denitrification (Deutsch et al. 2001) and anammox (Kuypers et al. 2005). In contrast, anoxic shelf sediments are a source for dissolved inorganic phosphate (P) as, under reducing conditions, P bound to metal oxides or biogenic apatite in fish debris is released into the water column (Van Cappellen & Ingall 1994; Lenton & Watson 2000). Thus, water masses that are already significantly below the canonical N:P Redfield ratio of 16 are transported by upwelling processes into the productive surface layer (Franz et al. 2012). Since changes in the nutrient stoichiometry have been observed to affect phytoplankton in respect of its community structure (Sommer et al. 2004), its elemental composition (Gervais & Riebesell 2001) and its nutritional value for higher trophic levels (Kiørboe 1989; Sterner & Schulz 1998), changes in the upwelled nutrient stoichiometry may have strong impacts on the primary and secondary production as well as the biogeochemical cycling off Peru. It has been accepted for decades that the overall productivity in the Peruvian coastal upwelling is limited by new nitrogen (Dugdale 1985). It is largely assumed that especially large-celled phytoplankton communities on the shelf rely on the vertical supply of nitrate as opposed to offshore pico- and nanoplankton dominated assemblages that take advantage of regenerated ammonium and urea (Probyn 1985). However, tracer uptake experiments conducted off Peru indicate that ammonium (NH_4^+) regenerated in surface waters can contribute up to 50% of total assimilated dissolved inorganic nitrogen (DIN, Fernández et al. 2009). The effect of non-Redfield N and P supply dynamics on the shelf phytoplankton assemblage has not been well studied yet, and field data describing the changes in community structure with increasing distance from the coastal upwelling are scarce (DiTullio et al. 2005; Franz et al. 2012). Traditionally, upwelling areas are

considered to be regions of short energy transfer across few trophic levels, with diatoms, calanoid copepods and small pelagic fish feeding on zoo- and partly phytoplankton as key players (Cushing 1989; Alheit & Niquen 2004). Furthermore, diatoms are considered the main drivers of export flux due to their large cell sizes, high sinking velocities and rapid flocculation (Buesseler 1998), thus channelling biomass into the OMZ. A plethora of studies exists describing the response of marine phytoplankton to nutrient enrichment experiments (see Downing et al. 1999 and references therein) in terms of biomass or chlorophyll-*a* (Chl-*a*) change relative to an unamended control. Although the use of batch assays has been criticized in low-nutrient environments (Hutchins et al. 2003), they have contributed pivotally to our understanding of nutrient limitation in many systems and are considered suitable to simulate pulsed nutrient supply in coastal upwelling areas. While a number of studies have been conducted in the eastern North Pacific (Kudela & Dugdale 2000; Wetz & Wheeler 2003; Fawcett & Ward 2011), little information is available on phytoplankton biomass regulation off Peru (Hutchins et al. 2002). Furthermore, no detailed studies exist that examine phytoplankton succession following an upwelling event in this area. The ability to fix elemental N by diazotrophic cyanobacteria is a major advantage in ecosystems prone to N limitation. Thus, it is argued that excess P in the euphotic zone as a result of N losses within the OMZ in the tropical eastern South Pacific could facilitate considerably higher N₂-fixation rates than previously assumed (Deutsch et al. 2007). This is well in line with observations reporting that the role of unicellular cyanobacteria in the nutrient cycle has been underestimated (Zehr et al. 2001; Montoya et al. 2004; Moisander et al. 2010) compared to the extensive surface blooms of *Trichodesmium* spp. in the warm surface waters of the oligotrophic ocean (Breitbarth et al. 2007).

The transfer of primary to secondary production (i.e., zooplankton growth) is driven by various factors, among which the quality of prey can be of equal or higher relevance than its quantity (Kleppel 1993). Within the biochemical composition of microalgae, the proportion of polyunsaturated fatty acids (PUFAs) in relation to saturated and monounsaturated fatty acids (SAFA and MUFA, respectively) form an integral part of the food quality of a primary producer to higher trophic levels (Müller-Navarra et al. 2000). PUFAs such as 20:5n-3 (eicosapentanoic acid, EPA) and 22:6n-3 (docosahexanoic acid, DHA) cannot be synthesized *de novo* by most metazoan consumers and are thus considered essential (Brett & Müller-Navarra 1997). It was demonstrated that PUFA content in the particulate matter can enhance secondary production of marine zooplankton (e.g. Jónasdóttir et al. 1995; Vargas et al. 2006). While carbon accumulation in nutrient-limited monoalgal phytoplankton cultures results in cells that are rich in lipids (Malzahn et al. 2010), N limitation may have a negative effect on relative PUFA content, as

shown by Klein Breteler et al. (2005). Furthermore, changes in the taxonomic composition of a phytoplankton assemblage under nutrient limitation may influence the availability of PUFAs depending on the physiology of the species involved (Mayzaud et al. 1989; Vargas et al. 2006).

We hypothesized that changes in inorganic N and P supply as well as their ratio would influence the community composition and total biomass development of the phytoplankton, in turn affecting the quality to higher trophic levels. To investigate this, nutrient limitation experiments were conducted using an *in situ* phytoplankton assemblage and meso-scale shipboard experimental containers.

I. 2 Materials and Methods

Experimental setup

Two short-term (6 and 7d) growth experiments were conducted during cruise M77/3 on the German R/V *Meteor* from Guayaquil (Ecuador) to Callao (Peru) from Dec 26, 2008 to Jan 21, 2009 (Table I.1). The experimental setup comprised twelve 70L mesocosm bags afloat in four gimbals-mounted cooling water baths connected to a flow-through system that allowed a complete water exchange of the water bath with surface seawater within 10 to 15 min (Fig. I.1 A). Surface water for the initial filling was obtained from repeated casts (10 m depth) using Niskin bottles mounted on a CTD-rosette at 12°02.05'S, 077°47.33'W for experiment 1 and at 16°0.01'S, 074°37.04'W for experiment 2 (Fig. I.1 B). The collected water from individual Niskin bottles was mixed in large barrels before filling the individual bags. Temperatures within the mesocosms varied with sea surface temperature and ranged from 19.0 to 23.0°C in experiment 1 and from 18.0 to 25.6°C in experiment 2. The water baths were shaded with nets to reduce light intensity to approximately 30% of surface irradiation. Daytime light intensity within the water baths ranged from 700 to 2600 $\mu\text{E s}^{-1} \text{m}^{-2}$. As an experimental treatment, inorganic N and P levels were manipulated by initial fertilization using ammonium nitrate (NH_4NO_3) and monopotassium phosphate (KH_2PO_4) to the respective target DIN:DIP ratios (Table 1), where DIN includes NH_4^+ and NO_3^- . Equal SiO addition ($10 \mu\text{mol L}^{-1}$) to all mesocosms using sodium metasilicate penta-hydrate ($\text{Na}_2\text{SiO}_3 \cdot 5\text{H}_2\text{O}$) as well as Provasoli PII metal mix (6 ml) prevented colimitation by Si or by trace elements. In experiment 1, either N or P (or none) was added in the presence or absence of mesozooplankton (removed by a 200- μm mesh screen), while experiment 2 was aimed at a closer investigation of N:P impact, and thus encompassed four N:P treatments, of which one (N:P=5) received no nutrient addition and thus represents the ambient nutrient conditions at the filling station. During experiment 2, the bottom

plate construction failed in two mesocosms in the course of the experiment, thus these were omitted from subsequent analyses. Due to the limited water volume in this first application of the setup and the volume requirements of sampling ($4\text{-}5\text{L d}^{-1}$), mesocosms had to be restocked (i.e. diluted to initial volume) on days 3 (14 L in experiment 1, 20 L in experiment 2) and 5 (8 L in experiment 1, 15 L in experiment 2) using $5\text{-}\mu\text{m}$ filtered surface seawater. In experiment 2, SiO was also restocked to $10\ \mu\text{mol L}^{-1}$ on day 5. However, due to the large differences in biomass and nutrient concentrations between sampling days, we did not attempt to calculate growth rates and correcting the data for the dilution as we concluded that an extrapolation of growth rates in the sampled water would introduce a considerable error.

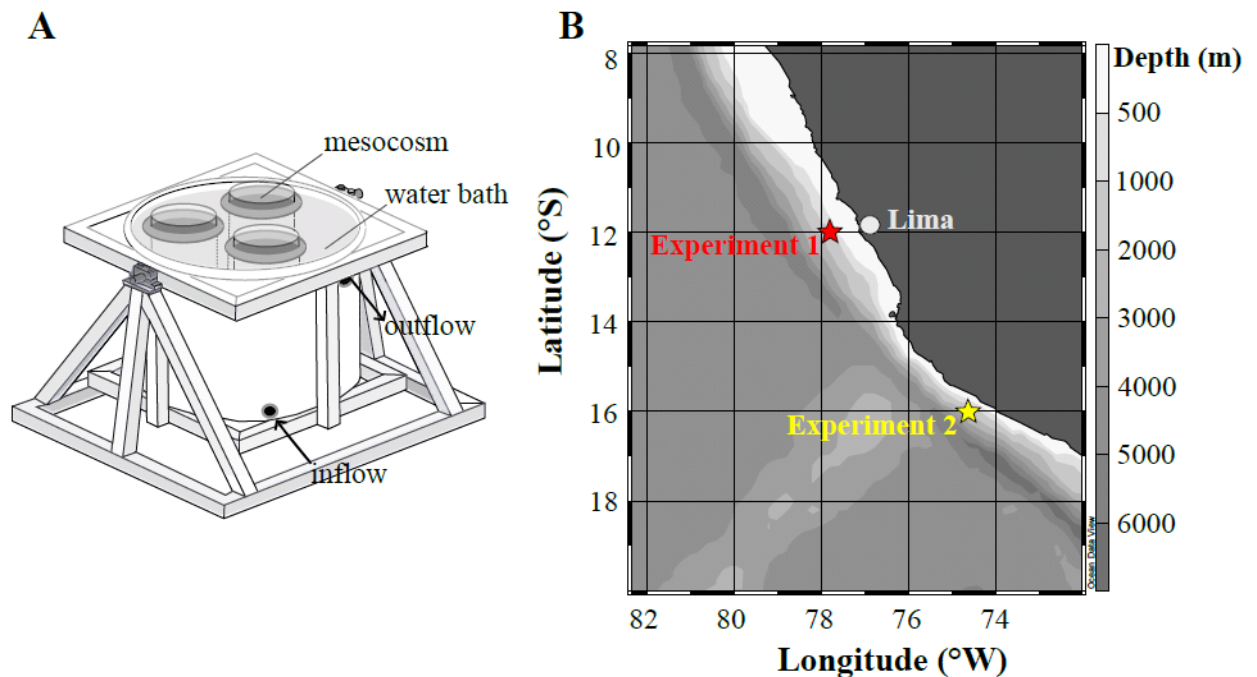


Figure I.1: Sketch of three mesocosms within gimbals-mounted water bath with flow-through cooling using surface seawater (panel A). Four water baths with a total of twelve mesocosms were used. Locations of initial filling of the two experiments are indicated by stars on panel B.

Table I.1: Overview of the initial and adjusted conditions of the two experiments.

		Experiment 1			Experiment 2			
initial conditions								
Latitude		12°02.05'S			16°0.01'S			
Longitude		077°47.33'W			074°37.04'W			
T (°C)		20.3			18.2			
DIN		5.5			5.0			
DIP		1.6			1.0			
SiO		3.2			3.7			
experimental conditions								
treatment		+N	none	+P	+N	+N&P	none	+P
N:P		20	3.4	2.8	16	8	5	2.5
N level		high	low	low	high	high	low	low
P level		low	low	high	low	high	low	high
adjusted DIN		32	5.5	5.5	16.0	16.0	5.0	5.0
adjusted DIP		1.6	1.6	2	1.0	2.0	1.0	2.0
adjusted SiO		10	10	10	10	10	10	10
replicates		2x zooplankton removed 2x zooplankton			3x			

Analyses

All samples except for fatty acid composition were taken on a daily basis after gentle mixing of each mesocosm by up-and-down stirring. Samples for dissolved inorganic nutrients (NO_3^- , NO_2^- , PO_4^{3-} , SiO) were filtered through 5 μm cellulose acetate filters (\varnothing 25 mm) and immediately analyzed on board according to Hansen & Koroleff (2007) using a Hitachi U-2000 spectrophotometer. For determination of NO_2^- , 0.2 ml sulphonamide and 0.2 ml naphthylethylenediamine were added to 10 ml of sample, incubated 30 min at room temperature, and absorbance was measured at 542 nm against double deionized water. To calculate the amount of NO_3^- in the sample, all NO_3^- compounds were reduced to NO_2^- using a cadmium reductor with the reagents sulphanilamide and N-1-naphthylethylenediamine dihydrochloride and incubating for 20min at room temperature before measuring. NH_4^+ analysis was conducted according to Holmes et al. (1999). Immediately after sampling, 10 ml of unfiltered sample was mixed with 2.5 ml of working reagent (WR) and incubated in the dark for 2 h 15 min, and its emission measured at 422 nm. The WR consisted of 2 L borate-buffer (80 g $\text{Na}_2\text{B}_4\text{O}_7 \cdot 10\text{H}_2\text{O}$

+ 2 L double deionized water), 10 ml of sodium sulfite (1 g Na₂SO₃ in 125 ml double deionized water) and 100 ml of OPA-solution (4 g orthophtaldialdehyde in 100 ml ethanol).

For the analysis of PO₄³⁻, 0.3 ml of a mixed reagent (4.5M H₂SO₄ + ammonium molybdate + potassium antimonyl tartrate) and 0.3 ml ascorbic acid were added to 10 ml sample, incubated at room temperature for 10 min and the absorbance measured at 882 nm against double deionized water.

Analysis of Si(OH)₄ was performed according to Hansen & Koroleff (2007). 0.3 ml of a mixed reagent (molybdate solution + 3.6 M H₂SO₄ in the ratio 1:1) was added to 10 ml of unfiltered sample. After 10-20 min of incubation, 0.2 ml oxalic acid and 0.2 ml of ascorbic acid were added, and after another 30min, absorption was measured against double deionized water at 810 nm wavelength in a spectrophotometer.

Cell counts of Lugol-stained microplankton were conducted daily on board using the inverted microscope method after Utermöhl (1958). Sedimentation volume was 50 ml. At least 100 cells per category were counted when possible. Biovolumes were calculated after approximation to geometric shapes (Hillebrand et al. 1999) and converted to biomass (µg C L⁻¹) using the carbon to volume relationships described in Menden-Deuer & Lessard (2000). Nanoplankton and bacterial abundance were assessed using a flow cytometer (FACScalibur, Becton Dickinson, San Jose, CA, USA). Samples (5 ml) were fixed with 2% formaldehyde, frozen at -80°C, transported to the laboratory and measured at a flow rate of 50.6 µl min⁻¹. Cells were distinguished by forward scatter (relative cell size) and fluorescence of Chl-*a*, phycoerythrin, and allophycocyanin. Biovolume was estimated assuming spherical shapes. For bacterial abundance, samples were diluted 1:3, stained with SYBR-Green and counted at lower flow rate (13.9 µl min⁻¹).

The fatty acids of bulk seston were measured as fatty acid methyl esters (FAMES). 250 or 500 ml water, depending on the concentration of phytoplankton, were filtered on precombusted 0.2 µm GF/F filters at the start (duplicate sample) and the end of the experiment (one sample per mesocosm) and frozen at -80°C. Lipids were extracted from the samples with dichloromethane:methanol:chloroform (1:1:1 volume ratios), and C23:0 standard added. After centrifugation, water-soluble fractions were removed by washing with a 1 M KCl solution and dried by addition of NaSO₄. The solvent was evaporated to dryness in a rotaryfilm evaporator (150-200 mbar) and the remainder transferred with 200 µl chloroform into a glass cocoon. Esterification was done over night using 2% H₂SO₄ in methanol at 50°C. The FAMES were washed from the H₂SO₄ using n-hexane, transferred into a new cocoon, and evaporated to dryness using nitrogen gas. N-hexane was added to a final volume of 100 µl. All chemicals used

were gas chromatography (GC) grade. FAMES were analyzed by GC using a Varian CP 8400 gas chromatograph equipped with a DB-225 column (JandW Scientific, 30 m length, 0.25 mm inner diameter, 0.25 mm film). The carrier gas was helium at a pressure of 82.737 Pa. Sample aliquots (1 μ l) were injected splitless. The injector temperature was set to 250°C. The column oven was set to 60°C for 1 min after injection, after which it was heated to 150°C at 15°C min⁻¹, then to 170°C at 3°C min⁻¹, and finally to 220°C at 1°C min⁻¹, which was held for 21 min. The flame ionization detector was set to 300°C. FAMES were quantified using calibrations set up for each fatty acid separately.

Samples for High Pressure Liquid Chromatography (HPLC) were vacuum-filtered (150 mbar) onto Whatman GF/F filters (25 mm) and immediately stored at -20°C until analysis in the laboratory. Filters were homogenized for 5 min with 2 mm and 4 mm glass beads and 2 ml acetone (90%). The supernatant was filtered through a 0.2 μ m teflon filter and stored at -80°C. The HPLC measurement was conducted by a Waters 600 controller in combination with a Waters 996 photodiode array detector (PDA) and a Waters 717plus auto sampler (modified after Barlow et al. 1997). Classification and quantification of the various phytoplankton pigments was performed with the software EMPOWERS (Waters).

Statistics

In order to estimate nutrient uptake rates, linear regressions were fitted to DIN and DIP over time in experiment 1. To be able to estimate nutrient drawdown dynamics in the different treatments in experiment 2, where the decrease in nutrient concentrations was nonlinear, three-parameter logistic regressions were fitted to nutrient concentrations over time:

$$(I.1) \quad [N] = \frac{a}{1 + \left(\frac{t}{t_{50}}\right)^b}$$

where $[N]$ is the concentration (μ mol L⁻¹) of the respective nutrient, t is time (days), and a , b , and t_{50} are regression parameters, so that t_{50} represents the time where half of the initially available nutrient concentration is consumed. Only values up to day four were included, as post-bloom conditions resulted in a slight increase in detected concentrations of N and P.

Diatom biomass was described using a lognormal function

$$(I.2) \quad BM = BM_{MAX} * e^{-0.5 * \left(\frac{\ln(t/t_{BM_{MAX}})}{b} \right)^2}$$

Where BM is the observed biomass at time t (d), BM_{MAX} is the maximum biomass reached during bloom development and $t_{BM_{MAX}}$ is the time when maximum biomass is reached.

A factorial ANOVA with time, initial N level and P level as factors was used to explore differences between treatments in the biomass of individual species as well as aphanizophyll. A correlation matrix was used to explore the relationships between total diatom biomass (maximum of the respective mesocosm during the entire experiment) and individual fatty acids and their ratios determined at termination of the experiment (i.e., after the bloom). Data were square-root transformed to approximate normality.

I.3 Results

Nutrients

In situ nutrient concentrations at the filling stations were 5.5 and 5 $\mu\text{mol L}^{-1}$ total DIN, 1.6 and 1.0 $\mu\text{mol L}^{-1}$ DIP, and 3.2 and 3.7 $\mu\text{mol L}^{-1}$ SiO in experiment 1 and 2, respectively. This translates into molar N:P ratios of 3.4 and 5 in experiment 1 and 2, respectively (Table 1).

After the start of the experiment, nutrient drawdown of the three macronutrients (DIN, DIP, SiO) began after a time lag of 1-2 days in experiment 1 and immediately in experiment 2. Generally, nutrient drawdown in experiment 1 (Fig. I.2) was slower than in experiment 2 (Fig. I.3), in which the initial phytoplankton assemblage contained more diatoms, with a mean (\pm SD) proportion of $6.9\pm 3.8\%$ and $60.2\pm 7.4\%$ of total microplankton biomass on day 1 in experiment 1 and 2, respectively. No significant differences in nutrient drawdown were detected within experiment 1 between the mesocosms with zooplankton present as opposed to the ones that were mesh-screened. Therefore, data were pooled into four replicates of the three nutrient treatments. Until the termination of the experiment, dissolved nutrients were detected in all mesocosms. The drawdown of DIN in the “high N” treatment was significantly faster (ANCOVA, $p < 0.001$) than in the two “low N” treatments, with a mean (\pm SE) uptake rate of $2.9(\pm 0.3)$ $\mu\text{mol N d}^{-1}$ in the +N treatment, $0.40(\pm 0.12)$ $\mu\text{mol N d}^{-1}$ in the +P and $0.40(\pm 0.13)$ $\mu\text{mol N d}^{-1}$ in the ambient treatment, respectively (Fig. I.2 A). Similarly, DIP uptake rates were similar in the two “low P” treatments over the course of the experiment, with $0.09(\pm 0.02)$ $\mu\text{mol P d}^{-1}$ in the ambient and +N treatment, respectively, and significantly higher (ANCOVA, $p < 0.001$) in the +P treatment with $0.12(\pm 0.03)$ $\mu\text{mol P d}^{-1}$. No continuous removal of SiO could be observed (Fig. I.2 C). In contrast to experiment 1, the DIN pool was completely depleted on the third day in experiment 2. Mean half consumption times $t_{50}(\pm$ SE) of DIN were significantly longer in the “high N” treatments ($p = 0.014$), with $1.84(\pm 0.07)$ and $1.9(\pm 0.08)$ days in the N:P=16 and 8, and $1.32(\pm 0.18)$ and $1.41(\pm 0.15)$ days in N:P=5 and 2.5 treatments, respectively. For DIP, mean half consumption times were significantly longer in the “high P” treatments ($p = 0.009$), with $1.23(\pm 0.07)$ and $1.73(\pm 0.09)$ days in the N:P=16 and N:P=8, and $1.34(\pm 0.2)$ and $2.23(\pm 0.3)$ days in the N:P=5 and 2.5 treatments, respectively. In the N:P=2.5 treatment, supplied P uptake was incomplete and a concentration of approximately $0.5 \mu\text{mol L}^{-1}$ remained until termination of the experiment. The ratio of drawdown velocity, expressed as $t_{50\text{N}}:t_{50\text{P}}$, was positively related to initial N:P supply (Fig. I.3, insert on panel B).

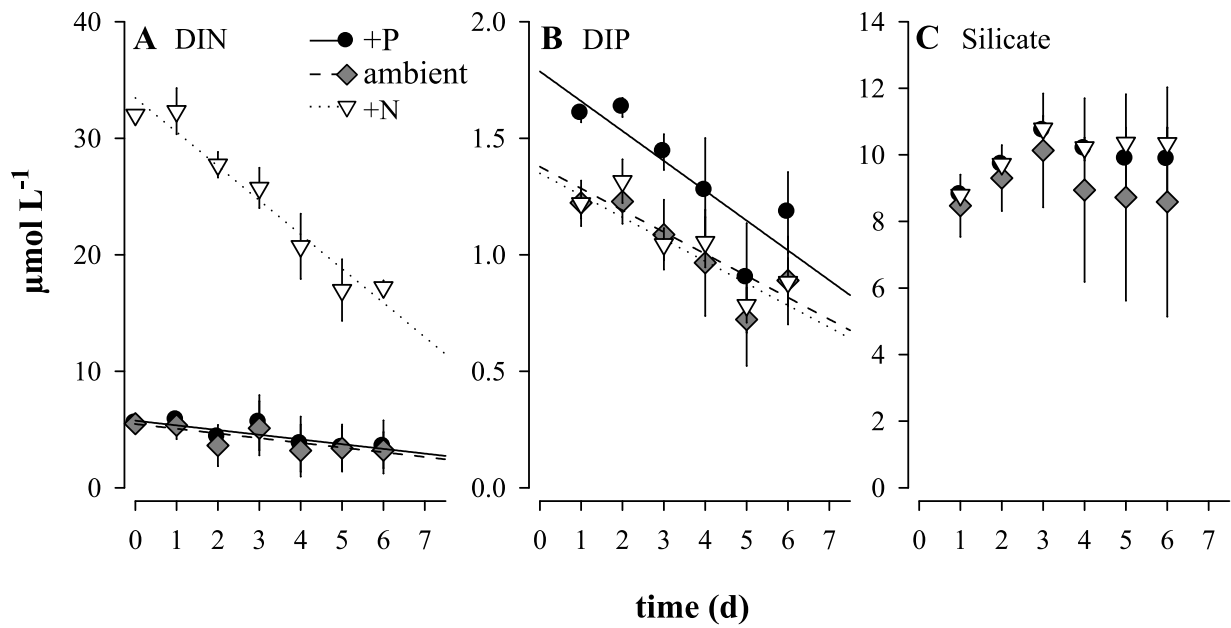


Figure I.2: Dissolved inorganic nutrient (DIP, panel A, DIN, panel B, and SiO, panel C) concentrations ($\mu\text{mol L}^{-1}$) in experiment 1 over time. Values are treatment means (\pm standard deviation). Data from mesocosms with mesozooplankton removed and not removed were pooled because of insignificant differences, hence $n=4$ for all treatments.

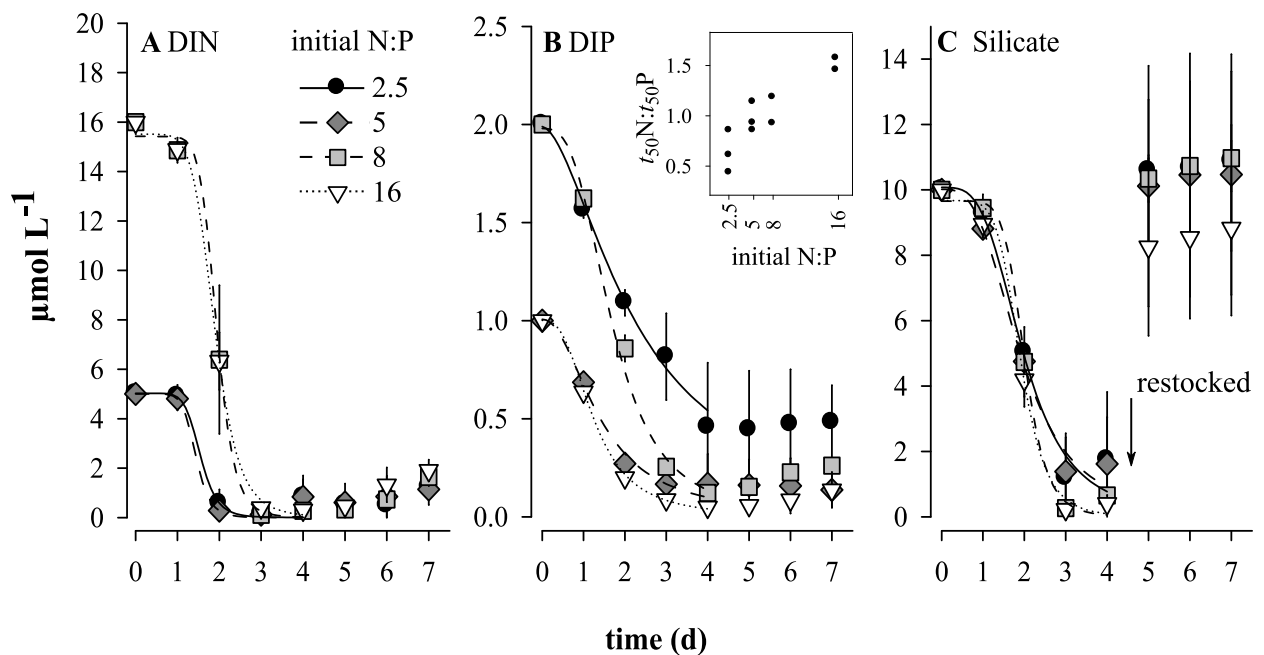


Figure I.3: Dissolved inorganic nutrient (DIP, panel A, DIN, panel B, and SiO, panel C) concentrations ($\mu\text{mol L}^{-1}$) in experiment 2 over time. Values are treatment means (\pm standard deviation, $n=2-3$). Lines are sigmoid regressions fitted through individual mesocosm values up to day four (indicated by dashed line). Insert on panel B indicates relationship between half consumption times ($t_{50N}:t_{50P}$) and initial N:P supply ratio.

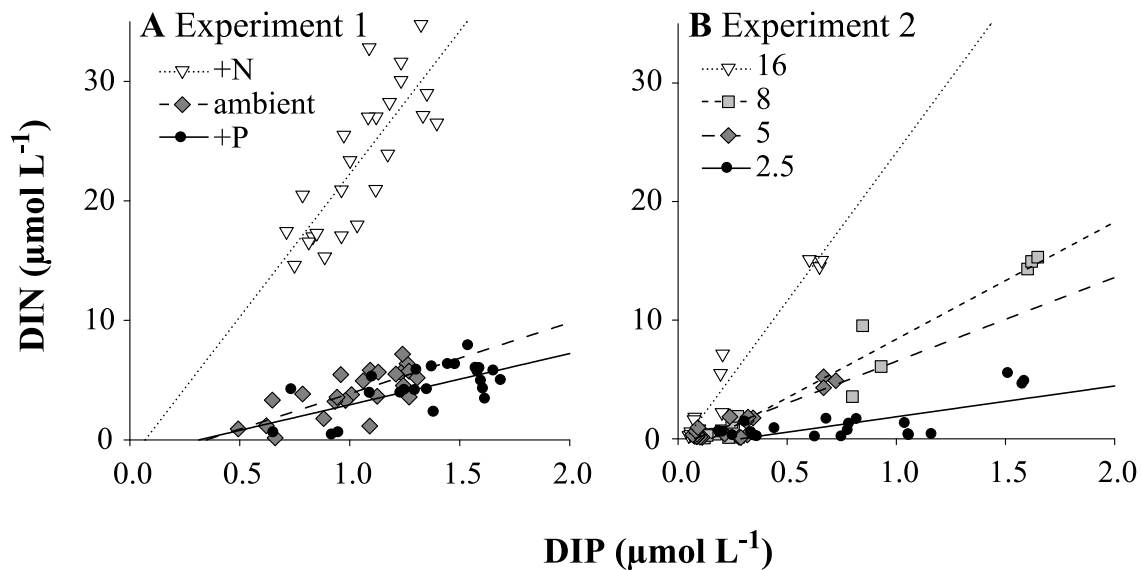


Figure I.4: Uptake ratios of inorganic nitrogen and phosphorus in experiment 1 (panel A) and experiment 2 (panel B). Values are individual data, slopes of linear regressions correspond to uptake ratios.

The uptake ratios of inorganic N and P in the different experimental treatments determined by linear regressions (Fig. I.4) were closely related to the initial N:P ratio provided in both experiments. In experiment 1, the regression slopes (\pm SE, $p < 0.001$) were $23.92(\pm 1.73)$, $5.9(\pm 1.15)$ and $4.28(\pm 1.05)$ in the +N (N:P=32), ambient (N:P=3.4) and +P (N:P=2.8) treatments, respectively. In experiment 2, the regression slopes (\pm SE, $p < 0.001$) were $25.01(\pm 1.48)$, $9.88(\pm 0.56)$, $7.07(\pm 0.75)$ and $2.59(\pm 0.56)$ in the +N (N:P=16), + N&P (N:P=8), ambient (N:P=5) and +P (N:P=2.5) treatments, respectively.

Total diatom biomass

In experiment 1, the removal of mesozooplankton larger than $200 \mu\text{m}$ resulted in about two-fold increase in diatom biomass development within the respective nutrient addition treatments (Fig. I.5). Nevertheless, diatom biomass was always higher in the +N treatments than in the other two. In experiment 2, diatom biomass was also higher in the two “high N” treatments (N:P=16 and N:P=8) than in the two “low N” treatments (N:P=5 and N:P=2.5) whereas no differences could be detected among the “high P” and “low P” treatments (Fig. I.6 A). The peak bloom was reached slightly earlier in the “low N” treatments.

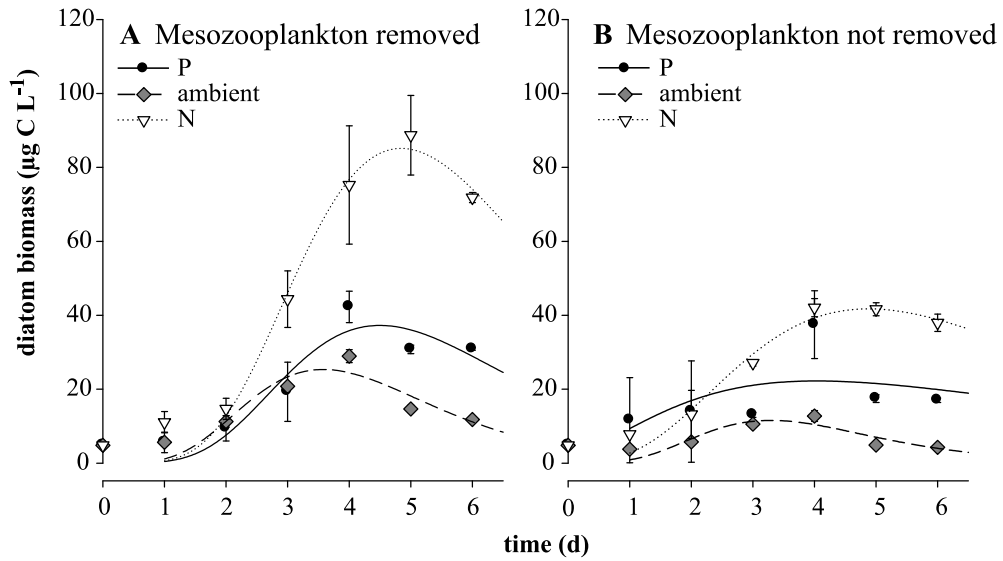


Figure I.5: Summed diatom biomass ($\mu\text{g C L}^{-1}$) in experiment 1 over time in mesocosms with mesozooplankton removed (Panel A) and not removed (Panel B). Values are means (\pm standard deviation, $n=2$) of the fertilization treatments (+N, +P, ambient). Lines are lognormal regressions fitted through individual mesocosm data over the entire time period.

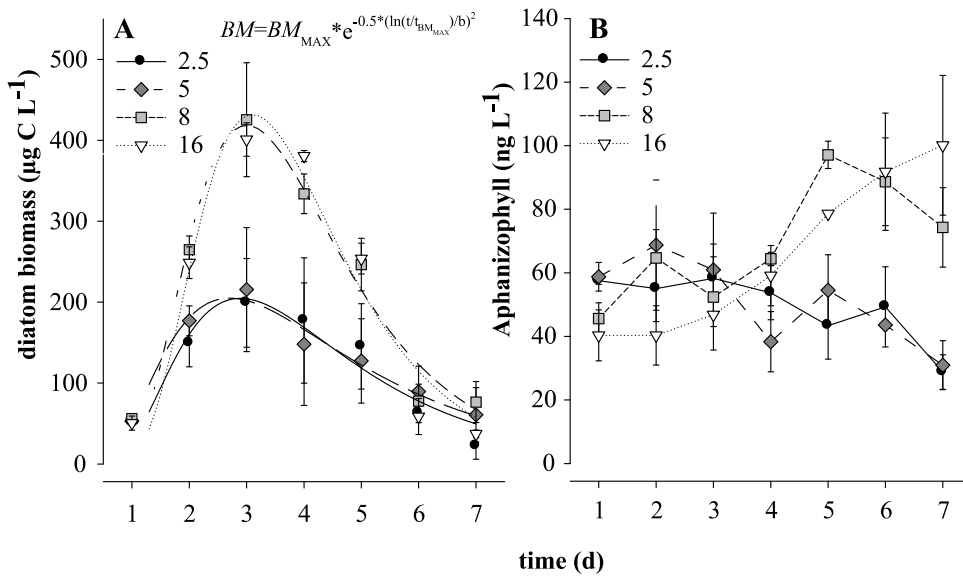


Figure I.6: Summed diatom biomass ($\mu\text{g C L}^{-1}$) in experiment 2 over time (Panel A) and Aphanizophyll concentration (ng L^{-1}) as determined by HPLC over time (Panel B). Values are treatment means (\pm standard deviation). Lines in Panel A are lognormal regressions fitted through individual mesocosm data over the entire time period. Values are treatment means (\pm standard error).

Cyanobacterial marker pigment

During the first three days of experiment 2, no significant differences in the amount of aphanizophyll between the different treatments could be detected (Fig. I.6 B). However, after day 3, two diverging trends in the distribution of the pigment were monitored in the “high N” and “low N” treatments. Initial DIN concentration had a significant impact ($p < 0.0001$) on the production of aphanizophyll (factorial ANOVA with N-level, P-level and time as factors), whereas neither initial P nor the interaction between the two were significant. Tukey’s HSD post-hoc comparison ($p < 0.01$) revealed a significant separation of the aphanizophyll concentration between the two N-levels on days 6 and 7. In the two “high N” treatments (16:1 and 8:1), aphanizophyll increased continuously up to maximum mean (\pm SE) concentration of 168.2(\pm 37.7) and 163.9(\pm 13.8) ng L⁻¹ in the 16:1 and 8:1 treatment, respectively. Only minor changes over time were detected in those tanks treated with initial “low N”, with final mean (\pm SE) values of 66.8(\pm 7.7) and 54.7(\pm 10.0) ng L⁻¹ in the 5:1 and 2.5:1 treatment, respectively.

Table I.2. Summary of maximum biomass and *p*-values of an ANOVA comparing biomass of individual taxa over the entire experiment 1.

Nutrient treatment	maximum biomass ($\mu\text{gC L}^{-1}$)						<i>p</i> -value			
	initial	ambient	+N	+P	ambient	+N	+P	time	zoo	nutrient
Nanoplankton										
<i>Prochlorococcus</i> -like	1.5	0.8	0.8	0.8	2.0	6.0	6.4	<0.001	0.041	0.699
mixed phototroph nanoplankton	16.1	164.9	193.8	198.1	193.7	256.9	239.0	<0.001	0.001	0.391
<i>Synechococcus</i> -like	0.0	2.8	2.3	2.1	3.9	5.5	6.2	<0.001	0.001	0.461
Ciliates										
<i>Laboea</i> sp.	6.0	3.0	7.5	6.9	2.1	7.7	3.0	<0.001	0.331	0.001
	0.1	1.2	4.9	3.6	1.2	4.1	6.0	<0.001	0.451	<0.001
	0.3	1.2	1.2	1.1	1.0	1.3	0.5	<0.001	<0.001	0.001
	0.4	1.2	5.0	1.0	0.4	0.7	1.5	<0.001	<0.001	<0.001
Dinoflagellates										
<i>Ceratium tripos</i>	1.1	0.3	5.3	0.7	0.7	5.1	1.8	<0.001	0.386	<0.001
<i>Ceratium furca</i>	14.8	4.5	19.8	6.8	6.2	19.3	8.5	<0.001	0.500	<0.001
<i>Dinophysis caudata</i>	7.9	35.6	199.4	24.9	12.3	137.7	17.6	<0.001	<0.001	<0.001
	0.3	0.5	2.0	0.6	0.6	0.7	0.4	0.016	<0.001	<0.001
	2.0	7.3	10.9	25.5	2.2	1.3	12.1	<0.001	<0.001	<0.001
<i>Protoperidinium depressum</i>	10.1	9.1	4.4	2.4	11.2	6.8	13.5	<0.001	0.009	0.142
<i>Protoperidinium</i> spp.	1.3	2.1	2.0	2.4	2.6	2.1	4.4	<0.001	0.034	<0.001
<i>Prorocentrum triestinum</i>	28.6	145.7	233.6	151.9	72.2	164.3	64.6	<0.001	<0.001	<0.001
Diatoms										
<i>Thalassiosira</i> sp.	2.3	4.6	7.1	3.2	1.3	3.6	16.9	0.161	0.902	0.180
<i>Thalassiosira subtilis</i>	0.0	19.2	33.8	37.5	8.4	11.9	24.6	<0.001	<0.001	<0.001
<i>Dactylosolen fragilissimum</i>	1.1	4.3	12.5	70.2	10.4	30.6	37.5	<0.001	0.023	<0.001
<i>Chaetoceros</i> spp.	0.1	3.9	64.9	3.7	2.5	36.4	2.3	<0.001	<0.001	<0.001
<i>Cerataulina pelagica</i>	1.1	3.6	5.8	5.8	12.5	7.4	4.5	0.977	0.165	0.924
<i>Thalassionema nitzschioides</i>	0.1	3.1	2.1	2.9	1.2	1.7	2.1	<0.001	0.023	0.935
<i>Nitzschia acicularis</i>	0.0	1.9	0.4	0.9	1.6	0.4	0.8	<0.001	0.036	<0.001
<i>Pseudonitzschia</i> sp.	0.1	166.4	195.2	114.8	151.0	175.9	146.4	<0.001	0.197	<0.001
other										
<i>Heterosigma</i> sp.	0.0	36.7	213.3	50.0	13.3	147.6	37.0	<0.001	<0.001	<0.001
<i>Dictyocha fibula</i>	2.2	12.5	72.8	31.1	20.5	39.6	20.5	<0.001	0.970	<0.001
<i>Carteria</i> sp.	8.8	36.1	213.0	29.2	18.1	147.4	25.2	<0.001	<0.001	<0.001
<i>Pyramimonas</i> sp.	1.6	7.1	15.5	12.6	4.2	11.9	10.6	<0.001	<0.001	<0.001

I: Changes of dissolved N:P influence phytoplankton composition (Pacific Mesocosm)

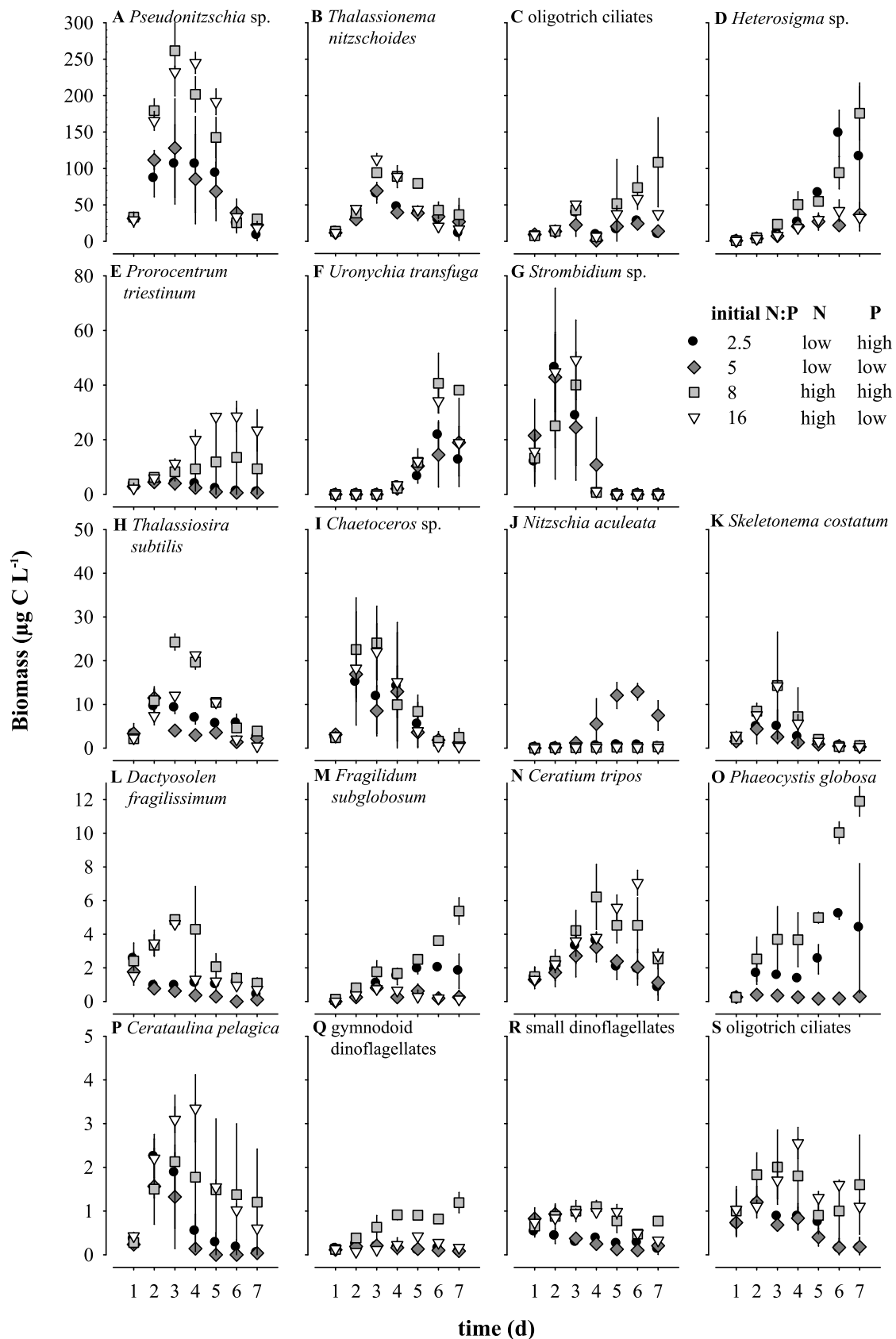


Figure I.7: Microplankton biomass ($\mu\text{g C L}^{-1}$) derived from microscopic counts in experiment 2. Diatoms: panels A, B, H, I, J, K, L and P; dinoflagellates (all mixotrophic): panels E, M, N, Q, R; ciliates: panels C, G, S; haptophytes: panel O; raphidophytes: panel D. Note different scaling on y-axis, with the taxa reaching the highest biomass in the top row, and lowest in the bottom row. Values are treatment means (\pm standard deviation).

Individual taxa

In experiment 1, there were taxon-specific differences in the response to nutrient treatments and presence of mesozooplankton. Table I.2 summarizes maximum biomasses of individual taxa as well as ANOVA significance levels of time (days), nutrient treatment (+N, +P, no addition) and zooplankton presence. Both zooplankton and nutrient supply significantly affected several microplankton species (Table I.2). The presence of zooplankton resulted in many (but not all) of the larger organisms reaching lower biomasses. For example, the dominant diatom group (*Pseudonitzschia* sp.) was not negatively affected by higher grazing pressure ($p=0.197$). In contrast, nanoplankton biomass was significantly ($p<0.001$) higher in the mesh-screened treatments, indicating a trophic cascade effect. Nutrient addition resulted in higher biomass in most groups, with N-addition having a larger impact than P-addition (compare Fig. I.5). The three dominant (biomass-based) dinoflagellate species (*Prorocentrum triestinum*, *Dinophysis caudata* and *Ceratium furca*) were all positively affected by N-addition, while P addition did not result in a biomass increase relative to the unamended control. Likewise, the two diatom groups contributing the largest proportion of biomass dominant diatoms (*Pseudonitzschia* sp. and *Chaetoceros* spp.) were positively affected by N ($p<0.001$), but not by P addition; however, in *Thalassiosira subtilis* and *Dactylosolen fragilissimum* the biomass response to P addition was significantly higher ($p<0.001$) than in the “ambient” treatment, while the two nutrient addition treatments (+N and +P) were not significantly different from each other.

Likewise, in experiment 2, the dinoflagellate *Prorocentrum triestinum* (Fig. I.7 E) and diatoms of the genus *Pseudonitzschia* (Fig. I.7 A) were favored by N-addition, while *Heterosigma* sp. (Fig. I.7 D) and *Phaeocystis globosa* (Fig. I.7 O) benefitted from increased P levels. The only species that reached significantly higher biomass in mesocosms with no nutrient addition was the diatom *Nitzschia aculeata* (Fig. I.7 J).

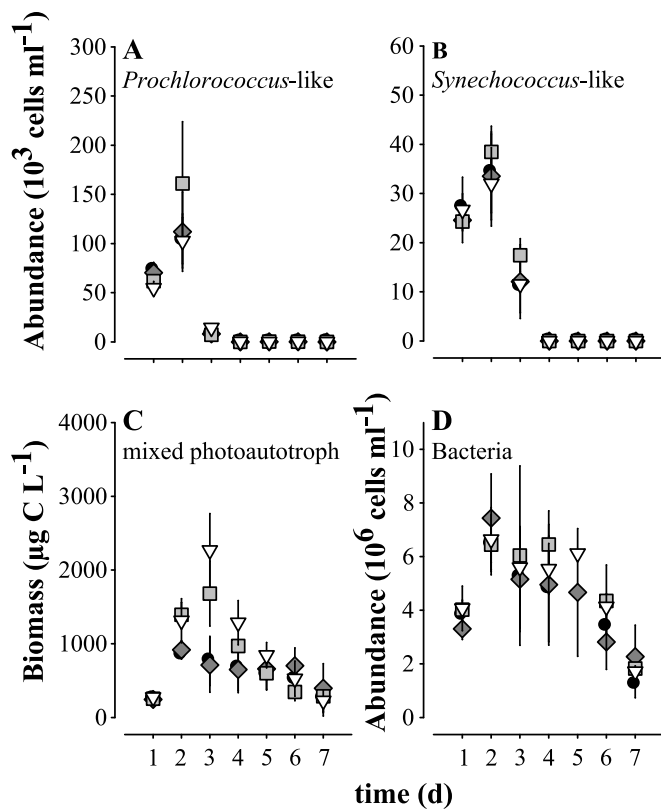


Figure I.8: Nanoplankton abundance (panels A and B, no. ml^{-1}) and biomass (panel C, $\mu\text{g C L}^{-1}$) and bacterial abundance (Panel D, cells ml^{-1}) over time as detected by flow cytometry. Labels as in Fig. I.7.

At the start of the experiment, a cluster with small ($<5 \mu\text{m}$) cells containing very little Chl-*a*, and phycoerythrin likely *Prochlorococcus* (Fig. I.8 A), and one of similar size with slightly more Chl-*a* and especially phycoerythrin, likely *Synechococcus* (Fig. I.8 B), were identified and initially increased in number, but disappeared after day 4, with no differences between treatments. As the forward scatter to size conversion is inaccurate for cells smaller than $5\mu\text{m}$, we were not able to convert their abundance data into biomass by measured cell sizes. However, assuming a cellular carbon content of 50 and $200 \text{ fg C cell}^{-1}$ for *Prochlorococcus*- and *Synechococcus*-like cells (Bertilsson et al. 2003) would result in a maximum biomass of approximately 8.0 and $7.6 \mu\text{g C L}^{-1}$, respectively. Mixed photoautotrophic nanoplankton comprised a considerable amount of the total calculated biomass (mean diameter $7.7 \mu\text{m}$, Fig. I.8 C), with a similar temporal development of biomass as the microplankton (estimated from microscopic counts), however exceeding its biomass. Again, a significant difference between the two N-levels, but not between P-levels, was detected ($p < 0.001$). The highest biomass was reached on day 3 with $2266(\pm 498)$ and $1680(\pm 441) \mu\text{g C L}^{-1}$ in the N:P=16 and N:P=8 treatments, respectively, and on day 2 with $916(\pm 126)$ and $847(\pm 33) \mu\text{g C L}^{-1}$ in the N:P=5 and N:P=2.5 treatments, respectively. Bacterial abundance developed in parallel with the phytoplankton bloom, reaching a maximum abundance on day 2 and declining afterwards (Fig. I.8 D). No treatment effects could be detected in bacterial abundance.

Fatty acid composition

No significant correlation between maximum diatom biomass and total lipid content or individual fatty acid components could be detected. Both EPA (20:5n-3) and DHA (22:6n-3) proportion decreased slightly in both experiments during the course of the experiments. EPA contributed a mean (\pm SD) proportion of 4.39(\pm 0.49) and 5.13(\pm 0.06)% of total FA at the start, and 2.47(\pm 0.6) and 4.23(\pm 2.14)% at the end of experiment 1 and 2, respectively, while DHA contributed a mean (\pm SD) proportion of 10.38(\pm 0.68) and 5.37(\pm 0.01)% of total FA at the start, and 4.89(\pm 0.78) and 5.15(\pm 1.74)% at the end of experiment 1 and 2, respectively. However, a significant correlation ($r=0.69$, $p<0.05$) existed between the relative amount of unsaturated fatty acids ($FA_{\text{unsat/sat}}$) and maximum diatom biomass (Fig. I.9).

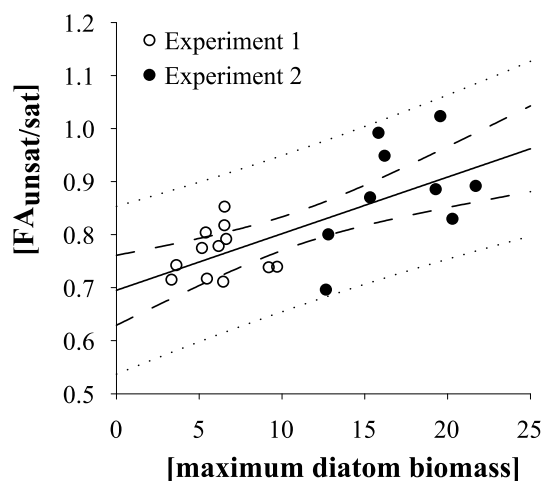


Figure I.9: Positive correlation ($r=0.69$, $p<0.05$) of the proportion of unsaturated fatty acids ($FA_{\text{unsat/sat}}$) at final day of the two experiments with the maximum diatom biomass during the experiment. Values are square-root transformed single mesocosm data. Dashed line indicates 95% confidence band, dotted line indicates 95% prediction band.

I.4 Discussion

The Peruvian upwelling system is characterized by strong spatial gradients in surface nutrient concentrations, both in absolute concentrations and relative to each other (Bruland et al. 2005; Franz et al. 2012), indicating that several macro- and micronutrients can potentially limit primary productivity. Particularly iron can limit phytoplankton growth (Hutchins et al. 2002), while silicate limitation of diatoms becomes more crucial further offshore (Franz et al. 2012). However, under low O_2 conditions on the shelf, the high solubility of iron supplies high concentrations of Fe(II) to surface waters along with P (Bruland et al. 2005), rendering N the macronutrient in shortest supply if OMZs are expanding. Phytoplankton counts revealed a considerable effect of nutrient availability on the community structure of the primary producers, and N addition significantly increased the total biomass of protists (Figs. I.5 and I.6), indicating an overall N-limitation of the system. Under N-repletion, diatom biomass doubled and biomass

of autotrophic dinoflagellates increased up to 4-fold compared to the treatments with relatively low concentrations of N, implying that an increasing N-deficit in the O₂-deficient waters of the eastern South Pacific can induce a shift in the taxa dominating the phytoplankton community at the expense of diatoms and dinoflagellates. Given the response of bulk diatom biomass, it becomes evident that biomass production at the primary producer level depends solely on the supply of inorganic N. This is surprising, as we expected at least a modulation of the response by P availability. Diatoms are frequently characterized as “bloomers” (Klausmeier et al. 2004; Arrigo 2005) that keep a high-rRNA growth machinery adapted to rapid exponential growth and, thus, display low N:P requirements (Loladze & Elser 2011) and are able to efficiently utilize excess P. Mills & Arrigo (2010) employed a dynamic ecosystem model to explore the relationship between nutrient uptake ratios of phytoplankton and marine N₂-fixation. They suggested that by non-Redfield uptake stoichiometry, fast-growing phytoplankton (i.e. diatoms) in upwelling areas utilize excess P and therefore ultimately control new nitrogen flux by N₂-fixation into the ocean, as then excess P would not be available to diazotrophs further offshore. However, the plasticity of uptake stoichiometry (i.e., N:P<Redfield, Fig. I.4) indicates that it is impossible to classify growth modes and uptake ratios of certain functional types of phytoplankton without taking into account that both growth and uptake ratio strongly depend on the limiting nutrient. This is partly reflected in the particulate matter (POM) pool (Franz, unpublished data), but also linked to higher release of dissolved organic phosphate (DOP; Franz, unpublished data). The partitioning of phytoplankton-derived organic matter between its dissolved and particulate fractions as a response to changes in nutrient supply has also been described by Conan et al. (2007). Hence, we cannot conclude that the observed uptake ratios described in the present study are directly translated to phytoplankton or POM.

Wetz & Wheeler (2003) observed complete depletion of NO₃⁻ by diatoms within three to five days, while SiO and PO₄³⁻ were still available, in deck incubation experiments off Oregon where deep water was seeded with a surface inoculum. Interestingly, the N:P uptake ratio before N depletion ranged from 13 to 15.6 in their study. N:P uptake ratios observed in yet another eastern boundary current system, the Benguela current, in microcosm incubations conducted by Pitcher et al. (1993) ranged from 13.5 to 19.8. Hence, it can be concluded that uptake ratios of diatom-dominated phytoplankton assemblages in upwelling areas are not necessarily low in N:P as suggested by Mills & Arrigo (2010); rather, the observed uptake ratios are directly related to supply. This can also be seen from the relative uptake velocity (estimated as “half consumption times” in our study) for the limiting and unlimiting nutrient, respectively. The ability of blooming diatoms to immediately utilize DIN and to outcompete smaller size fractions of

phytoplankton has recently been demonstrated in a simulated upwelling mesocosm experiment in Monterey Bay by Fawcett & Ward (2011). If the immediate growth response of fast-growing large diatoms to such upwelling events is directly related to the vertical supply of dissolved inorganic nitrogen across into the photic zone, this might further intensify this imbalanced nutrient budget in the Peruvian upwelling.

While Fawcett & Ward (2011) observed a succession of diatom species from “ubiquitous” *Pseudonitzschia* spp.-dominated to “upwelling” *Chaetoceros* spp.-dominated assemblages, we found quite the contrary: *Pseudonitzschia* spp. contributed substantially to the total developing biomass, which in parts may be due to their protection against grazing. It has to be noted that some species within the genus *Pseudonitzschia* are known to produce the neurotoxin domoic acid, although it is questionable whether this is harmful to copepods (Lincoln et al. 2001). As can be seen from results in Experiment 1, presence of mesozooplankton did not significantly influence biomass development in *Pseudonitzschia* spp. Their relative proportion of microplankton biomass thus increased when grazing pressure on other algal groups was increased in the unscreened treatments (Table I.2). However, since *Pseudonitzschia* numbers decreased after depletion of nutrients in both experiments, they apparently are consumed by microzooplankton. Their dominance might therefore also be caused by allelopathic effects that negatively affect the growth of other microalgae (Granéli & Hansen 2006). Further, *Pseudonitzschia pseudodelicatissima* has been reported to grow particularly well following high ammonium concentrations (Seeyave et al. 2009), making it a good competitor in both upwelling and post-upwelling conditions. In the California Current, *Pseudonitzschia* was found to be associated with the beginning or end of strong upwelling periods, when nutrients are elevated but declining (Kudela et al. 2002).

In our experiment, *Phaeocystis globosa* (although never dominating algal biomass) was clearly profiting from P addition. This is in line with a study by Riegman et al. (1992) in the southern North Sea, who observed a positive effect of decreasing dissolved N:P in riverine discharge on biomass development of *P. globosa*. The authors hypothesized that *P. globosa* is a good competitor under N-limitation and tested this hypothesis in laboratory competition experiments. They found that *P. globosa*, while being outcompeted at high N:P by the coccolithophore *Emiliana huxleyi* and the diatom *Chaetoceros socialis*, quickly became the dominant species under N limitation (N:P=1.5). Interestingly, *P. globosa* growth was also found to be enhanced under increased Fe supply in the eastern tropical South Pacific (Hutchins et al. 2002); it may thus be one of the “winners” of elevated P/Fe and low N conditions on the shelf under ocean deoxygenation. *P. globosa* is thought to be of comparably low nutritional value to zooplankton

consumers, as experimental studies using calanoid copepods and a monospecific diet of *Phaeocystis* resulted in low egg production rates (Tang et al. 2001; Turner et al. 2002). However, since adult survivorship and egg hatching success were high throughout these feeding experiments, the authors conclude that the low food quality is due to the lack of essential constituents rather than the content of chemical compounds that act as mitotic inhibitors (Turner et al. 2002). Moreover, its fatty acid composition was determined to be low in n3 PUFAs (Tang et al. 2001).

Within the biochemical make-up of primary producers, the fatty acid composition is recognized as one of the key factors of food quality. To metazoan consumers, particularly long-chained polyunsaturated fatty acids (PUFAs), such as eicosapentaenoic acid (EPA; 20:5n-3) and docosahexaenoic acid (DHA; 22:6n-3) are considered essential, as they usually cannot be synthesized *de novo* and thus have to be ingested in adequate amounts. In natural food webs, these components influence the growth and reproduction of zooplankton as well as trophic transfer efficiency (Kainz et al. 2004). Although a persistent effect on the bulk fatty acid composition could be detected at the end of the experiments (Fig. I.9), no differences were found in the relative amounts of essential PUFAs such as EPA and DHA. Although the relative contribution of these components decreased during the experiments, they still contributed substantially to total lipids. It is therefore unlikely that consumers will be limited by PUFAs as a consequence of nitrogen-limited diatom growth in this assemblage. It has to be noted that the fatty acid analysis took place at the termination of the experiment, when a large proportion of the primary producers' biomass constituting the peak bloom was transferred to protozoan grazers such as various ciliates (Fig. I.7 C) and mixotroph dinoflagellates such as *Fragilidium subglobosum* (see Fig. I.7 M). For copepods, it has been demonstrated that protozoans contribute relatively more to the diet in oligotrophic ocean regions or under post-bloom conditions when phytoplankton concentrations are low (Calbet & Saiz 2005). While it is generally accepted that marine ciliates contribute to the availability of phytoplankton biomass to mesozooplankton by repackaging of cells that are too small to be consumed directly (Sherr & Sherr 1999), they are considered incapable of synthesizing PUFAs beneficial to higher trophic levels, a process dubbed "trophic upgrading" (Klein Breteler et al. 1999).

While nitrogen fixing cyanobacteria may be able to partially compensate the lack of available nitrogen, this appears to happen in a distinct succession rather than a direct response to P availability. Several studies in limnetic (Smith 1983; Vrede et al. 2009), brackish (Niemi 1979) and marine (Michaels et al. 1996) environments have reported on cyanobacterial blooms triggered by low inorganic N:P stoichiometry. Analysis of the pigment inventory by HPLC

revealed that the photosynthetic accessory pigment aphanizophyll increased considerably after the complete depletion of both inorganic N and P after the diatom bloom in those tanks that received high initial N load (Fig. I.6 B). This xanthophyll is solely produced by cyanobacterial phytoplankton (Hertzberg & Jensen 1966), but not by all cyanobacterial genera. It is even regarded indicative of N-fixing cyanobacteria (Hall et al. 1999) in freshwater systems, which is supported by the negative correlation between $\delta^{15}\text{N}$ in particulate organic matter (low $\delta^{15}\text{N}$ characterizes atmospheric fixed N) and the concentration of aphanizophyll in lakes (Patoine et al. 2006). Nevertheless, since aphanizophyll has also been detected in *Microcystis aeruginosa* (Soma et al. 1993), a freshwater species which lacks the ability to fix dinitrogen, its detection might not necessarily imply the abundance of diazotrophic cyanobacteria. However, up to now there is no marine non-diazotroph cyanobacterium known to synthesize aphanizophyll. The widely abundant oceanic non-diazotrophs picoautotrophs *Prochlorococcus* and *Synechococcus* lack this pigment. No filamentous cyanobacteria such as *Trichodesmium* were detected by microscopic inspection, which is not surprising as they are not recorded in the nutrient-rich waters of the Peruvian Shelf. In general, *Trichodesmium* is encountered in oligotrophic waters with sea surface temperatures $>20^\circ\text{C}$ (Breithbarth et al. 2007). However, in contrast to filamentous species that often reach lengths of $200\mu\text{m}$ and form dense colonies, unicellular diazotrophic cyanobacteria with sizes of approximately $1\text{-}8\mu\text{m}$ cannot be identified using light microscopy, neither could they be distinguished from other photoautotrophs by flow cytometry. Only little is known about the pigment composition of N-fixing cyanobacteria such as the lately found “Group A” (Zehr et al. 2001) or diatom-diazotroph associations (DDAs) such as the endosymbiotic *Richelia intracellularis*. According to Řezanka & Dembitsky (2006), pigments from *Richelia* have not yet been isolated. However, their phylogeny (order Nostocales, family Nostocaceae) could indicate that they might be able to synthesize this pigment. DDAs have been found to substantially contribute to the diazotroph community in subtropical and tropical waters. Their occurrence has been reported from ocean areas as different as the Amazon River plume (Foster et al. 2007), the eastern tropical Atlantic (Foster et al. 2009), the southwest Indian Ocean (Poulton et al. 2009) and the southern California Current (Kimor et al. 1978). Since we did not assess N_2 -fixation rates in this study, and could not concomitantly detect other diazotroph carotenoids such as myxoxanthophyll, we cannot conclude whether the cyanobacteria present in the experiment were diazotrophic. Furthermore, even if diazotrophs were present in our experiment, N_2 -fixation might be down-regulated due to preferential uptake of DIN (Holl & Montoya 2005). Further studies to investigate this succession pattern are recommended,

preferably applying molecular techniques and N₂-fixation rate assays, as it might be an important driver of the onshore-offshore differences in dominating algal functional groups.

I.5 Acknowledgements

We would like to thank the crew of R/V *Meteor* for excellent support, Peter Fritsche for on-board nutrient measurements, and Thomas Hansen and Arne Malzahn for help in the lab. We thank Dr. Rainer Kiko and two anonymous reviewers for critically commenting on an earlier version of the manuscript. This work is a contribution of the DFG-supported project SFB754 (www.sfb754.de).

Chapter II

Impact of changes in dissolved N:P on phytoplankton biomass and its functional and elemental composition and resulting effects on zooplankton in the Eastern Tropical North Atlantic

Helena M. Hauss, Jasmin Franz and Ulrich Sommer

Abstract

To explore effects of changes in nitrogen and phosphorus supply on the pelagic community of the Eastern Tropical North Atlantic, we conducted a shipboard nutrient manipulation experiment off the Senegalese coast using the natural surface plankton assemblage in October 2010. Experimental units were twelve 150L mesocosm bags, adjusted to four N:P ratios ranging from 2.8 to 16, with initial addition of either high N/low P (16), low N/high P (2.8), high N/ high P (8) or low N/low P (5.5), where high and low N concentrations were 12 and 4.14 $\mu\text{mol L}^{-1}$, and high and low P concentrations were 1.5 and 0.75 $\mu\text{mol L}^{-1}$. The developing community was observed over a time period of 11 days. The developing primary bloom peaked already two days after the start of the experiment and was significantly higher in the two treatments that received N addition. No effect of P addition on total biomass could be detected. After the collapse of the primary bloom, a secondary bloom developed, again with higher primary producer standing stocks in the N-fertilized treatments. Bacterial abundance was likewise higher in the “high N” treatments, apparently dependent on phytoplankton biomass. Composition of particulate matter (PON:POP) responded to the respective fertilization ratios, and in turn affected the $\text{NH}_4^+/\text{PO}_4^{3-}$ excretion ratio of a herbivorous copepod, *Undinula vulgaris*, incubated for three days using the respective mesocosm community as food medium. The mesozooplankton community within the mesocosms was dominated by the cladoceran *Penilia avirostris*, but also comprised small calanoid copepods such as *Temora* sp., *Centropages* sp. and unidentified calanoid copepodite stages as well as cyclopoid (*Oithona* sp. and *Oncaea* sp.) and harpacticoid (*Macrosetella* sp. and *Miracia* sp.) species. The final abundance of the respective species was influenced by the initial N:P treatment, with *P. avirostris* abundance increasing with initial N:P, while the cyclopoid and harpacticoid copepods were most numerous in those mesocosms receiving no nutrient addition. Calanoid abundance tended to be negatively affected by the addition of P, however differences were not significant due to high variability among replicates.

II.1 Introduction

The Eastern Tropical North Atlantic (ETNA) is an area with sharp horizontal gradients in vertical diffusivity of macronutrients. While the upwelling off the north-western African coasts fuels highly productive areas, together forming the large marine ecosystem of the Canary current, the majority of the offshore ocean tends to be highly stratified and very oligotrophic, except where bathymetric features and eddy formation (often spin-offs of the coastal upwelling) contribute to an increased vertical flux such as off Cape Verde and in the Guinea Dome area. Of all ocean basins, the North Atlantic receives the highest input of Aeolian dust originating from the Sahara desert, providing pulsed input of both bioavailable trace elements (most importantly iron) and macronutrients such as inorganic N and P. In the oligotrophic open ocean, and especially in the western part of the basin, both dissolved and particulate N:P tend to be very high due to atmospheric N₂-fixation by diazotrophic cyanobacterial, leading to “excess N” relative to Redfield conditions at depth (~150-400 m) below the photic zone (Gruber & Sarmiento 1997; Hansell et al. 2004). In a model that allocated N and P resources to either assembly (e.g. nucleic acids, high P) or resource acquisition (e.g. pigment, high N), Klausmeier et al. (2004) predicted optimal N:P stoichiometry of phytoplankton in the oligotrophic ocean to range between 35 and 45, implying that phytoplankton communities tend to be nitrogen limited even when the deep-water supply is higher than 16, which is in line with observations on the picophytoplankton taxa characteristic for these regions such as *Prochlorococcus* and *Synechococcus* (Davey et al. 2008).

In the eastern part of the basin, however, N:P in the euphotic zone is largely below the canonical Redfield ratio, and the vertical distribution of nitrate and phosphate, with the phosphocline being both shallower and thicker than the nitracline, suggests overall N-limitation of phytoplankton productivity (see chapter IV). This is remarkable, as the eastern margin of the ocean receives the highest dust input with quite high inorganic N:P (Formenti et al. 2003) and Fe, and the filamentous cyanobacterium *Trichodesmium* is frequently present in the nutrient-depleted surface waters even far east (Tyrell et al. 2003), up to the African continental shelf (Margalef 1973; Vallespinós 1985). Apart from *Trichodesmium*, unicellular cyanobacteria (Großkopf et al. submitted) and diatom-diazotroph associations (DDAs) contribute diazotrophically fixed N to the surface ocean (Foster et al. 2009). These two sources (dust, N₂-fixation) of inorganic bioavailable nitrogen do not seem to be balanced by loss processes: The oxygen concentrations in the ETNA oxygen minimum zone (OMZ) are not sufficiently low to trigger large-scale water column N loss via denitrification and anammox; however, some evidence for benthic anammox has recently been documented (Jaeschke et al. 2010). As the extent of the oxygen minimum zone

in the ETNA was observed to increase (Stramma et al. 2008), these N loss processes may gain momentum in the future. Changes in N:P stoichiometry of dissolved nutrient flux to the photic zone potentially impact the taxonomic and elemental composition, in turn affecting the trophic transfer to consumers. In the marine environment, both the limitation of zooplankton growth by elemental imbalances of their prey and the influence of changes in zooplankton N:P regeneration remain controversial. Hessen (1992) proposed that both freshwater and marine copepod growth could be limited by low prey N content. The common perception is that marine copepods are limited by C (i.e., food quantity), owing to the low food C:N ratios of the surface ocean (Anderson & Hessen 1995), and that food quality effects, if observed, are rather due to biochemical compounds such as essential amino acids or fatty acids. Likewise, the comparably high N cell quotas in marine phytoplankton (as opposed to very low P cell quotas in P-limited freshwater systems) suggest that the impact of marine zooplankton on nutrient recycling might be lower.

To some extent, mesozooplankton may be able to remove bioavailable nitrogen from surface waters when N:P of particulate matter is lower than their requirements for growth, because they then preferentially retain N relative to P, lowering their excretion ratio in surface waters. This effect has been observed in the Gulf of Guinea by LeBorgne (1982a). The underlying mechanisms for N:P homeostasis in marine copepods are largely unexplored compared to copepods and cladocerans in freshwater ecosystems (Sterner & Elser 2002). In a laboratory study with the copepod *Acartia tonsa*, Liu et al. (2006) found that the P assimilation efficiency of copepods fed on diatoms with different P cell quotas remained unchanged, while their P excretion rate was higher when feeding on algae with higher P cell quotas. However, this study did not address nitrogen excretion or retention, so the relative role of both remained unclear. In the same species, Saba et al. (2009) observed a significant change in N:P excretion ratio among copepod groups fed different diets (either heterotrophic dinoflagellates, or phototrophic diatoms, or a mix of both), which was due to changes in both N and P excretion. The P content (and thus PON:POP) of the food cultures was not determined. To the best of our knowledge, the influence of different food PON:POP in a natural phytoplankton community manipulated with different N:P supply ratio on zooplankton excretion has not been investigated in the marine environment yet.

A single-pulse nutrient addition experiment conducted in the present study resembles a simulation of an upwelling event. Following the characteristic succession of phytoplankton functional groups in such experiments can therefore help to explain their spatial distribution patterns, both in respect to the vertically stratified water column and in the shelf-slope-open

ocean regions adjacent to eastern boundary current systems. At the same time, we aimed to investigate whether the nutrient-manipulated phytoplankton assemblage influences the food quality in terms of fatty acid composition of particulate matter, the resulting abundance of different zooplankton groups, the nutritional condition of copepods after several days of feeding as well as their N:P excretion ratio.

II.2 Materials and Methods

Experimental Setup

An 11-day mesocosm experiment was conducted on a cruise with R/V *Meteor* in October/November 2010 in which the natural plankton community was manipulated by an initial fertilization to four target inorganic N:P ratios ranging from 2.8:1 to 16:1. Mesocosm bags (150 L volume) were floating in gimbals mounted flow-through water baths. For a detailed description of the setup see chapter I.2. The initial filling station was located at 15°0.01'N, 017°45.0'W and characterised by a SST of 27.6°C with a shallow pycnocline (25 m) and low surface nutrient concentrations, with 0.3, 0.1 and 1.4 $\mu\text{mol L}^{-1}$ DIN, DIP and SiO, respectively. For the filling, a deck-based peristaltic pump (intake hose submerged to approximately 5 m depth) was used to minimize damage to fragile plankton. The mesocosms were shaded by white plastic lids to approximately 50% of surface irradiation (mean 560 $\mu\text{E m}^{-2} \text{s}^{-1}$, range 100-1000 $\mu\text{E m}^{-2} \text{s}^{-1}$, depending on cloud cover) and the average temperature was 29.96°C (ranging from 28.9 to max. 31°C) which is approximately 2°C warmer than the *in situ* conditions at the filling station (see above). Sampling was conducted on a daily basis for dissolved inorganic nutrients, chlorophyll-*a*, particulate and dissolved organic matter as well as for phytoplankton community analyses.

Sampling and analyses: Phytoplankton/POM

For the determination of chl-*a*, 0.25 to 1 L samples (depending on the concentration) were filtered onto 0.2- μm GF/F filters (Whatman) and extracted using acetone, frozen at -80°C for >5 h and measured against a blank in a Turner fluorometer calibrated with a chl-*a* standard (Sigma C5753) dilution series. For microplankton counts, 100 ml samples were lugol-fixed, while flow cytometry samples for the nanoplankton fraction were fixed using 2% formaldehyde

and immediately frozen at -80°C until analysis. Nano-phytoplankton abundance was measured using a flow cytometer (FACScalibur, Becton Dickinson, San Jose, CA, USA) at a flow rate of $50.6\ \mu\text{l}\ \text{min}^{-1}$. Cells were distinguished by size (forward scatter) and fluorescence of chlorophyll-*a*, phycoerythrin, and allophycocyanin. Biovolume was estimated based on the FSC calibration assuming spherical shapes. For bacterial abundance, samples were diluted 1:3, stained with SYBR-Green and counted at lower flow rate ($13.9\ \mu\text{l}\ \text{min}^{-1}$).

Samples for analysis of phytoplankton pigments by High Pressure Liquid Chromatography (HPLC) were vacuum-filtered (150 mbar) onto Whatman GF/F filters (25 mm) and immediately stored at -20°C until analysis. Filters were homogenized for 5 min with 2 mm and 4 mm glass beads and 2 ml acetone (90%). The supernatant was filtered through a $0.2\text{-}\mu\text{m}$ teflon filter and stored at -80°C . The HPLC measurement was conducted by a Waters 600 controller in combination with a Waters 996 photodiode array detector (PDA) and a Waters 717plus auto sampler (modified after Barlow et al. 1997). Classification and quantification of the various phytoplankton pigments was accomplished with the software EMPOWERS (Waters).

On days 0 (duplicate initial sample), 3 and 8 (one sample per mesocosm), samples were prepared for bulk seston fatty acid (FA) analysis by filtering 0.5 L on a precombusted GF/F filter ($0.2\ \mu\text{m}$) and frozen at -80°C . Lipids were extracted over night using 3 ml of a solvent mixture (dichloromethane:methanol:chloroform in 1:1:1 volume ratios). A five component fatty acid methyl ester (FAME) Mix (Restek, Bad Homburg, Germany; $c=8.5\ \text{ng}\ \text{component}^{-1}\ \mu\text{l}^{-1}$) was added as an internal standard, and a 23:0 FA standard ($c=25.1\ \text{ng}\ \mu\text{l}^{-1}$) was used as an esterification efficiency control (usually 80-85%). Water-soluble fractions were removed by washing with 2.25 ml of KCl solution ($c=1\ \text{mol}\ \text{L}^{-1}$), and the remainder dried by addition of NaSO_4 . The solvent was evaporated to dryness in a rotaryfilm evaporator (100-150 mbar), redissolved in chloroform and transferred into a glass cocoon. Again, the solvent was evaporated to dryness (10-30 mbar), and esterification was performed overnight at 50°C using $200\ \mu\text{l}$ 1% H_2SO_4 (in CH_3OH) and $100\ \mu\text{l}$ toluene. Unfortunately, three samples were lost during this process due to cocoon leakage, so that no replicate measurements were available for N:P=16, day 3 and N:P=5.5, day 8. Phases were split by adding $300\ \mu\text{l}$ 5% sodium chloride solution, and FAMES were separated using *n*-Hexane, transferred into a new cocoon, evaporated, and $100\ \mu\text{l}$ added (final volume). All solvents used were gas chromatography (GC) grade. FAMES were analyzed in $1\text{-}\mu\text{l}$ aliquots injected in a Thermo Fisher Trace GC Ultra equipped with a nonpolar column (Thermo Fisher TRACE™ TR-FAME, $10\ \text{m} \times 0.1\ \text{mm} \times 0.2\ \mu\text{m}$) and a flame ionization detector (FID, base temperature 260°C) with helium as a carrier gas at a constant flow of $0.8\ \text{ml}\ \text{min}^{-1}$. The column oven was initially set to 50°C , and heated at a $30^{\circ}\text{C}\ \text{min}^{-1}$ increase to

120°C, at 3° C min⁻¹ to 165°C, at 10° C min⁻¹ to 180°C and at 30°C min⁻¹ to 220°C, which was held for 2 min. The system was calibrated with a 37-component FAME-mix (Supelco, Germany) and chromatograms were analysed using Thermo Chrom-Card Trace-Focus GC software.

Sampling and analyses: Zooplankton

On day 11 of the mesocosm experiment, a 20 L subsample of each mesocosm was sieved through a 100-µm mesh and fixed in 4% borax-buffered formaldehyde seawater solution. These samples were enumerated under a dissecting microscope. Crustacean zooplankton was identified to genus level, and copepods were divided into adult and copepodite stages.

Two satellite feeding experiments were conducted using the calanoid copepod *Undinula vulgaris*, a large omnivorous copepod that is widely abundant in the epipelagic zone of the ETNA. Adult females were sorted from vertical hauls (ca. 0.2 m s⁻¹ heave speed) from 50 m to the surface with a 150-µm WP-2 net equipped with a solid cod end. Three individuals were placed in a 500-ml Kautex bottle filled with algal suspension from the mesocosms (one bottle per mesocosm), which was exchanged daily. Time period of incubation was from days 3 to 5 and 8 to 10 in trial 1 and 2, respectively. Upon termination of trial 2, females were transferred into bottles containing 0.2-µm filtered seawater, with two blank bottles without copepods. After 75min of incubation, samples were taken for analysis of excretion products. Dissolved ammonium and phosphate were immediately analysed on board using a four-channel Quattro autoanalyzer with an external fluorometer (Jasco FP-2020 excitation: 370 nm, emission: 460 nm) for NH₄⁺ analysis (K erouel et al. 1997). Standard deviations for NH₄⁺ and PO₄³⁻ were 0.03 and 0.01 µmol L⁻¹, respectively, and detection limits were 0.01 and 0.01 µmol L⁻¹, respectively. Copepods were then individually transferred into 1.5-ml cap vials and immediately frozen at -80°C, and their RNA-DNA ratio as an indicator of nutritional condition was analysed in the laboratory ashore. Samples were freeze-dried for >16 h, their dry weight determined, and concentrations of RNA and DNA measured fluorometrically according to Malzahn et al. (2007), with ethidium bromide as fluorophore and digesting RNA with Ribonuclease A (bovine pancreas, Serva 34388). Nucleic acid standards were Bacteriophage λ-DNA (Roche 745782) and Ribosomal 16s, 23s RNA (E.coli, Roche 206936). To ensure consistency over time, two control samples (from a pooled stock homogenate) were measured within each 96-well microplate.

Statistical analysis

To be able to compare initial nutrient drawdown dynamics across treatments, three-parameter logistic regressions were fitted through the nutrient concentration $[N]$ data over time t , where t_{50} is the time period after which 50% of the initially available nutrient is taken up:

$$(II.1) \quad [N] = \frac{a}{1 + \left(\frac{t}{t_{50}}\right)^b}$$

In those cases where a detectable, low concentration remained (this was the case for silicate), a four-parameter regression was used:

$$(II.2) \quad [N] = y_0 + \frac{a}{1 + \left(\frac{t}{t_{50}}\right)^b}$$

A factorial ANOVA with time, initial N level and P level as factors was used to explore differences in the biomass response of phytoplankton types distinguished by flow cytometry, bacterial abundance, chlorophyll-*a*, POC, fatty acids (FA), and PON:POP. Cytometry counts were log-transformed and proportions of individual FAs were arcsine-transformed to approximate normality. A principal component analysis (PCA) based on correlations was used to explore changes in the FA composition of particulate matter over time and treatments. Because the final zooplankton abundance and pigment data failed to fulfill assumptions on normality and homogeneity of variances, a nonparametric comparison (Mann-Whitney *U* Test) was used to explore differences between high and low initial DIN and DIP supply, respectively.

II.3 Results

Dissolved nutrients

In all experimental treatments, inorganic nutrient pools were rapidly exhausted after an initial period of 1-2 days (Fig. II.1). The mean half consumption time t_{50} was influenced by the absolute N concentration. For DIN, drawdown was decelerated in those mesocosms receiving N addition, with t_{50} values (\pm SE) being 1.08(\pm 0.26), 1.08(\pm 0.22), 1.63(\pm 0.06) and 1.72(\pm) days in the N:P 2.8, 5.5, 8 and 16 treatment, respectively, with the two former ones being those receiving no N addition (Fig. II.1, panel A). For DIP and SiO, drawdown was faster in “high N” conditions. For

DIP, t_{50} were 3.24(\pm 0.33), 3.25(\pm 0.26), 1.88(\pm 0.15) and 1.48(\pm 0.09) days in the N:P 2.8, 5.5, 8 and 16 treatment, respectively (Fig. II.1, panel B). For SiO, t_{50} were 3.43(\pm 0.25), 3.90(\pm 0.39), 2.22(\pm 0.11) and 2.28(\pm 0.07) days in the N:P 2.8, 5.5, 8 and 16 treatment, respectively.

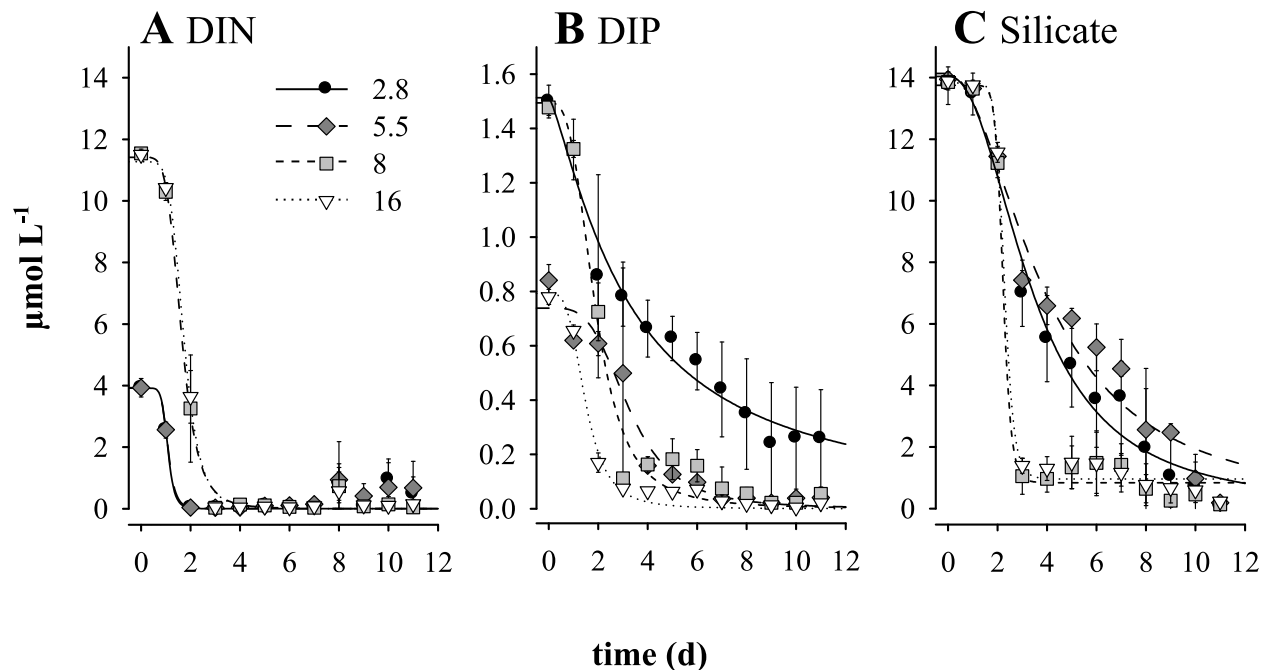


Figure II.1: Dissolved inorganic macronutrient concentrations ($\mu\text{mol L}^{-1}$) over time in the four N:P treatments. Panel A: total inorganic nitrogen DIN ($\text{NO}_3^- + \text{NO}_2^- + \text{NH}_4^+$), Panel B: dissolved inorganic phosphorus DIP, C: silicate SiO. Values are treatment means (\pm SD). Lines are fitted logistic regressions.

Phytoplankton biomass

Temporal development of chlorophyll-*a*, monitored during the experiment on board, revealed an immediate phytoplankton bloom response, with maximum values recorded in all treatments on day 2 (Fig. II.2, panel A). However, those treatments with N addition reached approximately twice the chl-*a* concentration of the two treatments without N addition, with a mean (\pm SD) of 9.0(\pm 1.0) and 9.0(\pm 1.7) $\mu\text{g L}^{-1}$ in the N:P= 16 and 8 treatments, respectively, and 4.7(\pm 0.4) $\mu\text{g L}^{-1}$ in both the N:P=2.8 and 5.5 treatment. This primary bloom declined rapidly until a minimum was reached on day 4. In the developing secondary bloom (with a peak on day 9), variability among replicates increased. However, only time and initial N level as well as their interaction were statistically significant ($p < 0.001$) factors in the ANOVA.

The bulk POC development generally confirms the chl-*a* patterns (Fig. II.2, panel B), but lacks the drop on day 4. Again, only time and initial N level as well as their interaction were

significantly ($p < 0.001$) impacting POC. The two “high N” and “low N” treatments are significantly ($p < 0.001$) different from each other and develop in parallel, with the former being approximately 30-50% higher than the latter. Likewise, phytoplankton biomass estimated from flow cytometry counts revealed the same pattern with a primary and secondary bloom and significant differences between N levels and time ($p < 0.001$), but the peak abundance occurred one day later in comparison to the chl-*a* fluorescence peak (Fig. II.2, panel C). In contrast, the PON:POP ratio was influenced by the N:P fertilization ratio. In the factorial ANOVA, both initial N and P levels (besides time) are significant ($p < 0.001$), as well as the interaction between the two. The PON:POP ratio began to separate between the different treatments after entering nutrient limitation on day 2 (Fig. II.2, panel D). From day 3 until termination of the experiment, mean (\pm SD) PON:POP values were 8.76(\pm 1.42), 11.65(\pm 1.77), 11.16(\pm 1.61) and 16.08(\pm 1.65) in the N:P=2.5, 5.5, 8 and 16 treatment, respectively. When assessing PON:POP in a factorial ANOVA with time and the four treatment levels as factors, the two intermediate treatments with N:P=5.5 and 8 were not significantly different from each other (Tukey’s HSD, $p=0.98$), while PON:POP in the 2.5 treatment was significantly lower and in the 16 treatment significantly higher (Tukey’s HSD, $p < 0.005$) than in the remaining three N:P treatments.

The initial microplankton community included *Trichodesmium* filaments, diatoms (*Rhizosolenia* sp., *Chaetoceros* spp., *Pseudonitzschia* spp., *Odontella sinensis*, *Hemiaulus* sp., *Leptocylindrus* sp.), heterotrophic and autotrophic dinoflagellates (*Prorocentrum triestinum*, *Heterocapsa* sp., *Protoperidinium* spp., *Ceratium* spp.), and ciliates. The immediate biomass response, however, was mainly due to nanoplanktonic autotrophs ($< 64 \mu\text{m}$); cell numbers peaked one day after the chl-*a*. Both time and N-level were significant predictors of nanophytoplankton biomass ($p < 0.0001$).

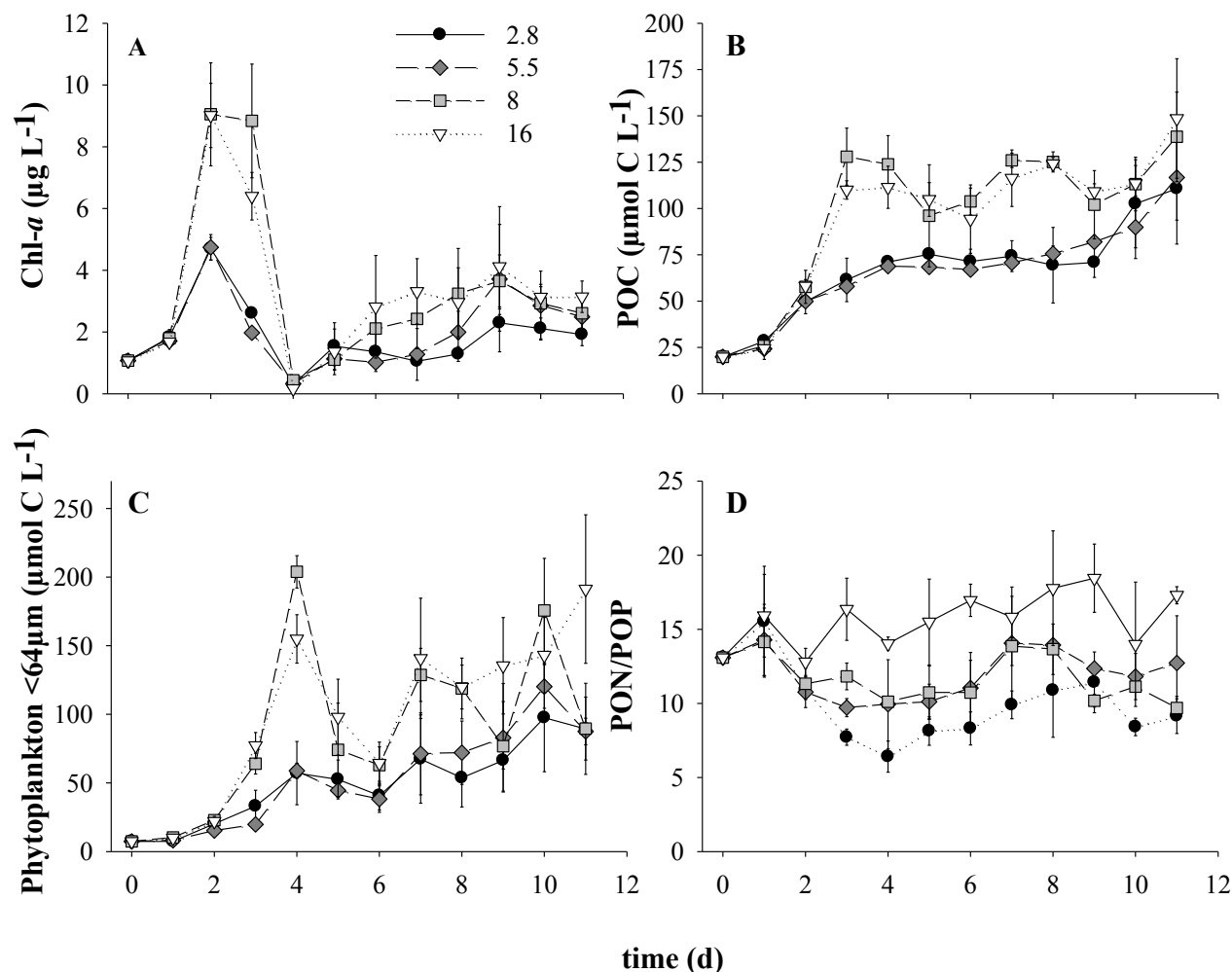


Figure II.2: Temporal development of bulk chlorophyll a (panel A), particulate organic carbon (panel B), phytoplankton biomass derived from flow cytometry counts (panel C) and the ratio of particulate organic nitrogen to phosphorus (panel D). Values are treatment means (\pm SD).

Cell counts

The response of the different cell clusters distinguished by flow cytometry to the nutrient manipulation treatments was variable. The two smallest clusters, which were *Synechococcus*-like and *Prochlorococcus*-like cells, were positively influenced by high initial N load, and negatively by high initial P load ($p < 0.001$). In contrast, the three larger phytoplankton clusters (all chl-*a* only, separated by size) responded only to increased N level ($p < 0.001$). Neither P nor the interaction N*P was significant in the model. Likewise, bacterial biomass responded significantly to N ($p < 0.0001$), but not to P, but here, the interaction between the two was significant ($p < 0.05$). Days 7-9 were excluded from this analysis due to an incomplete dataset.

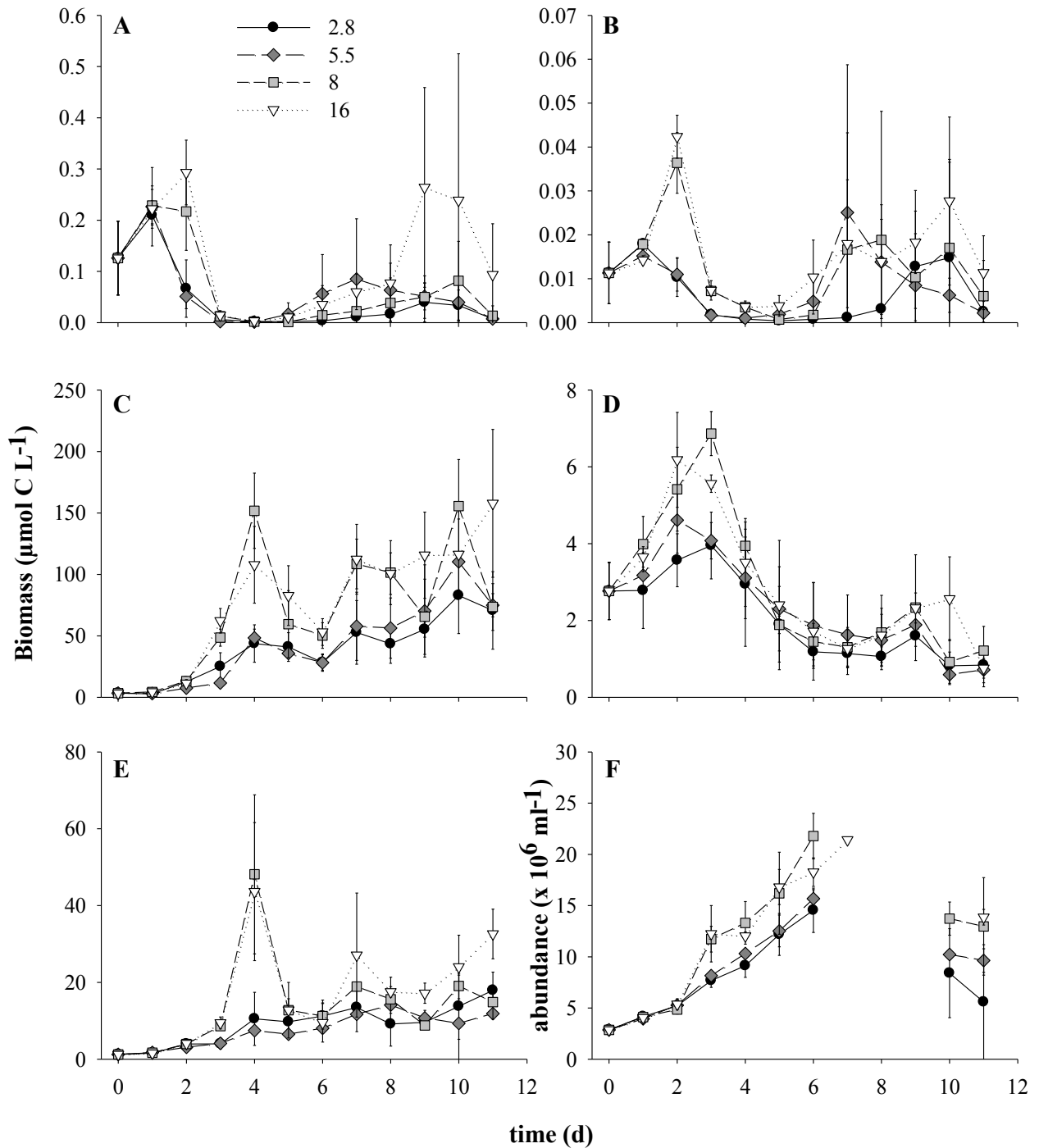
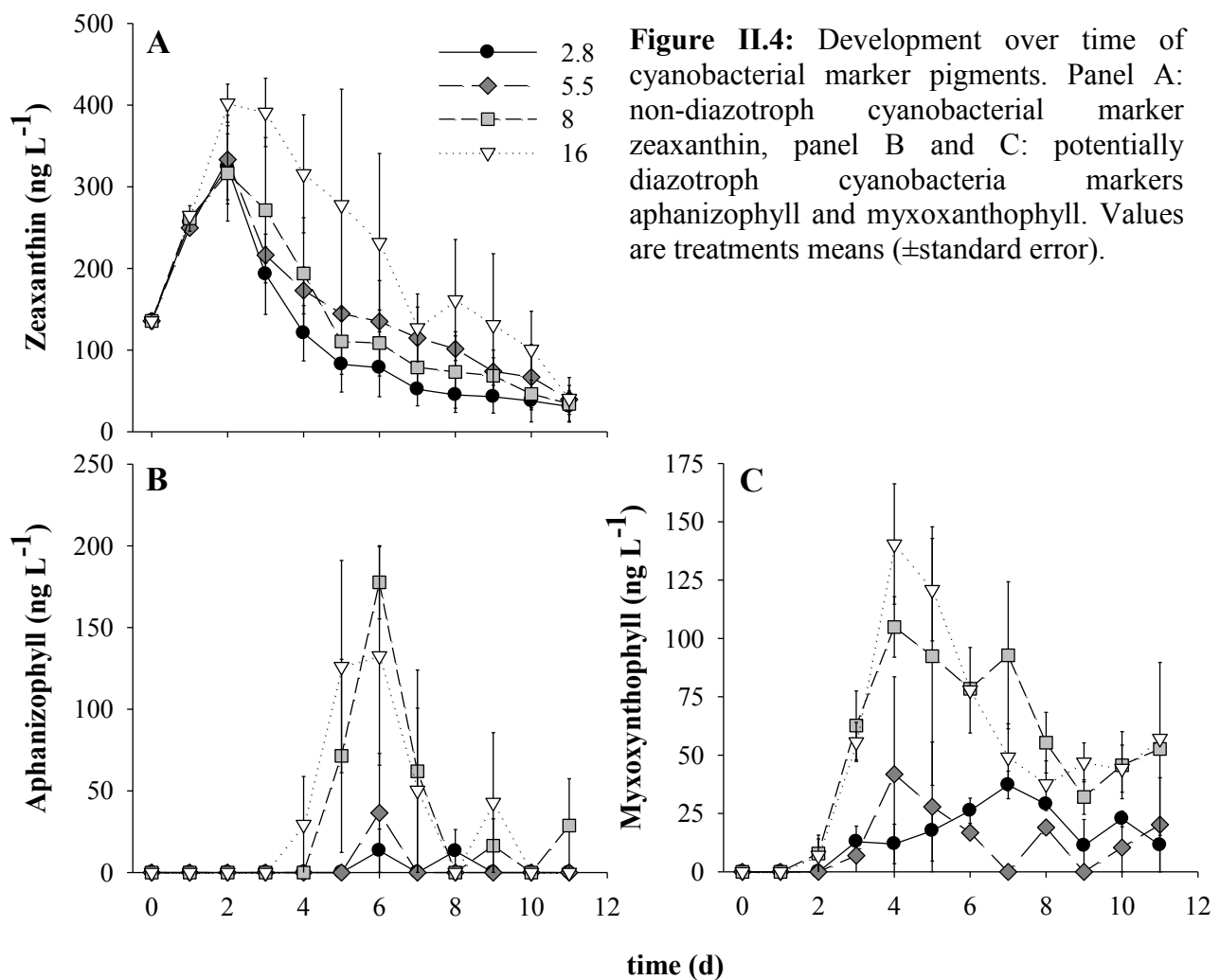


Figure II.3: Phytoplankton biomass (panels A-E) and bacterial abundance (panel F) development determined by flow cytometry counts. Panel A: *Synechococcus*-like cells, panel B: *Prochlorococcus*-like cells, panel C: phytoplankton cells with a mean (\pm SD) equivalent spherical diameter (ESD) of $7(\pm 1.7) \mu\text{m}$ and high chl-*a* content, panel D: phytoplankton cells $3.5(\pm 0.2) \mu\text{m}$ and high chl-*a*, panel E: phytoplankton cells $6.5(\pm 2.1) \mu\text{m}$ and low chl-*a*, panel F: Bacterial abundance (10^6 ml^{-1}). Values are treatment means (\pm SD) of the four N:P treatments.



Phytoplankton pigments

The temporal development of the three cyanobacterial marker pigments (Fig. II.4) was similar for aphanizophyll and myxoxanthophyll, and different for zeaxanthin, as the latter responded with immediate growth until day 2 and subsequently declined, while the former two were not detected within the first days and began to increase after the DIN pool was depleted (Fig. II.4 B and D, Fig II.1 A). Variability among replicates was quite high, but significant differences between treatments were detected by the Mann-Whitney U test. While zeaxanthin was negatively influenced by high initial DIP ($p < 0.05$), the effect of initial DIN load was not significant ($p = 0.054$). Both aphanizophyll and myxoxanthophyll amounts were higher in those mesocosms that had received a higher DIN addition ($p < 0.05$ and $p < 0.0001$, respectively), and were not significantly influenced by DIP ($p = 0.907$ and $p = 0.665$, respectively).

Fatty acid (FA) composition

Twenty-two FAs were detected in the particulate organic matter (table II.1). The principal component analysis (PCA) of FA composition showed distinctive clustering of sampling days 3 and 8 as well as the initial sample (Fig. II.5). PC 1 explained 46.9% of the variability (Fig. II.6) and was strongest negatively correlated with 20:5n3 ($r^2=0.95$), 16:1 ($r^2=0.94$), 18:3n6 ($r^2=0.76$), 14:0 ($r^2=0.76$), 14:1 ($r^2=0.74$) and 20:4n6 ($r^2=0.72$), and positively with 16:0 ($r^2=0.96$), 18:1n9cis ($r^2=0.96$), 18:0 ($r^2=0.91$) and 20:0 ($r^2=0.82$). PC 2 explained 22.6% of the variability in the data and was negatively correlated with 22:6n3 ($r^2=0.78$), 24:0 ($r^2=0.62$), 22:0 ($r^2=0.61$) and 18:2n6cis ($r^2=0.59$), and positively with 12:0 ($r^2=0.79$), 17:1 ($r^2=0.75$) and 14:0 ($r^2=0.56$). Thus, low or negative loadings on PC 1 and 2 indicate relatively high proportions of the essential FAs EPA (20:5n3), ARA (20:4n6) and GLA (18:3n6), while the same is the case for PC 2 and DHA (22:6n3) and LA (18:2n6). In the initial sample, the saturated fatty acids 16:0, 18:0 and 14:0 were dominating the FA composition and together contributed 64.5% of the total FA. The total amount of particulate matter increased over time, as did the proportion of PUFAs and the $FA_{\text{unsat}}/FA_{\text{sat}}$ ratio (Fig. II.6 A and B). This was mainly due to marked increases in 20:5n3, 20:4n6 and 16:1 over time (table II.1). Thus, a higher proportion of these components led to clustering of day 3 and 8 FA composition on decreasing PC 1 and 2 scores (Fig. II 5). On both sampling days of the manipulated mesocosms, FA composition in the lowest N:P treatment (2.8) reaches highest loadings of the PC 1, thus being most similar to the initial sample. However, for none of the individual components was the proportion significantly lower in the N:P=2.8 treatment than in the other three, although the low 16:1/16:0 and EPA/ARA ratios (Fig. II 6 B and C) tend to be in the lowest part of the range observed on the respective sampling days.

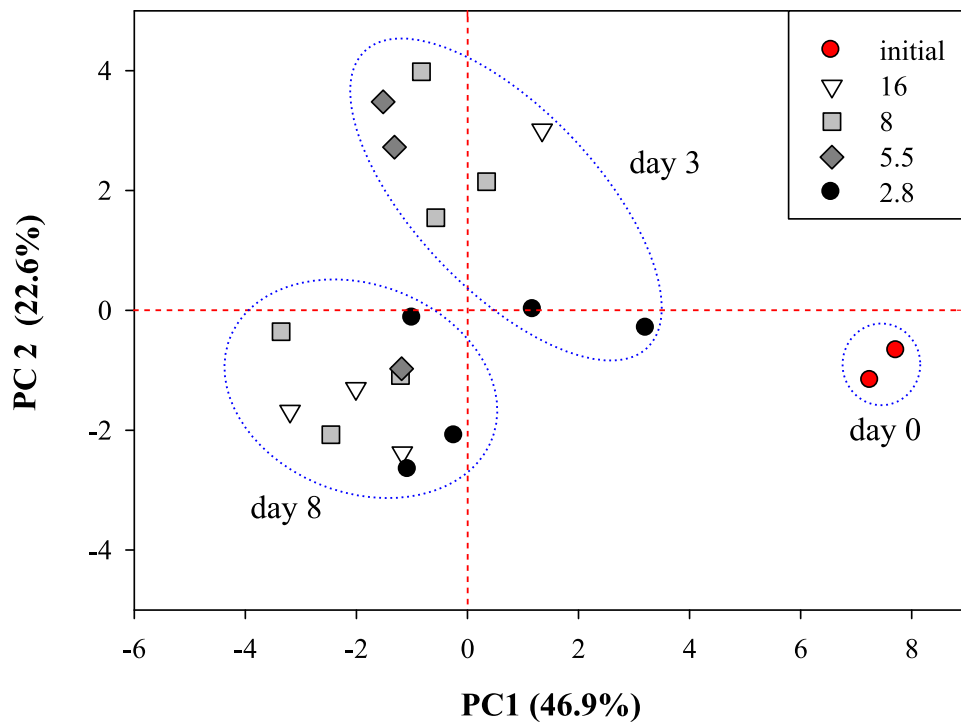


Figure II.5: Principal component analysis (PCA) of fatty acid (FA) composition in particulate organic matter in a duplicate initial sample and on days 3 and 8 in the four N:P manipulation treatments.

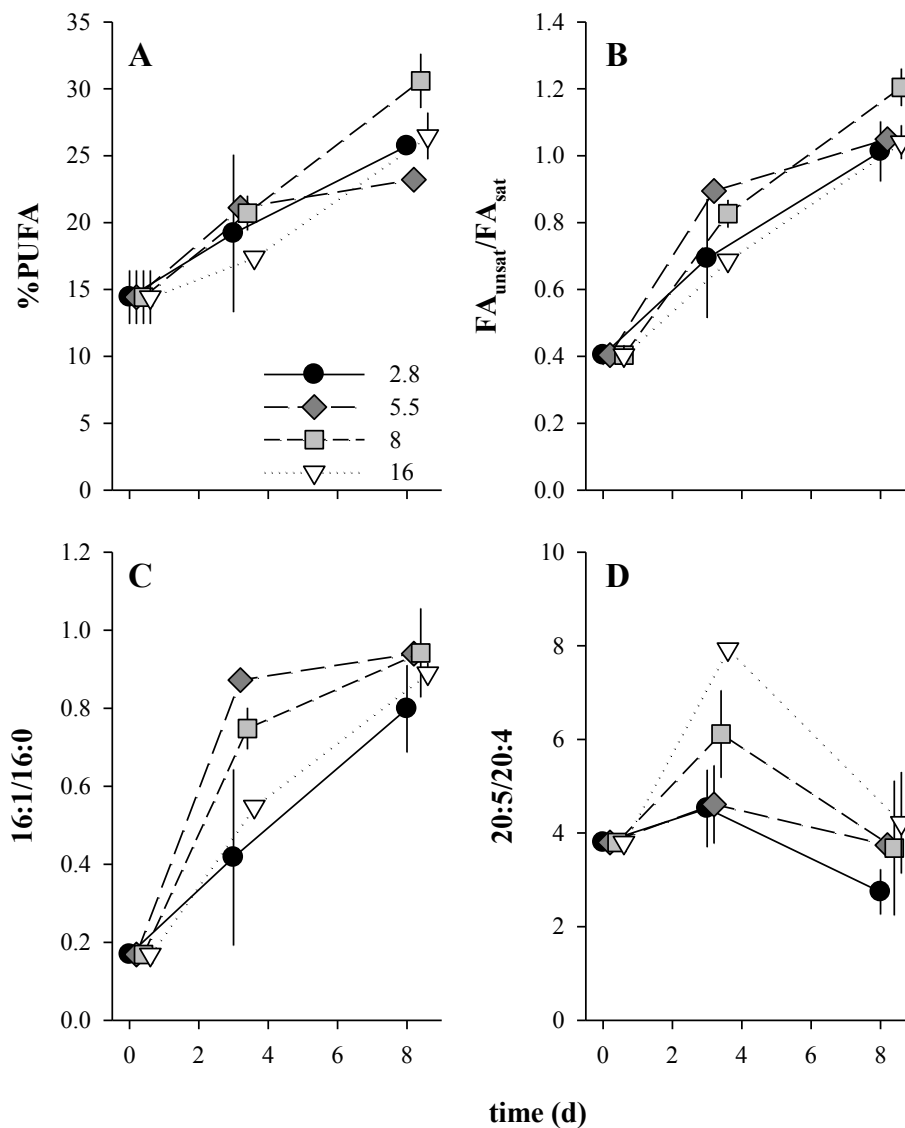


Figure II.6: Development of fatty acid (FA) composition of particulate matter over time in the four N:P manipulation treatments. Panel A: Proportion of polyunsaturated fatty acids (PUFAs) of total FA, panel B: Ratio of unsaturated to saturated FAs, panel C: Ratio of 16:1 to 16:0, panel D: Ratio of 20:5n₃ to 20:4n₆. Day 0 values are from a duplicate subsample (mean \pm SD) of the initial water, day 3 and 8 values are treatment means (\pm SD).

Table II.1: Individual fatty acid (FA) proportions (%) of total FA in particulate organic matter within the four nutrient manipulation treatments (N:P=2.8 to 16) on days 0 (initial sample) 3 and 8. Values are treatment means (\pm SD).

FA	day 0				day 3				day 8				
	all	2.8	5.5	8	16	2.8	5.5	8	16	2.8	5.5	8	16
C8:0	0.0 (\pm 0.0)	0.0 (\pm 0.0)	0.0 (\pm 0.0)	0.4 (\pm 0.6)	0.0 (n/a)	0.0 (\pm 0.1)	0.0 (n/a)	0.0 (n/a)	0.0 (\pm 0.0)	0.0 (n/a)	0.0 (n/a)	0.0 (\pm 0.0)	0.0 (\pm 0.0)
C10:0	1.7 (\pm 0.7)	1.2 (\pm 0.6)	1.0 (\pm 0.3)	0.1 (\pm 0.2)	0.0 (n/a)	0.0 (\pm 0.0)	0.0 (n/a)	0.2 (\pm 0.3)	0.1 (\pm 0.1)	0.0 (n/a)	0.0 (n/a)	0.2 (\pm 0.3)	0.1 (\pm 0.1)
C12:0	1.4 (\pm 0.1)	1.5 (\pm 0.5)	2.0 (\pm 0.3)	1.6 (\pm 0.5)	1.8 (n/a)	1.2 (\pm 0.7)	1.0 (n/a)	1.0 (\pm 0.4)	0.9 (\pm 0.3)	1.0 (n/a)	1.0 (n/a)	1.0 (\pm 0.4)	0.9 (\pm 0.3)
C14:0	12.5 (\pm 0.3)	14.7 (\pm 6.0)	22.9 (\pm 1.0)	22.0 (\pm 2.1)	19.3 (n/a)	18.1 (\pm 1.6)	19.2 (n/a)	19.0 (\pm 1.6)	20.1 (\pm 0.2)	19.2 (n/a)	19.0 (n/a)	19.0 (\pm 1.6)	20.1 (\pm 0.2)
C14:1	0.0 (\pm 0.0)	0.7 (\pm 0.8)	0.6 (\pm 0.0)	0.2 (\pm 0.3)	0.7 (n/a)	0.9 (\pm 0.1)	1.0 (n/a)	1.0 (\pm 0.3)	1.1 (\pm 0.2)	1.0 (n/a)	1.0 (n/a)	1.0 (\pm 0.3)	1.1 (\pm 0.2)
C16:0	35.4 (\pm 1.8)	28.2 (\pm 4.5)	21.7 (\pm 1.4)	25.4 (\pm 1.3)	27.5 (n/a)	21.8 (\pm 1.6)	20.8 (n/a)	20.2 (\pm 1.5)	21.5 (\pm 0.9)	20.8 (n/a)	20.2 (n/a)	20.2 (\pm 1.5)	21.5 (\pm 0.9)
C16:1	6.0 (\pm 0.0)	11.1 (\pm 5.1)	18.9 (\pm 0.7)	19.0 (\pm 0.4)	15.1 (n/a)	17.3 (\pm 1.3)	19.6 (n/a)	18.4 (\pm 0.7)	19.1 (\pm 0.2)	19.6 (n/a)	18.4 (n/a)	18.4 (\pm 0.7)	19.1 (\pm 0.2)
C17:1	0.3 (\pm 0.4)	0.1 (\pm 0.2)	2.2 (\pm 0.1)	1.4 (\pm 1.0)	1.8 (n/a)	0.9 (\pm 0.2)	1.2 (n/a)	0.8 (\pm 0.1)	0.5 (\pm 0.1)	1.2 (n/a)	0.8 (n/a)	0.8 (\pm 0.1)	0.5 (\pm 0.1)
C18:0	16.6 (\pm 0.1)	9.7 (\pm 5.5)	4.2 (\pm 0.0)	3.9 (\pm 1.7)	9.1 (n/a)	6.0 (\pm 0.7)	5.6 (n/a)	4.6 (\pm 1.2)	4.9 (\pm 0.4)	5.6 (n/a)	4.6 (n/a)	4.6 (\pm 1.2)	4.9 (\pm 0.4)
C18:1n9c	4.5 (\pm 0.2)	3.0 (\pm 0.2)	1.8 (\pm 0.6)	2.1 (\pm 0.6)	2.2 (n/a)	1.9 (\pm 0.2)	2.1 (n/a)	1.7 (\pm 0.2)	1.4 (\pm 0.5)	2.1 (n/a)	1.7 (n/a)	1.7 (\pm 0.2)	1.4 (\pm 0.5)
C18:2n6c	2.3 (\pm 0.1)	1.8 (\pm 0.3)	1.2 (\pm 0.0)	1.1 (\pm 0.1)	1.0 (n/a)	1.9 (\pm 0.4)	1.4 (n/a)	1.5 (\pm 0.3)	1.3 (\pm 0.1)	1.4 (n/a)	1.5 (n/a)	1.5 (\pm 0.3)	1.3 (\pm 0.1)
C18:3n6	0.2 (\pm 0.0)	0.5 (\pm 0.5)	0.4 (\pm 0.1)	0.4 (\pm 0.0)	0.2 (n/a)	0.6 (\pm 0.1)	0.6 (n/a)	0.6 (\pm 0.1)	0.6 (\pm 0.0)	0.6 (n/a)	0.6 (n/a)	0.6 (\pm 0.1)	0.6 (\pm 0.0)
C18:3n3	2.7 (\pm 0.4)	2.5 (\pm 0.3)	1.7 (\pm 0.1)	1.7 (\pm 0.2)	1.8 (n/a)	0.7 (\pm 0.1)	0.5 (n/a)	0.5 (\pm 0.1)	0.4 (\pm 0.1)	0.5 (n/a)	0.5 (n/a)	0.5 (\pm 0.1)	0.4 (\pm 0.1)
C20:0	0.7 (\pm 0.0)	0.4 (\pm 0.2)	0.2 (\pm 0.0)	0.2 (\pm 0.1)	0.3 (n/a)	0.3 (\pm 0.0)	0.2 (n/a)	0.2 (\pm 0.2)	0.2 (\pm 0.2)	0.2 (n/a)	0.2 (n/a)	0.2 (\pm 0.2)	0.2 (\pm 0.2)
C20:3n6	0.0 (\pm 0.0)	0.0 (\pm 0.0)	0.1 (\pm 0.1)	0.0 (\pm 0.1)	0.0 (n/a)	0.2 (\pm 0.1)	0.0 (n/a)	0.1 (\pm 0.2)	0.1 (\pm 0.1)	0.0 (n/a)	0.0 (n/a)	0.1 (\pm 0.2)	0.1 (\pm 0.1)
C20:4n6	0.4 (\pm 0.6)	1.5 (\pm 0.6)	2.4 (\pm 0.4)	1.7 (\pm 0.2)	1.0 (n/a)	4.3 (\pm 0.8)	3.2 (n/a)	4.5 (\pm 1.2)	3.2 (\pm 1.1)	3.2 (n/a)	3.2 (n/a)	4.5 (\pm 1.2)	3.2 (\pm 1.1)
C22:0	0.3 (\pm 0.0)	0.3 (\pm 0.2)	0.2 (\pm 0.0)	0.2 (\pm 0.0)	0.2 (n/a)	0.4 (\pm 0.1)	0.4 (n/a)	0.2 (\pm 0.1)	0.3 (\pm 0.1)	0.4 (n/a)	0.4 (n/a)	0.2 (\pm 0.1)	0.3 (\pm 0.1)
C20:5n3	3.1 (\pm 0.4)	6.8 (\pm 3.3)	10.9 (\pm 0.2)	10.1 (\pm 0.3)	8.0 (n/a)	11.6 (\pm 0.3)	11.8 (n/a)	14.2 (\pm 1.5)	12.6 (\pm 0.8)	11.8 (n/a)	14.2 (n/a)	14.2 (\pm 1.5)	12.6 (\pm 0.8)
C22:1n9	0.3 (\pm 0.0)	0.7 (\pm 0.6)	0.2 (\pm 0.1)	0.2 (\pm 0.0)	2.0 (n/a)	0.1 (\pm 0.0)	0.1 (n/a)	0.2 (\pm 0.2)	0.3 (\pm 0.0)	0.1 (n/a)	0.2 (n/a)	0.2 (\pm 0.2)	0.3 (\pm 0.0)
C24:0	0.7 (\pm 0.1)	1.1 (\pm 0.7)	0.3 (\pm 0.1)	0.3 (\pm 0.0)	0.4 (n/a)	0.5 (\pm 0.0)	0.6 (n/a)	0.4 (\pm 0.0)	0.6 (\pm 0.2)	0.6 (n/a)	0.4 (n/a)	0.4 (\pm 0.0)	0.6 (\pm 0.2)
C24:1	0.1 (\pm 0.1)	0.1 (\pm 0.1)	0.1 (\pm 0.0)	0.0 (\pm 0.1)	0.2 (n/a)	0.1 (\pm 0.1)	0.0 (n/a)	0.2 (\pm 0.1)	0.3 (\pm 0.0)	0.0 (n/a)	0.0 (n/a)	0.2 (\pm 0.1)	0.3 (\pm 0.0)
C22:6	8.0 (\pm 0.6)	7.9 (\pm 2.7)	5.7 (\pm 0.8)	6.7 (\pm 0.9)	6.3 (n/a)	8.4 (\pm 1.1)	7.1 (n/a)	9.1 (\pm 2.7)	9.5 (\pm 0.7)	7.1 (n/a)	9.1 (n/a)	9.1 (\pm 2.7)	9.5 (\pm 0.7)
16:1/16:0	0.2 (\pm 0.0)	0.4 (\pm 0.2)	0.9 (\pm 0.0)	0.7 (\pm 0.1)	0.5 (n/a)	0.8 (\pm 0.1)	0.9 (n/a)	0.9 (\pm 0.1)	0.9 (\pm 0.0)	0.9 (n/a)	0.9 (n/a)	0.9 (\pm 0.1)	0.9 (\pm 0.0)
20:5/20:4	3.8 (\pm 0.0)	4.5 (\pm 0.8)	4.6 (\pm 0.8)	6.1 (\pm 0.9)	7.9 (n/a)	2.7 (\pm 0.5)	3.7 (n/a)	3.7 (\pm 1.4)	4.2 (\pm 1.1)	3.7 (n/a)	3.7 (n/a)	3.7 (\pm 1.4)	4.2 (\pm 1.1)
% PUFA	14.4 (\pm 2.0)	19.2 (\pm 5.9)	21.1 (\pm 0.2)	20.7 (\pm 1.3)	17.4 (n/a)	25.7 (\pm 0.6)	23.2 (n/a)	30.6 (\pm 2.0)	26.5 (\pm 1.7)	23.2 (n/a)	30.6 (n/a)	30.6 (\pm 2.0)	26.5 (\pm 1.7)
FA _{unsat} /FA _{sat}	0.4 (\pm 0.0)	0.7 (\pm 0.2)	0.9 (\pm 0.0)	0.8 (\pm 0.0)	0.7 (n/a)	1.0 (\pm 0.1)	1.0 (n/a)	1.2 (\pm 0.1)	1.0 (\pm 0.1)	1.0 (n/a)	1.2 (n/a)	1.2 (\pm 0.1)	1.0 (\pm 0.1)

Copepod (U. vulgaris) RNA/DNA and excretion

Since three copepods were incubated for one day in 500 ml of algal suspension, mean (\pm SD) daily available POC was $277(\pm 28)$, $260(\pm 25)$, $464(\pm 69)$ and $435(\pm 14)$ $\mu\text{C ind}^{-1} \text{d}^{-1}$ in the 2.8, 5.5, 8 and 16 treatment in the first trial (d3-5), respectively, and $324(\pm 75)$, $330(\pm 29)$, $454(\pm 46)$ and $462(\pm 31)$ $\mu\text{C ind}^{-1} \text{d}^{-1}$ in the 2.8, 5.5, 8 and 16 treatment in the second trial (d8-10), respectively. Inter-individual variability in field-caught copepod RNA/DNA was high, ranging from 1.5 to 4.7 in the initial sample of trial 2 (d8-10). However, neither did the RNA/DNA change significantly compared to the initial sample, nor were there significant treatment effects on copepod RNA/DNA (Kruskal-Wallis ANOVA, $p=0.37$ for day 3-5 and $p=0.81$ for day 8-10, Fig. II.7 A). However, the excretion N:P was significantly correlated to the mean PON:POP of the corresponding days 8-10 ($r=0.69$, $p<0.05$, Fig. II.7 B), which in turn was responding to the different nutrient amendment treatments (Fig. II.7 B, see also Fig. II.2 D).

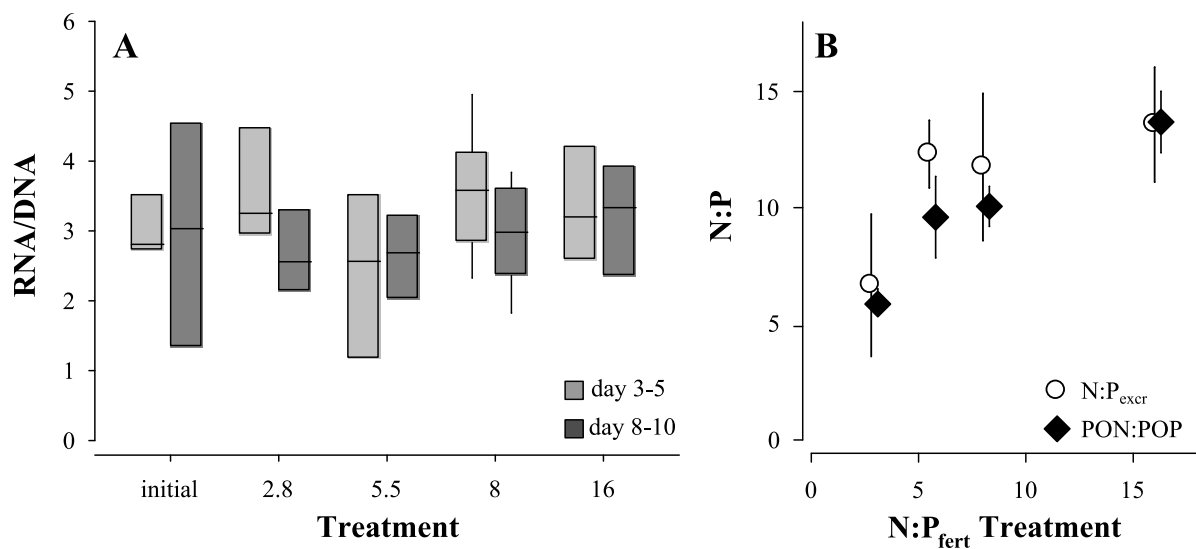


Figure II.7: RNA/DNA of *Undinula vulgaris* females after three days of incubation with mesocosm phytoplankton manipulated to four different nutrient scenarios (panel A) and excretion N:P (panel B, white circles) of *U. vulgaris* after incubation days 8 to 10 in relation to initial N:P fertilization treatments as well as corresponding N:P of particulate organic matter. Values are treatment means \pm standard deviation.

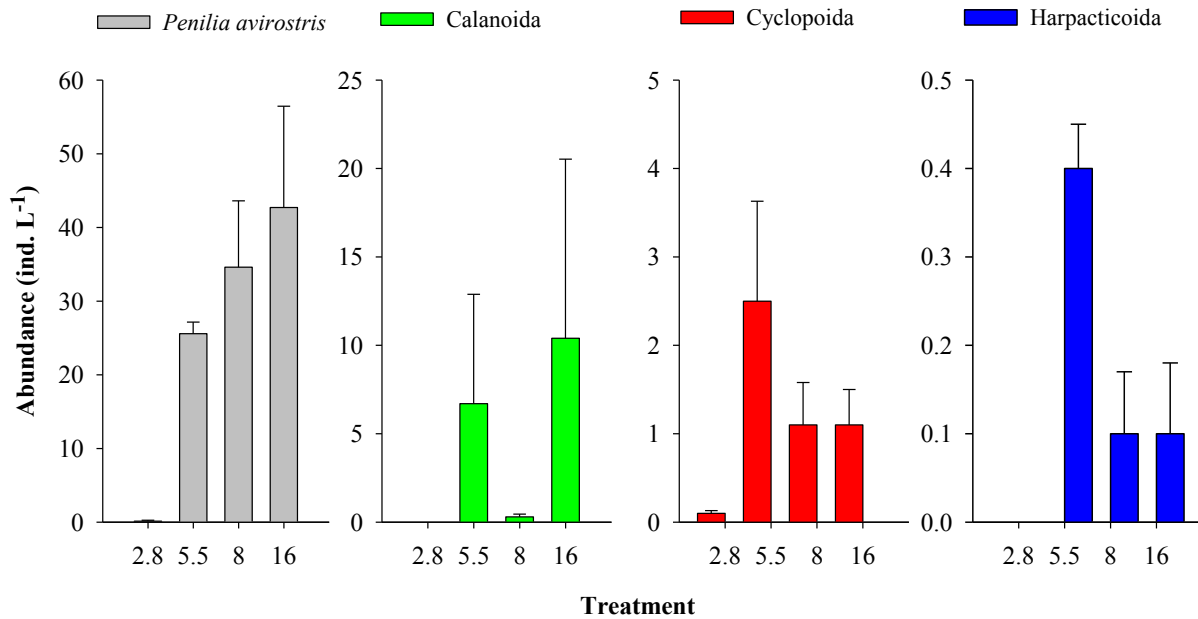


Figure II.8: Final mesozooplankton abundance (individuals L⁻¹) in mesocosms of the four N:P treatments. Calanoid copepods comprise *Temora* sp., *Centropages* sp. and unidentified copepodite stages, the cyclopoida were *Oncaea* sp., *Oithona* sp. and *Corycaeus* sp., and the harpacticoida include *Miracia* sp. and *Macrosetella* sp. Values are treatment means (\pm standard error).

Zooplankton abundance

Final zooplankton abundances in the experimental mesocosms after 11 days of incubation were highly variable and were influenced by initial fertilization treatment. Mesozooplankton comprised several species of pelagic calanoid, cyclopoid, and harpacticoid copepods. However, the single most dominant species in most mesocosms was the cladoceran *Penilia avirostris* (Figure II.8). Abundance of *P. avirostris* (and hereby also total mesozooplankton density) was positively correlated with increasing N:P fertilization ratio ($r=0.71$, $p<0.05$), from close to zero in the lowest to 42.7(\pm 13.8) *P. avirostris* L⁻¹ in the highest N:P treatment. The difference between low and high initial N fertilization was significant (Mann-Whitney *U*-test, $p<0.05$). No significant differences between the “high N” and “low N” treatments were detected in the copepod abundance, where also variability among replicates was very high. Nevertheless, both calanoid (mainly *Temora* sp.) and harpacticoid abundance was significantly lower (Mann-Whitney *U*-test, $p<0.05$) in those treatments with P addition. Both mean cyclopoid and harpacticoid abundance were highest in the unamended control treatment (N:P=5.5), however this difference was not significant.

II.4 Discussion

Given the overall excess N in the tropical North Atlantic Ocean, it is striking that on the more local scale (continental shelf surface waters) the near-field nutrient concentrations as well as their ratio experienced by the phytoplankton community are very similar to the coastal upwelling off Peru (chapter I). Only the supply level of dissolved nitrogen determined the magnitude of phytoplankton biomass increase and community nutrient uptake, with no modulation by the extent of P addition. While our initial station was located close to the West African coast and might be to some extent influenced by coastal nutrient sources (e.g. Sénégal River and Gambia River), our results are generally confirmed by results of Davey et al. (2008), who determined N to be the proximate limiting nutrient at six stations in the offshore ETNA (between 15.5 and 49.5°W) in short-term bioassay experiments. However, these authors found that primary production was significantly higher in the N+P amended bottles, and even higher in the N+P+Fe, than in those where only N was added, and concluded that N₂-fixation in the ETNA is P and Fe-limited. Although N₂-fixation (measured as ¹⁵N₂ uptake in three of these experiments) did increase when only P and Fe (no N) was added (Mills et al. 2004), this never enhanced primary productivity and chl-*a* compared to the unamended control.

The temporal development of non-diazotroph cyanobacteria (such as *Prochlorococcus* and *Synechococcus*) and suspected diazotrophs (such as *Richelia* and *Trichodesmium*) as reflected by their respective marker pigments (Fig. II.4) is complementary to each other. While the non-diazotrophs grow initially until dissolved nutrients are depleted and then gradually decline (Fig. II.1 A), the potentially diazotroph marker pigments begin to appear after complete DIN-depletion (Fig. II.4 B and C, Fig II.1 A). Remarkably, the increase in the latter is more pronounced in those mesocosms initially treated with a higher DIN load. Following general assumptions about the environmental conditions where the ability to fix N₂ becomes profitable, one would assume that rather the low N:P treatments trigger such an increase, especially the lowest one where additional P was added. Traditionally, large-scale N input by N₂-fixation has been attributed largely to the central and western part of the North Atlantic based upon the dominance of *Trichodesmium* and the high N:P export ratio. More recently, the role of unicellular cyanobacteria as well as diatom-cyanobacteria associations (DDAs) have been increasingly acknowledged, but are still largely based on the assumption that high diapycnal supply of DIN prevents the necessity of N₂-fixation. The group-specific abundance of *nifH* (the structural gene for nitrogenase reductase) only partly confirms results from pigment analysis. While *Trichodesmium*-specific *nifH* gene abundance increased exponentially over time (Fig. II.9), other groups (DDA, *Crocospaera*-like, γ -Proteobacteria, group A) were only detected

sporadically on some sampling days, indicating that their overall abundance was lower than that of *Trichodesmium*. Thus, there is a discrepancy between *nifH*-gene abundance and pigment concentration both over time and treatment-wise. Highest aphanizophyll and myxoxanthophyll values were recorded between days 4 and 8 (Fig. II.4), but the most abundant *nifH*-gene (assigned to *Trichodesmium*) showed the highest copy numbers towards the end of the experiment. Both aphanizophyll and myxoxanthophyll were significantly higher in the “high N” than in the “low N” treatments, while *Trichodesmium nifH*-gene abundance was not. For DDAs, even the contrary was found on days 5 and 6, where considerable amounts of DDA-specific *nifH*-genes were found in the two “low N” treatments. Very little information exists on the interplay between cell number, pigment amount per cell, and N₂-fixation in the various N-fixing groups; this is certainly an area of rewarding future research.

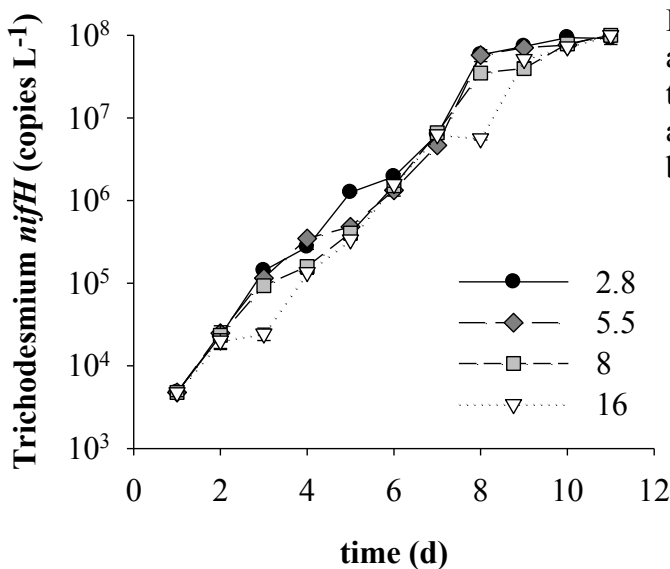


Figure II.9: *Trichodesmium nifH* gene abundance (copies L⁻¹) development over time in the four N:P treatments. Symbols as in Fig. II.6. Gene abundance determined by Carolin Löscher, IFAM Kiel.

Considerations of resource limitation and resulting profitability of certain functional groups are often focused entirely on measured nutrient standing stocks and their ratios rather than their supply and depletion dynamics. As such, natural successions are often neglected. However, it has been hypothesized before, following observations of Margalef (1973) and model predictions by Hood et al. (2004) that the succession sequence diatoms-cyanobacteria-flagellates might be characteristic of the ETNA. In fact, co-occurrence of diatom-dominated assemblages at depth and a *Trichodesmium* bloom at the surface are not uncommon. In regions where high vertical DIN supply is balanced by high primary productivity, and thus quickly depleted in the surface, a niche for diazotrophs is created shortly after every upwelling event.

Penilia avirostris, the only marine species of the cladoceran order Ctenopoda, is an important component of surface zooplankton in tropical and subtropical waters (Marazzo & Valentin

2003), however increasingly occurring also in temperate regions during summer months (Lochhead 1954; Johns et al. 2005). Its life cycle is notably different from marine copepods, since developmental time is much shorter (estimated 6 to 8 days, Aienza et al. 2007) and does not include major metamorphic changes. In conjunction with the parthenogenetic reproduction of adults, this can lead to an immediate population growth response to favourable environmental conditions. Indeed, very high densities of this species characterize stratified post-bloom conditions (Johns et al. 2005). Although early studies claimed that the feeding size spectrum of *P. avirostris* was rather small, Katechakis et al. (2004) demonstrated in a selectivity study that the species is grazing most efficiently on intermediate prey sizes ranging from 15 to 70 μm , covering a range from 2.5 to 100 μm (longest linear extension). However, the large contribution of small-celled phytoplankton in our experiments seemed to have favored *P. avirostris* as an efficient filter feeder compared to the copepods. Moreover, the copepod groups that were most abundant in the lowest nutrient addition treatments (N:P=5.5, low N/low P) are characteristic for stratified oceanic waters, such as *Miracia* and *Macrosetella* sp.

It remains uncertain why *Temora* was negatively affected by P-additions. The fatty acid composition of particulate organic matter suggested that the effect of increased light and decreased grazing impact in our mesocosm setup, triggering a phytoplankton bloom in all nutrient treatments, was more important for the increase in the proportion of essential PUFAs (such as 20:5n3 and 22:6n3) over time than the N:P supply. Although the lowest N:P treatment (N:P=2.8) had slightly lower 16:1 and 20:5n3 proportions compared to the other nutrient treatments (Fig. II.6 C and D) and scored highest on the PC1 (Fig. II.5), differences were small compared to the changes over time. A factor that has received little (if any) attention in the natural marine environment is the influence of irradiation on the fatty acid composition of phytoplankton (Guschina & Harwood 2009). While the impact of irradiation on lipid synthesis is acknowledged (Wainman et al. 1999), its differential impact on fatty acid composition remains somewhat ambiguous (e.g. Thompson et al. 1990). The underwater light climate experienced can be very different among ocean regions with differing stratification and turbidity. Especially in the highly stratified oligotrophic ocean, phytoplankton is strongly light limited when the nutricline deepens. In a freshwater field study where different regions of a shallow fluvial lake were compared, Pommier et al. (2012) found that EPA and DHA(22:6n-3) concentrations in the seston were negatively correlated to light attenuation, and that this correlation was strongest at wavelengths close to the absorption maximum of chl-*a*. In summary, it seems unlikely that low food quality in terms of FA availability caused the detrimental effect on calanoid copepods.

Phytoplankton quantity was very similar between the N:P=8 and 16 treatments, and so was the fatty acid composition of the particulate matter. Possibly, the lower PON:POP in the N:P=8 treatment (see Fig. II.2 D) was more suitable for *P. avirostris* than for the calanoid copepods: Traditionally, and partly because substantial differences found in freshwater systems (e.g. Andersen & Hessen 1991), copepods are considered high N:P organisms, while cladocerans are considered low N:P. However, marine data on body N:P of different taxa remain quite scarce. Those available indicate that this difference is far less pronounced in the marine realm, as marine cladocerans (mainly *Evadne* spp.) were found to have a body N:P in the lower range of marine herbivorous copepods, yet constantly beyond the canonical Redfield N:P of 16 (Walve & Larsson 1999; Sommer & Sommer 2006). No data are available on *P. avirostris* body C:N:P, but Atienza et al. (2006) found no detectable phosphate excretion in this species and proposed that it efficiently retains P to fuel parthenogenetic reproduction, which requires high contents of P-rich nucleic acids. Thus, high abundance of *P. avirostris* can potentially relieve N-limitation in surface waters, however, its low growth in the low N:P treatments in the present study indicate that there is a tradeoff between prey abundance and its elemental composition that we are not able to fully resolve with the available data.

We did not observe significant differences in nutritional condition (assessed as RNA/DNA ratio) in large omnivorous copepods after being fed with the mesocosm algal suspension. This is likely due to the very high food density in all incubations (compared to natural abundances encountered by *U. vulgaris*), which may have outweighed food quality effects. Although we did not determine actual ingestion rates, high food availability is also reflected in weight-specific ammonium and phosphate excretion rates that were four- to tenfold higher than in incubations field-caught individuals of the same species (see chapter III). Nevertheless, a significant effect in the ratio of the two was detected, which was due to a diminished NH_4^+ excretion rate at low PON:POP, while phosphate excretion remained constant. This downregulation can help the copepod to sustain its biochemical body composition; however, the selective retention of N in N-poor environments can also provide a feedback to dissolved nutrient pools exploited by phytoplankton. Nevertheless, the lowest ammonium to phosphate ratio was still higher than the lowest PON:POP, which was likewise higher than the initial N:P fertilization ratio, so that the effect appears somewhat dampened.

Our results indicate that changes in the nutrient inventories in the ETNA have profound effects on primary productivity, elemental composition of phytoplankton, trophic efficiency to zooplankton consumers, and nutrient recycling by zooplankton. However, to fully understand the

role of nutrient limitation in this ecosystem, each of these aspects deserves dedicated research efforts.

Chapter III

Can tropical marine zooplankton excretion exacerbate dissolved nutrient imbalances?

Abstract

Zooplankton plays a pivotal role in the cycling and vertical flux of carbon (C), nitrogen (N), and phosphorus (P) in the ocean. Due to physiological restrictions in body C/N:P ratios, egestion and excretion of organic and inorganic nitrogen and phosphorus may be variable depending on the available prey stoichiometry. We investigated inorganic N and P excretion in three common epipelagic copepods at five stations in the Eastern Tropical North Atlantic, *Euchaeta marina*, *Scolecithrix danae* and *Undinula vulgaris*, with the first being a predatory species and the latter two largely herbivorous. Individuals were incubated in groups at two temperatures (11 and 23°C), and the accumulation of NH_4^+ and PO_4^{3-} measured immediately on board at four time points. At the respective stations, particulate organic N and P concentrations were determined at eight depths within the upper 150 m. Excretion was strongly temperature dependent, with *U. vulgaris* being the most temperature-sensitive species. In addition, stoichiometric N:P_{excr} (molar ratios) was significantly different between the two feeding types, with $17.0(\pm 0.78)$ in *E. marina* compared to $9.1(\pm 0.19)$ and $9.1(\pm 0.38)$ in *U. vulgaris* and *S. danae*, respectively, which can be accounted for by the more rigid N:P of the prey items of the former (metazoan prey) compared to N-limited phytoplankton consumed by the latter. For the stations sampled, N:P_{excr} increased for all species with the average PON:POP in the water column. We suggest that body mass and temperature alone are not sufficient as universal predictors of metabolic rates, and especially in the light of nutrient limitation feedbacks, prey stoichiometry should be taken into account.

III.1 Introduction

Mesozooplankton are both a sink and a source for macronutrients in the pelagic environment, as they simultaneously remove particulate matter from the water column and incorporate it into their biomass, and release bioavailable dissolved nutrients. Therefore, besides grazing control of phytoplankton biomass, they can relieve phytoplankton from nutrient limitation by recirculation of dissolved nutrients within the photic zone that otherwise would be lost with sinking biomass. Especially in the highly stratified oligotrophic open ocean, excretion by mesozooplankton in surface waters is an important process in the remineralization of organic matter to bioavailable nutrients. While, to a certain extent, diurnal vertical migration (DVM) of zooplankton may mediate a net downward flux of both nitrogen and phosphorus (Longhurst et al. 1989), a large fraction of nutrients required by microalgae is directly resupplied in the photic surface waters. Thus, mesozooplankton excretion provides a substantial fraction of the dissolved inorganic nitrogen (N) and phosphorus (P) requirements of phytoplankton. This proportion exceeds 50% in the oligotrophic tropical and subtropical Atlantic (Isla et al. 2004a and 2004b) and Pacific (Eppley et al. 1973). Copepods excrete mainly ammonium (NH_4^+), which is easily accessible to phytoplankton, and therefore immediately consumed and often undetectable in the water column. The percentage of copepods in the total mesozooplankton biomass is therefore positively related to the percentage of ammonium in total N excretion products (Le Borgne 1982a), although urea leaching from fecal pellets may also contribute substantially to recycling of bioavailable N (Saba et al. 2011). The large vertical flux of dissolved N in upwelling areas suggests that regeneration by zooplankton excretion only plays a minor role. However, analyses in the upwelling system off Peru (Whitledge 1981) and Mauritania (Smith & Whitledge 1977) revealed that zooplankton resupplied approximately 25% of phytoplankton N requirements.

The factors controlling ingestion and metabolism in zooplankton are manifold. While body size and temperature have long been identified to scale metabolic rates (Ikeda et al. 1985; Wen & Peters 1994; Ikeda et al. 2001; Sereda & Hudson 2011) and the relationships are quite rigid, others cannot be easily determined. Nitrogen excretion rates of zooplankton have been extensively measured, and empirical allometric relationships have been established that describe excretion rates as a function of body size and temperature (Vidal & Whitledge 1982; Ikeda 1985; Ikeda et al. 2001). In contrast, data on P excretion, in particular in relation to N and available food quantity and elemental composition, are quite scarce. Although N and P excretion are highly correlated and predict each other with an r^2 of 0.88 (absolute units, not weight normalized, Wen & Peters 1994), a considerable variability remains that can be crucial in terms

of the elemental balance resupplied to phytoplankton. To maintain stoichiometric balance of their body mass, zooplankton feeding on prey with a low N:P ratio must adjust their growth efficiency in order to retain the element in short supply (N) relative to that (P) in surplus (Sterner & Elser 2002). Because once incorporated in zooplankton biomass, the major fraction of this element eventually leaves the photic zone when the animals die or are preyed upon themselves, zooplankton may exacerbate nutrient limitation of phytoplankton by effectively removing the element in greatest shortage from the surface (Sterner 1990). This effect is predicted to be proportional to the difference in N:P ratio between the consumer and its prey. Under nutrient limitation, phytoplankton can deviate substantially (Hecky & Kilham 1988) from the C/N:P observed at maximal growth rate (i.e. high diffusive flux of dissolved nutrients), when C/N:P ratios are close to Redfield (106:16:1). This concept has been confirmed by observations in freshwater ecosystems, when the relatively P-rich cladocerans are the main grazers on phytoplankton, effectively drain P from the system and thus drive the system to P-limitation (e.g. Balseiro et al. 1997; Sommer 2003). For example, a mesocosm study investigating the impact of a mesozooplankton gradient on northeast Atlantic phytoplankton nutrient limitation revealed that N-limitation increased with copepod density (Sommer et al. 2004). However, this appeared to be due to a trophic cascade effect rather than direct biomass/excretion differentiation, because copepod growth (and thus PON incorporation) during the experiment was rather low and microplankton biomass was reduced by copepod consumption, in turn positively affecting phytoplankton growth and nutrient uptake. Because of the lack of observational evidence in these mesocosm experiments conducted in the Baltic and a Norwegian fjord, Sommer (2003) concluded that marine copepods were not capable of changing the nutrient limitation scenario due to the relatively small difference between zooplankton and phytoplankton N:P (Walve & Larsson 1999).

In field observations on mixed zooplankton in the Eastern Tropical North Atlantic, Le Borgne (1982a) observed a positive relationship between the N:P of excreted dissolved inorganic nutrients and the N:P of particulate organic matter (PON:POP). While the slope of this relationship was close to 1, the intercept was -5.2, thus, zooplankton excreted consistently less N than they acquired by feeding. Copepods and most other mesozooplankton are not unselectively consuming suspended particulate matter, but actively and passively select suitable prey items according to their size, shape, motility, and biochemical composition. Therefore, the ingested algae do not necessarily reflect the elemental ratios measured in bulk particulate matter. Some algae that are inconvenient to eat or contain toxic grazing protection products are avoided by almost all consumers. For example, the oceanic filamentous cyanobacterium *Trichodesmium* spp.

was found to be grazed upon only by a few specialized copepods (e.g. O’Neil et al. 1996). Thus, it remains somewhat uncertain to which extent its biomass, which is very high in N:P due to its ability to fix atmospheric nitrogen, is incorporated in consumer biomass and directly fuels secondary production. Avoidance of this food item would thus lead to a considerably lower N:P excretion ratio than would be expected from bulk PON:POP.

III.2 Materials and Methods

Measurements of N and P excretion rates were conducted during cruise M83-1 on R/V *Meteor* in November 2010. At 5 stations (Fig. III.1), zooplankton was caught using a WP-2 net (150- μ m mesh) equipped with a solid cod end hauled vertically from 100 m depth to the surface with a heave speed of 0.2 m s⁻¹. Zooplankton was immediately diluted in two 30 L buckets filled with seawater and sorted under a dissecting scope. Groups of three to eight adult females of the epipelagic calanoid copepod species *Undinula vulgaris*, *Scolecithrix danae* and *Euchaeta marina* were incubated in triplicate in 500-ml Kautex bottles at 11 and 23°C (corresponding to conditions at the surface and at ca. 200 m depth) under dim light. Samples for ammonium (NH₄⁺) and phosphate (PO₄³⁻) determination were taken at four time points using a plastic syringe and measured immediately using a Quattro autoanalyzer with an external fluorometer (Jasco FP-2020 excitation: 370 nm, emission: 460 nm) for NH₄⁺ analysis (K erouel et al. 1997). Standard deviations for NH₄⁺ and PO₄³⁻ are 0.03 and 0.01 μ mol L⁻¹, respectively, and detection limits are 0.01 and 0.01 μ mol L⁻¹, respectively. Upon termination of the experiment, copepods were placed without water in 1.5-ml cap vials and frozen at -80°C.

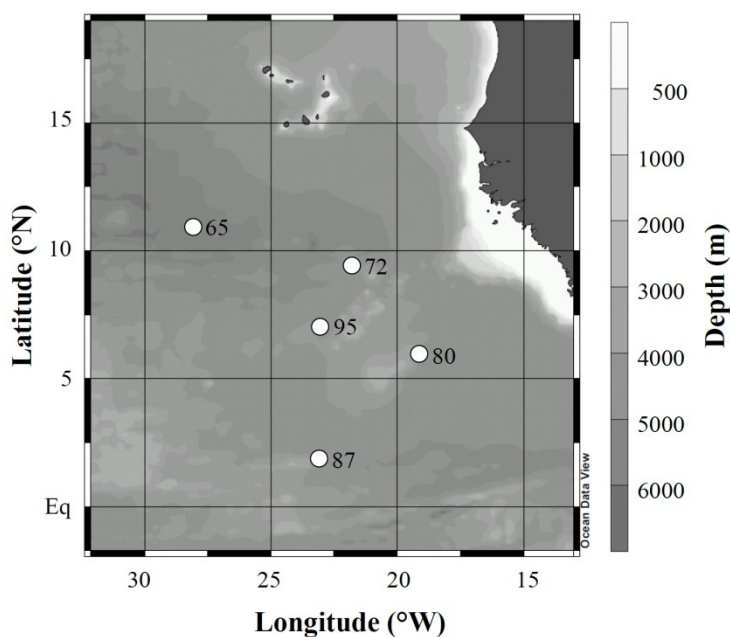


Figure III.1: Map of investigation area with white circles marking sites of excretion incubations.

Copepods were freeze-dried in opened cap vials for 16 h, using a Christ Alpha 1–4 freeze-drier and weighed individually to the nearest 0.1 μg (Sartorius microbalance SC2). For carbon and nitrogen analysis (Table III.1), samples of copepods from the same stations (two individuals per sample, three samples per species) were collected in tin cups (3.2x4 mm, Hekatech) for C/N analysis and dried for 24 h at 50°C. Measurements were performed on a Flash-EA 2000 coupled to a Delta V isotope-ratio mass spectrometer (Thermo Fisher Scientific).

Samples for particulate organic carbon, nitrogen and phosphorus were collected at 25 stations in the ETNA (see Fig. III.2 A), including those stations where excretion incubations were conducted (Fig. III.1), sampling at eight fixed depths within the upper 150 m (150, 100, 80, 60, 40, 20, and 10 m) and one additional sample within the chl-*a* maximum. Samples were filtered onto pre-combusted (450°C for 5 h) Whatman GF/F filters (0.7 μm pore size; 25 mm diameter) at low vacuum pressure (200 mbar) and stored frozen at -20°C until analysis. Filters for POC/PON were fumed with hydrochloric acid (37%) for ~15 h to remove the inorganic carbon, dried at 60°C for 12 h and wrapped in tin foil for combustion. Final measurements of POC and PON were made according to Sharp (1974) using an elemental analyzer with a heat conductivity detector (Thermo Flash 2000).

Particulate organic phosphorus (POP) was measured using a modified method according to Hansen and Koroleff (2007). Filters were defrosted and incubated for 30min with the oxidation reagent Oxisolv (Merck) and 40 ml of ultrapure water in a pressure cooker. Addition of ascorbic acid (1.25 ml) and a mixed reagent (4.5M H₂SO₄ + NH₄⁺ molybdate + potassium antimonyl tartrate; 1.25 ml) to the resulting orthophosphate formed a blue complex which was measured colorimetrically against ultrapure water at 882 nm with a Hitachi U-2000 spectrophotometer. To compare rate measurements, the slopes of individual concentration point measurements over time were compared in an ANCOVA, with Tukey's HSD for post-hoc comparison.

Table III.1: Mean (\pm standard deviation) dry weight *DW*, carbon C, nitrogen N, and C/N ratio of copepods at the five different stations.

Species	Station #	<i>DW</i> (\pm SD) (μ g)	C (\pm SD) (μ g)	N(\pm SD) (μ g)	C:N (\pm SD) (molar)
<i>S. danae</i>	65	205.3 (\pm 40.4)	96.0 (\pm 2.0)	18.7 (\pm 10.8)	5.6 (\pm 0.6)
<i>S. danae</i>	87	194.5 (\pm 20.7)	68.3 (\pm 8.4)	15.7 (\pm 1.9)	5.1 (\pm 0.06)
<i>S. danae</i>	95	182.1 (\pm 54.8)	62.5 (\pm 11.8)	13.9 (\pm 2.8)	5.2 (\pm 0.01)
<i>U. vulgaris</i>	72	217.0 (\pm 41.7)	86.1 (\pm 7.2)	19.8 (\pm 1.4)	5.1 (\pm 0.08)
<i>U. vulgaris</i>	95	202.6 (\pm 0.85)	66.0 (\pm 8.0)	15.3 (\pm 1.8)	5.0 (\pm 0.01)
<i>E. marina</i>	80	284.0 (\pm 71.6)	104.1 (\pm 13.1)	21.0 (\pm 3.7)	5.8 (\pm 0.3)
<i>E. marina</i>	95	291.0 (\pm 34.8)	117.1 (\pm 37.7)	25.1 (\pm 7.5)	5.4 (\pm 0.01)

III.3 Results and Discussion

Bulk particulate matter in terms of C, N, and P was variable in the study area, but tended to decrease with depth. Highest standing stocks were recorded in the upper 50 m (Fig. III.2 A-C). The eastern area, which comprised four stations located at the shelf edge, reached highest surface concentrations of particulate matter, and the southern part lowest. PON:POP at the surface was similar among areas and close to Redfield (Fig. III.2 D), but diverged at depth, with the PON:POP in the northern and southernmost stations exceeding Redfield, while in the eastern, central (Guinea Dome) and western part of the study area PON:POP was generally below Redfield, ranging from 7.3(\pm 1.3) to 13.7(\pm 1.0). Three of the five stations where excretion incubations were conducted were located in the “low PON:POP” range (#65, 72 and 95), while two were in the higher PON:POP range, with an average PON:POP in the upper 150 m of 19.7(\pm 4.48) and 17.7(\pm 2.6) at station # 87 and 80, respectively.

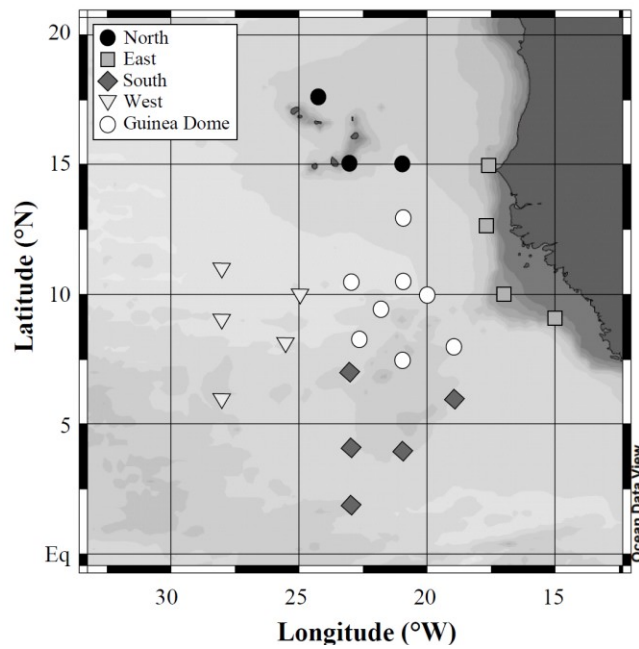
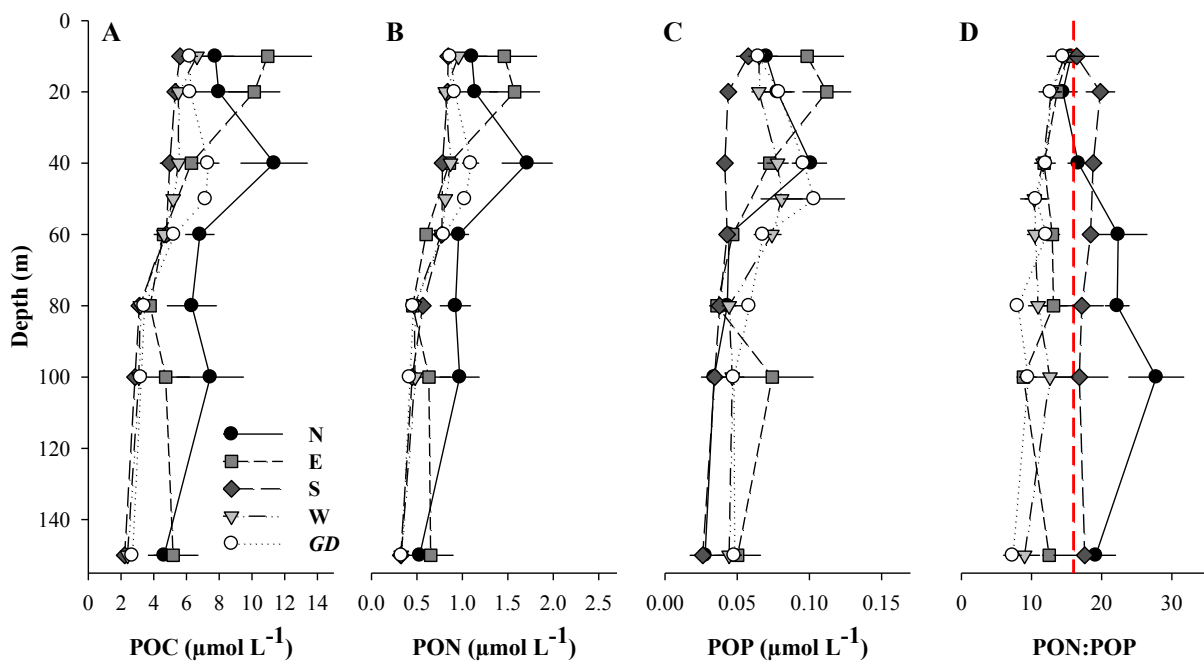


Figure III.2: Left: Map of stations investigated during M83-1 assigned to five areas: North (N, $n=3$), East (E, $n=4$), South (S, $n=5$), West (W, $n=5$) and Guinea Dome ($n=8$). Below: Vertical distribution of particulate organic carbon (POC, panel A), nitrogen (PON, panel B), phosphorus (POP, panel C) and the PON:POP (panel D) within the upper 150m. Values are area means (\pm SE).



Weight-specific excretion rates varied between both species and stations, with the highest range covered by *S. danae*, ranging from $13.17(\pm 3.02) \mu\text{mol NH}_4^+ \text{gDW}^{-1} \text{h}^{-1}$ at station 65 to $23.42(\pm 1.28) \mu\text{mol NH}_4^+ \text{gDW}^{-1} \text{h}^{-1}$ at station 87 (Table III.2).

Table III.2: Summary of weight-specific excretion rates (NH_4^+ and PO_4^{3-}) of copepods incubated at different temperature with the respective mean particulate organic nitrogen (PON) and phosphorus POP) in the upper 150m of the water column (\pm SD) at the respective stations.

Species	Station #	T (°C)	NH_4 excr (\pm SD) ($\mu\text{mol g DW}^{-1} \text{h}^{-1}$)	PO_4 excr (\pm SD) ($\mu\text{mol g DW}^{-1} \text{h}^{-1}$)	N:P _{excr}	PON (\pm SD) ($\mu\text{mol L}^{-1}$)	POP (\pm SD) ($\mu\text{mol L}^{-1}$)	PON:POP (\pm SD)
<i>S. danae</i>	65	11	6.84 (\pm 0.97)	0.60 (\pm 0.2)	11.4	0.72 (\pm 0.36)	0.06 (\pm 0.02)	13.75 (\pm 5.99)
<i>S. danae</i>	65	23	13.17 (\pm 3.02)	1.39 (\pm 0.4)	9.5	0.72 (\pm 0.36)	0.06 (\pm 0.02)	13.75 (\pm 5.99)
<i>S. danae</i>	87	23	23.42 (\pm 1.28)	1.71 (\pm 0.06)	13.7	0.62 (\pm 0.18)	0.03 (\pm 0.01)	19.70 (\pm 4.48)
<i>S. danae</i>	95	21.7	14.01 (\pm 1.25)	1.84 (\pm 0.3)	7.6	0.58 (\pm 0.2)	0.06 (\pm 0.01)	11.36 (\pm 6.44)
<i>U. vulgaris</i>	72	11	4.79 (\pm 0.98)	0.51 (\pm 0.20)	9.4	0.69 (\pm 0.32)	0.06 (\pm 0.02)	10.89 (\pm 3.48)
<i>U. vulgaris</i>	72	23	20.32 (\pm 0.16)	2.38 (\pm 0.24)	8.5	0.69 (\pm 0.32)	0.06 (\pm 0.02)	10.89 (\pm 3.48)
<i>U. vulgaris</i>	95	21.7	17.07 (\pm 0.85)	1.84 (\pm 0.1)	9.3	0.58 (\pm 0.2)	0.06 (\pm 0.01)	11.36 (\pm 6.44)
<i>E. marina</i>	80	11	9.75 (\pm 0.58)	n.d. n.d.	n.d.	0.77 (\pm 0.34)	0.04 (\pm 0.02)	17.73 (\pm 2.60)
<i>E. marina</i>	80	23	20.51 (\pm 2.23)	0.99 (\pm 0.14)	20.7	0.77 (\pm 0.34)	0.04 (\pm 0.02)	17.73 (\pm 2.60)
<i>E. marina</i>	95	21.7	22.81 (\pm 2.46)	1.38 (\pm 0.27)	16.5	0.58 (\pm 0.2)	0.06 (\pm 0.01)	11.36 (\pm 6.44)

At the only station where all three species were measured (station 95), the ammonium excretion rate in *E.marina* was significantly higher ($p<0.001$) than that of the other two (Fig. III.3 A). At the same time, its phosphate excretion rate was lower ($p<0.001$) than that of the other two (Fig. III.3 B), leading to the highest N:P_{excr} (16.5) in this species. While the rate of ammonium excretion was not significantly different between *S. danae* and *U. vulgaris*, phosphate excretion rate was significantly ($p<0.05$) higher in the latter (Fig. III.3). When all stations where incubations at surface temperature were conducted were considered, mean N:P_{excr} of *E. marina* was 17.0(\pm 0.78), while that of *U. vulgaris* and *S. danae* was 9.1(\pm 0.19) and 9.1(\pm 0.38), respectively (Fig. III.4). Thus, the feeding ecology of the respective species strongly influenced its nutrient efflux.

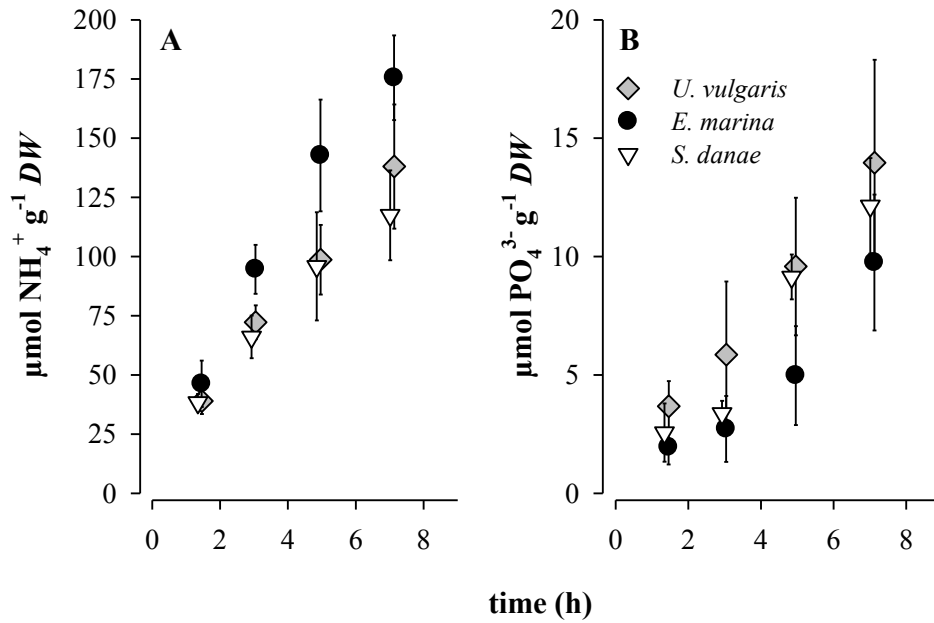


Figure III.3: Weight-specific excretion over time (h) of ammonium (panel A) and phosphate (panel B) of three copepods from the same station incubated at 21.7°C (Station 95).

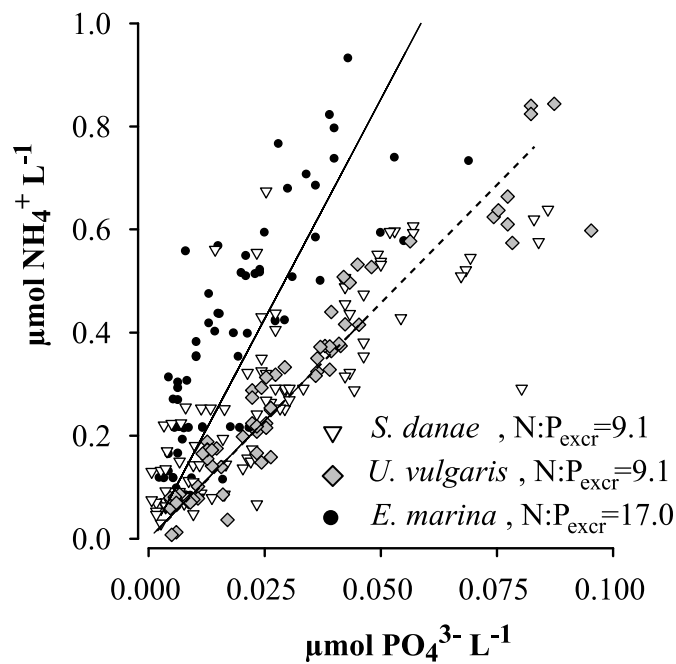


Figure III.4: Summarized ammonium and phosphate concentrations determined in copepod incubations at 21.7 to 23.0°C. Slopes of regressions represent mean N:P_{excr} .

In all species N:P_{excr} was higher at those stations with a higher mean PON:POP (Fig. III.5) in the upper 150 m, although variability in water column PON:POP is very high, hampering the establishment of a functional relationship. Complementary feeding experiments can help to resolve which fraction of ingested matter is egested as fecal pellets, excreted as dissolved inorganic nutrients, or becomes incorporated in zooplankton biomass.

Weight-specific zooplankton excretion is a function of temperature and body size (Ikeda 1985; Ikeda et al. 2001), but is also strongly influenced by phytoplankton biomass, size distribution, and taxonomic composition as well as internal nutrient ratios.

Because of changing interactions between phytoplankton biomass as well as taxonomic and elemental composition, quantification of the zooplankton contribution to N and P cycling remains challenging.

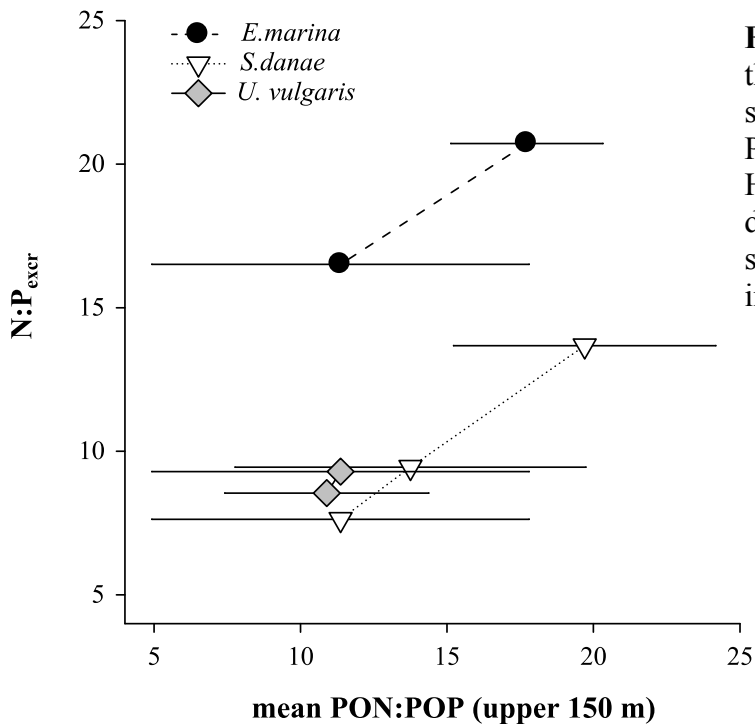


Figure III.5: N:P excretion ratio of three epipelagic copepods at different stations characterized by the mean PON:POP in the upper 150 m. Horizontal error bars represent standard deviation of the mean PON:POP from 8 sampling depths. Copepods were incubated at 21.7 to 23.0°C.

Regarding temperature effects on excretion rate, *U. vulgaris* was the most sensitive species (Fig. III.6). Q_{10} values calculated by the difference in ammonium and phosphate excretion rate were 1.7 and 2.0 for *S. danae*, respectively, and 3.3 and 3.6 for *U. vulgaris*. In *E. marina*, the Q_{10} value estimated using ammonium excretion rate was 1.9. The warmer incubation temperature approximately represents that of the 40-50 m depth, where the deep chlorophyll-*a* maximum is located. The colder temperature corresponds to approximately 200-250 m depth at the stations sampled. The three copepod species measured in the present study are considered epipelagic species that are usually non-migratory and largely reside in the upper 200 m of the water column (Hayward 1980; Ambler & Miller 1987; Séguin 2010). Thus, 11°C represents the lower end of the temperature range that is experienced by these species in the tropical ocean. As the presented dataset is rather limited, we cannot conclude whether the different Q_{10} values estimated for P and N excretion (slightly lower in the latter) represent a true differential impact of temperature of these metabolic processes. In his first comprehensive study on the allometric scaling of

metabolic rates as a function of temperature, Ikeda (1985) estimated Q_{10} values for phosphate excretion to be slightly lower (on average 1.55) than those for ammonium excretion (1.91 to 1.93). This was confirmed in a later analysis (Ikeda et al. 2001), albeit with a smaller difference between the two (1.6-1.9 and 1.8-2.0 for P and N excretion, respectively). No significant impact of temperature on the N:P excretion ratio was detected. However, these calculations were performed on a dataset where surface-dwelling species from different ocean regions (and the respective *in situ* temperature) were compared. If this differential effect of temperature (i.e., region) on N and P cycling, it would mean that tropical species excrete relatively more N than their boreal counterparts.

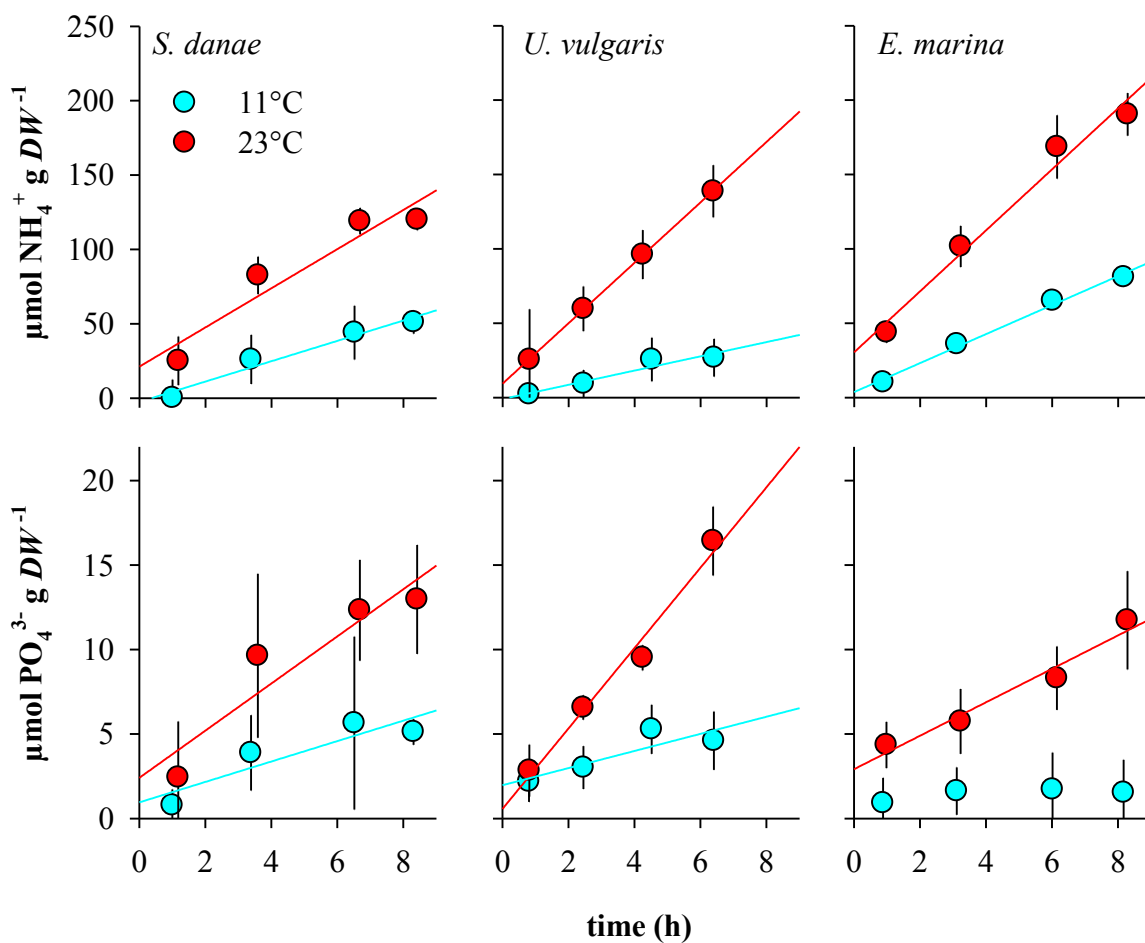


Figure III.6: Weight-specific excretion of ammonium (NH_4^+ , top row) and phosphate (PO_4^{3-} , bottom row) of three copepod species at two temperatures (red: 23°C, blue: 11°C) over time. Values are means \pm standard deviation. Lines are linear regressions fitted through the data.

Recent findings by Sartoris et al. (2010) suggest that there is a seasonal accumulation of ammonium in diapausing Antarctic copepods that undergo ontogenetic vertical migration, which may contribute to neutral buoyancy. It seems possible that in species that perform DVM, the discharge of (positively buoyant) nitrogenous waste products may be delayed before and during ascent and increased before descent, which would be energetically favourable and could be controlled by temperature. To our knowledge, this has not been investigated yet in oceanic migrant zooplankton, however diel periodicity in ammonium excretion in coastal waters has been documented but largely assigned to nighttime feeding rather than metabolic downregulation at depth (e.g. Harris & Malej 1986).

These findings support our initial hypotheses that herbivores may be able to exacerbate imbalances in dissolved inorganic nutrient supply in the photic zone. Our results emphasize the need for a thorough assessment of zooplankton functional types with respect to their vertical distribution as well as migration patterns. Further, concomitant ingestion, excretion and fecal pellet production measurements should be conducted if the contribution of mesozooplankton to surface nutrient recycling is to be understood.

The dependence of excretion ratios of different zooplankton functional groups on food quality, quantity, and abiotic conditions therefore needs to be studied further in order to parameterize the impact of zooplankton on the nutrient balance in biogeochemical models. Besides being important for the nutrient balance within the euphotic zone, zooplankton organisms have a high potential to impact dissolved nutrient dynamics in tropical oceans, especially those that feed in surface waters during night-time and migrate below 200 m water depth at day-time to avoid visual predators. These Diurnal Vertical Migrations (DVMs) are an important factor in oxygen losses within the ocean interior, acting both directly, via zooplankton respiration at depth during daytime (Marcus 2001) and indirectly, via enhanced transfer of organic matter from the euphotic zone to deeper water layers.

As Hannides et al. (2009) pointed out, little research has focused on the migrant-mediated export and recycling of P, while the majority of literature data comprises only C and N fluxes (e.g. Al-Mutairi & Landry 2001; Steinberg et al. 2002). We are only aware of two studies that has evaluated migrant-mediated P export from and recirculation within surface waters (Le Borgne & Rodier 1997; Hannides et al. 2009) of which the latter compared the active transport with passive sinking flux. However, nitrogen and phosphorus excretion were not measured directly, but derived from empirical allometric relationships. Thus, the impact of zooplankton community and phytoplankton elemental composition was not taken into account.

In order to parameterize the impacts of zooplankton on fluxes of nutrients in biogeochemical models, detailed information on abundance, biomass and vertical migration patterns are necessary. Furthermore, as synergistic effects of low temperature, low pO_2 and high pCO_2 could potentially result in strong metabolic rate reductions, field studies investigating zooplankton metabolism at *in situ* conditions are a challenging but needed task to provide a more mechanistic basis for biogeochemical models.

Chapter IV

Relative contribution of upwelled and atmospheric nitrogen to the eastern tropical North Atlantic food web: Spatial distribution of $\delta^{15}\text{N}$ in mesozooplankton biomass and relation to dissolved nutrient dynamics

Helena M. Hauss, Jasmin Franz, Thomas Hansen, Ulrich Struck and Ulrich Sommer

Abstract

The Eastern Tropical North Atlantic (ETNA) is characterized by a strong east to west gradient in the vertical upward flux of dissolved inorganic nitrogen to the photic zone. During a study of stable nitrogen isotope ($\delta^{15}\text{N}$) signatures of various zooplankton taxa covering twelve stations in the ETNA (04°-14°N, 016-030°W) in fall 2009, we found that $\delta^{15}\text{N}$ values were markedly different among stations. These differences were greater than those between trophic levels and revealed an increasing atmospheric input of nitrogen by N_2 -fixation and Aeolian dust in the open ocean as opposed to remineralized NO_3^- close to the NW African upwelling. In order to investigate the spatial distribution of upwelling-fuelled versus diazotroph-derived production more closely, we examined the stable nitrogen signatures in size-fractionated zooplankton as well as in three widely distributed copepod species on a second cruise in fall 2010 in the ETNA (02-17°35'N, 015-028°W). Sampling was conducted on 25 stations along with dissolved nutrients determined at eight depths <150m, continuous chlorophyll-*a* profiles, and copepod RNA/DNA ratio of the three species as a proxy for nutritional condition. High standing stocks of chl-*a* were associated with shallow mixed layer depth and thickening of the nutricline. As the nitracline was generally deeper and less thick than the phosphocline, it appears that non-diazotroph primary production was limited by N rather than P throughout the study area. Estimated by the $\delta^{15}\text{N}$ in zooplankton, atmospheric sources of new N contributed less than 20% close to the African coast and in the Guinea Dome area and up to 60% at the offshore stations, depending on the depth of the nitracline. $\delta^{15}\text{N}$ was highly correlated between three different copepod species in spite of their distinctly different feeding ecology as indicated by spatial patterns of their RNA/DNA ratio.

IV.1 Introduction

In the Eastern Tropical North Atlantic (ETNA), a marked east to west gradient exists in the dissolved inorganic nutrient load between surface waters affected by coastal upwelling and large oligotrophic areas in the central and western parts of the basin. Remote sensing of ocean colour indicates high standing stocks of phytoplankton biomass within and close to the Mauritanian Upwelling off NW Africa, contrasting vast areas of low productivity in the tropical North Atlantic (Longhurst et al. 1995; Hoepffner et al. 1999). Within these coastal upwelling zones, the supply of inorganic nutrients to the upper mixed layer is low in nitrogen relative to phosphorus, and the export of organic nitrogen from the photic zone exceeds the vertical supply of DIN (Agusti et al. 2001). Both result in overall N-limitation of non-diazotroph primary production at the surface. In turn, this supposedly leads to a competitive advantage of diazotrophic cyanobacteria that are ultimately P and Fe-colimited and therefore benefit from the DIP surplus as well as from the atmospheric iron input by Saharan dust deposition (Mills et al. 2004). Biogeochemical estimates of N₂-fixation in the North Atlantic support this view (Hansell et al. 2004). These estimates are based on the observation of net “excess N” (N* as a measure of deviation from the Redfield ratio) in the pool of inorganic nutrients at depth (~150-400 m) due to the remineralization of diazotroph-derived N-rich particulate organic matter (Gruber & Sarmiento 1997). However, the relative importance of diazotroph and non-diazotroph primary production often remains somewhat unclear, especially in regions of strong spatial gradients in the vertical flux of nutrients to the photic zone.

N₂-fixation by filamentous cyanobacteria of the genus *Trichodesmium* has been demonstrated to contribute significantly to the nitrogen pool of the oligotrophic tropical and subtropical Atlantic (Capone et al. 2005). While most observations emphasize its importance in the western part of the basin (Carpenter & Romans 1991; Montoya et al. 2002; Capone et al. 2005; Goebel et al. 2010), direct measurements of cyanobacterial abundance and/or N₂-fixation in the ETNA, and especially in the Guinea Dome area, are scarce and vary by orders of magnitude depending on the season and the methods used (Voss et al. 2004; Capone et al. 2005; Staal et al. 2007). Satellite imagery has revealed some seasonality in the formation of *Trichodesmium* blooms in the ETNA (Westberry & Siegel 2006), with the largest areal expansion in the fall quarter (Sep-Nov). However, the authors point out that the pattern is less distinct than in other ocean basins and likely due to single dust pulses. Still, this would be consistent with point observations on Atlantic Meridional Transect (AMT) cruises in fall and spring (Tyrrell et al. 2003) and observations close to the NW African coast (16-22°N) by Margalef (1973) and Vallespinós

(1985). Using a coupled biological-physical model, Hood et al. (2004) predicted high abundances of *Trichodesmium* and, consequently, high rates of N₂-fixation in the ETNA based upon ecological characteristics of this genus. Because it was considered the only diazotroph in this model, this might be rather an underestimation, as non-filamentous cyanobacteria and heterotrophic bacteria comprising *nifH*-genes were found even at depth and when nitrate was still available (Langlois et al. 2005), contrasting the optimal environmental conditions of *Trichodesmium* (warm, N-depleted surface waters). Further, it was suggested that small diazotroph play a larger role compared to *Trichodesmium* east of 40°W (Montoya et al. 2007). Using an improved N₂ fixation measurement technique, Mohr et al. (2010) demonstrated that especially non-filamentous cyanobacterial N₂-fixation is vastly underestimated with standard methods, suggesting the importance of unicellular diazotroph contribution to the overall N-budget.

As zooplankton in the oligotrophic open ocean are expected to rely relatively more on protozoan prey compared to direct consumption of phytoplankton (Stoecker & Capuzzo 1990; Sommer & Sommer 2006), and phagotrophic flagellates and ciliates directly ingest unicellular cyanobacteria, this contingent may quite efficiently enter the metazoan food web (Sommer et al. 2006). As a result of pulsed N₂ tracer incubations near Cape Verde, Wannicke et al. (2010) estimated that direct grazing accounts for approximately half of gross mesozooplanktonic N incorporation, while the rest was channelled through the microbial loop. Direct foraging on *Trichodesmium* filaments has only been observed for few zooplankton species, especially harpacticoid copepods (O'Neil & Roman 1994), but *Trichodesmium*-associated communities include diatoms, dinoflagellates and ciliates (Sheridan et al. 2002) that provide suitable prey items for a variety of zooplankton species. Furthermore, diatom-diazotroph associations (DDAs, e.g. *Rhizosolenia* and *Chaetoceros* associated with *Calothrix rhizosoleniae* and *Richelia intracellularis*, respectively) can provide a pathway of direct transfer of diazotroph N to consumers (Foster et al. 2009). In this context, the export efficiency of surface diazotroph-derived N also depends on the composition of the diazotroph community. The large and spiny diatom host cells of DDAs not only aggregate and sink fast, but are also readily consumed and repackaged into fecal pellets by mesozooplankton. Mesozooplankton contribute significantly to export of matter from surface waters, not only due to active diel vertical migration with nighttime feeding at the surface and daytime metabolic activity (defecation and excretion) at depth (Steinberg et al. 2002), but also by repackaging of particles into fecal pellets and thus increasing their sinking velocity. However, a considerable fraction (Isla et al. 2004) of ingested nitrogen is also directly recycled by excretion within the photic zone.

Stable carbon and nitrogen isotopes have been widely used to examine trophic interactions in aquatic systems, as well as characterizing sources and sinks. Specifically, low $\delta^{15}\text{N}$ values of particulate organic matter are known to correspond to high rates of biological N_2 -fixation and/or dust input (Ryabenko et al. 2011). Montoya et al. (2002) found that the $\delta^{15}\text{N}$ values of size-fractionated mesozooplankton was decreasing from east to west in the western and central tropical North Atlantic (approximately 030° to 055°W), corresponding to increasing abundance of *Trichodesmium*. In a recent study spanning the subtropical Atlantic at 32°N , the contribution of fixed N_2 to the pelagic food web at different depth layers was quantified (Landrum et al. 2011) by attributing low $\delta^{15}\text{N}$ values entirely to phototrophic N_2 -fixation. However, dust deposition is not only providing an iron source to surface waters, fuelling N_2 -fixation, but also contains substantial amounts of inorganic dissolved nitrogen as NO_x and NH_x (Baker et al. 2003; Formenti et al. 2003) with an isotopic signature <0 that is readily available to phytoplankton (Aberle et al. 2010).

In this study, we aimed to spatially resolve the differential impact of new (i.e. atmospheric) and remineralized (upwelled) inorganic nitrogen to the food web via stable nitrogen isotopic signatures of zooplankton. An additional aim was to assess whether the choice of analyzed species influences the resulting observed spatial distribution of zooplankton $\delta^{15}\text{N}$ values due to differences in feeding ecology.

IV.2 Materials and Methods

Sampling and analyses

Sampling was conducted during two cruises with RV *Meteor* in the ETNA (Fig. IV.1) from Nov 26 to Dec 22, 2009 (M80-2), and from Oct 14 to Nov 13, 2010 (M83-1). Zooplankton was collected at 22 and 25 stations in 2009 and 2010, respectively, using a WP-2 plankton net with a mesh size of $150\ \mu\text{m}$ and a solid cod-end that was heaved vertically from 100 or 50 m depth to the surface with a speed of $0.2\ \text{m s}^{-1}$. After careful rinsing, zooplankton was diluted in three 30 L buckets filled with filtered seawater and sorted under a dissecting microscope. On M80-2, a greater variety of taxa was sampled for stable isotope analysis with varying number of replicate samples and number of individuals pooled per sample, depending on the abundance in the sample and size of the species. On M83-1 we focused on three epipelagic copepod species that are found throughout the study area, and sampled in parallel for stable isotope analysis and RNA/DNA analysis. For single species stable isotope analysis, adult females were dipped in distilled water, transferred into tin capsules ($3.2 \times 4\ \text{mm}$, Hekatech) with two individuals per tin

vial and three replicate samples per haul and dried for 24 h at 50°C. For RNA/DNA analysis, up to five adult females per species and station were individually transferred into 1.5-ml cap vials and immediately frozen at -80°C to be analysed in the laboratory ashore. Subsequent sieving of the remaining zooplankton samples onto 500, 200 and 100- μm mesh screens created three size fractions (<200 μm , 200-500 μm and >500 μm) which were scraped into cap vials and dried to constant weight at 50°C. Size-fractionated samples were then ground to powder, a subsample transferred in a pre-weighed 5x9 mm Hekatech tin capsule, its dry weight determined and stored until analysis in a desiccator. On the same stations, vertical profiles of temperature, salinity, and chl-*a* were obtained by a Seabird 9 plus CTD (conductivity/temperature/depth) with a Dr. Haardt fluorescence probe mounted on a 24x10 L Niskin bottle sampling rosette.

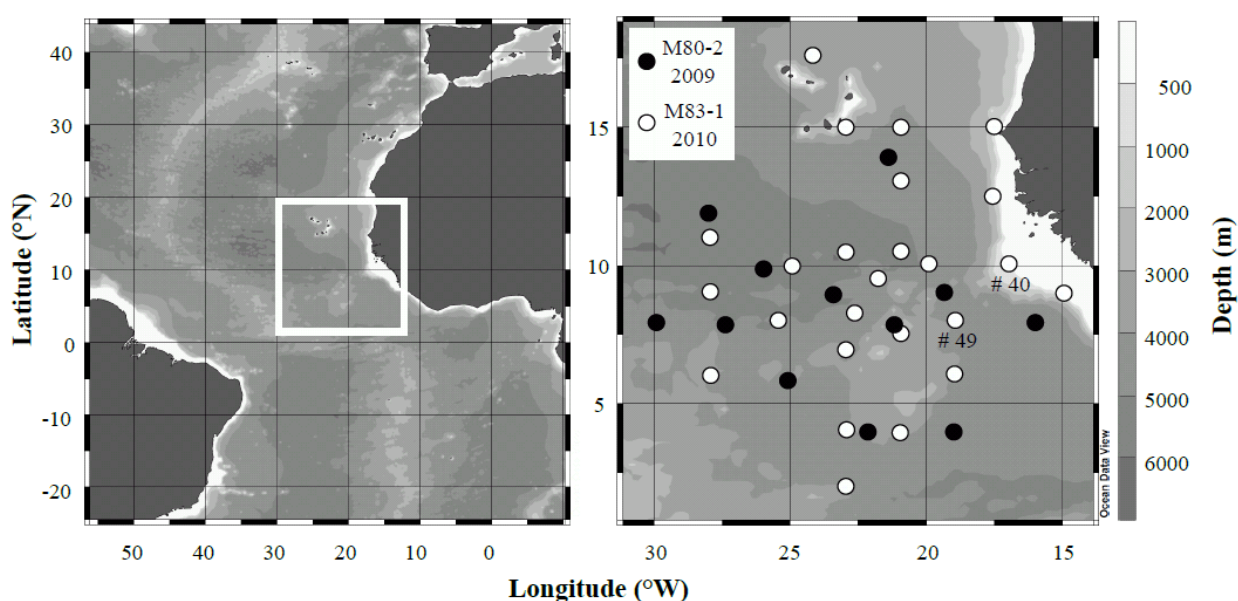


Figure IV.1: Overview of sampling area (white rectangle) in the tropical eastern North Atlantic. Sampling stations are indicated by black (M80-2) and white (M83-1) circles. The two stations marked (profiles 40 and 49) are those represented in figure IV.2.

The fluorescence probe was cross-calibrated with 353 chl-*a* samples along the cruise that were 0.2 μm -filtered and extracted using acetone, frozen at -80°C for >5 h and measured against a blank in a Turner fluorometer calibrated with a chl-*a* standard (Sigma C5753) dilution series. Integrated chl-*a* values (mg m^{-2}) were calculated using 1m-depth interval fluorescence-derived profiles to a maximum depth of 150 m. Dissolved inorganic macronutrients (NO_3^- , NO_2^- , NH_4^+ , PO_4^{3-}) were sampled at 8 depths within the upper 150 m (fixed depths 150, 100, 80, 60, 40, 20, and 10 m, plus one sample within the chl-*a* maximum) and analysed immediately on board using a four-channel Quatro autoanalyzer. Standard deviations for NO_3^- , NO_2^- , and PO_4^{3-} in these

analyses are 0.03, 0.04, and 0.01 $\mu\text{mol L}^{-1}$, respectively, and detection limits are 0.03, 0.01, and 0.01 $\mu\text{mol L}^{-1}$, respectively.

The RNA-DNA ratio as an indicator of nutritional condition was analysed in individual female copepods. Samples were freeze-dried for >16 h, their dry weight determined, and concentrations of RNA and DNA measured fluorometrically according to Malzahn et al. (2007), with ethidium bromide as fluorophore and digesting RNA with Ribonuclease A (bovine pancreas, Serva 34388). Nucleic acid standards were Bacteriophage λ -DNA (Roche 745782) and 16s, 23s rRNA (*E. coli*, Roche 206936). To ensure consistency over time, two control samples (from a pooled stock homogenate) were measured within each 96-well microplate.

Due to limited laboratory capacity and different biomass requirements for single species and size-fractionated bulk zooplankton, stable isotope samples had to be measured with differing analytical setups: Stable isotope measurements of samples with low biomass taken from the M80-2 cruise were performed using a high sensitive elemental analyzer (CE INSTRUMENTS EA1110) connected to a stable isotope ratio mass spectrometer (Delta^{Plus} Advantage, Thermo Fisher Scientific, Bremen, Germany). As an internal standard, acetanilide with a mean (\pm SD) $\delta^{15}\text{N}$ and $\delta^{13}\text{C}$ of $-2.56(\pm 0.24)\text{‰}$ and $-30.44(\pm 0.2)\text{‰}$ was measured after every sixth sample (Hansen & Sommer 2007). Stable isotope measurements of the M83-1 single species samples were performed on a Flash-EA 2000 coupled to a Delta V isotope-ratio mass spectrometer (Thermo Fisher Scientific). Peptone as an internal lab standard with a known isotopic composition ($\delta^{15}\text{N}=7.6\text{‰}$; $\delta^{13}\text{C}=-14.3\text{‰}$) was used after every fifth unknown sample. The standard deviation for replicate samples was $<0.2\text{‰}$ for both isotopes. Size-fractionated samples from M83-1 were measured using a PDZ Europa ANCA-GSL elemental analyzer interfaced to a PDZ Europa 20-20 isotope ratio mass spectrometer (Sercon Ltd., Cheshire, UK). During analysis, samples were interspersed with several replicates of at least two different laboratory standards selected to be compositionally similar to the samples being analyzed. The long term standard deviation for $\delta^{15}\text{N}$ is 0.3‰. All system calibrations were implemented by the combustion of international accepted standards (IAEA-N1, -N2, -N3, USGS-40, -41 and NBS22). Stable isotope ratios are expressed in conventional δ notation, i.e. parts per thousand deviations from a standard (air), using the equation $\delta^{15}\text{N}(\text{‰}) = [(R_{\text{Sample}}:R_{\text{Standard}}) - 1]*1000$, where R is the $^{15}\text{N}:^{14}\text{N}$ ratio.

Data analysis

For M80-2, the resolution of nutrient measurements in the surface layers was too low to accurately determine nutricline depth; for M83-1, the depth of the nitracline and phosphacline was determined by fitting sigmoid functions through the observed NO_3^- and PO_4^{3-} concentrations at depths down to 150 m:

$$(IV.1) \quad C = \frac{a}{(1 + e^{-(z-z_{50})/b})}$$

Where C is the observed concentration ($\mu\text{mol L}^{-1}$) of the respective nutrient, z is depth and z_{50} is the inflection point of the nutrient concentration increase with depth (i.e., the steepest slope) and defined as the nutricline depth (Fig. IV.2). All regressions were significant, with r^2 values ranging between 0.95 and 0.99. To estimate the thickness of the nutricline H , the functions were then used to calculate the depths at which 10% and 90% of the respective subsurface nutrient concentration were reached, and the vertical distance between them defined as H (Fig. IV.2). We chose to use nitrate concentrations rather than total DIN in this approach, because NO_2^- and NH_4^+ are regenerated within the photic zone and thus have different vertical distributions and dynamics.

A multiple linear regression with $\delta^{15}\text{N}$ depending on the $z_{50\text{N}}$, H_{N} , and $H_{\text{N}}-H_{\text{P}}$ was used to determine the maximum $\delta^{15}\text{N}$ of each species or size fraction analyzed under strong upwelling ($\delta^{15}\text{N}_{\text{REF}}$) when regenerated nitrogen represents 100% of N available to biological production, i.e. $\delta^{15}\text{N}_{\text{REF}}$ is the regression intercept. While we cannot distinguish between N input by Aeolian dust and by N_2 -fixation, we assumed an average isotopic signature of diazotroph-derived N of $\delta^{15}\text{N}_{\text{D}} = -2\text{‰}$, which is in line with diazotroph POM $\delta^{15}\text{N}$ values (Montoya 2008) and slightly higher than average dust $\delta^{15}\text{N}$ (-3‰ , Baker et al. 2007), and calculated its contribution to zooplankton production following Landrum et al. (2011):

$$(IV.2) \quad \%N_{\text{D}} = 100 * \frac{(\delta^{15}N_{\text{ZOO}} - \delta^{15}N_{\text{REF}})}{(\delta^{15}N_{\text{D}} - \delta^{15}N_{\text{REF}})}$$

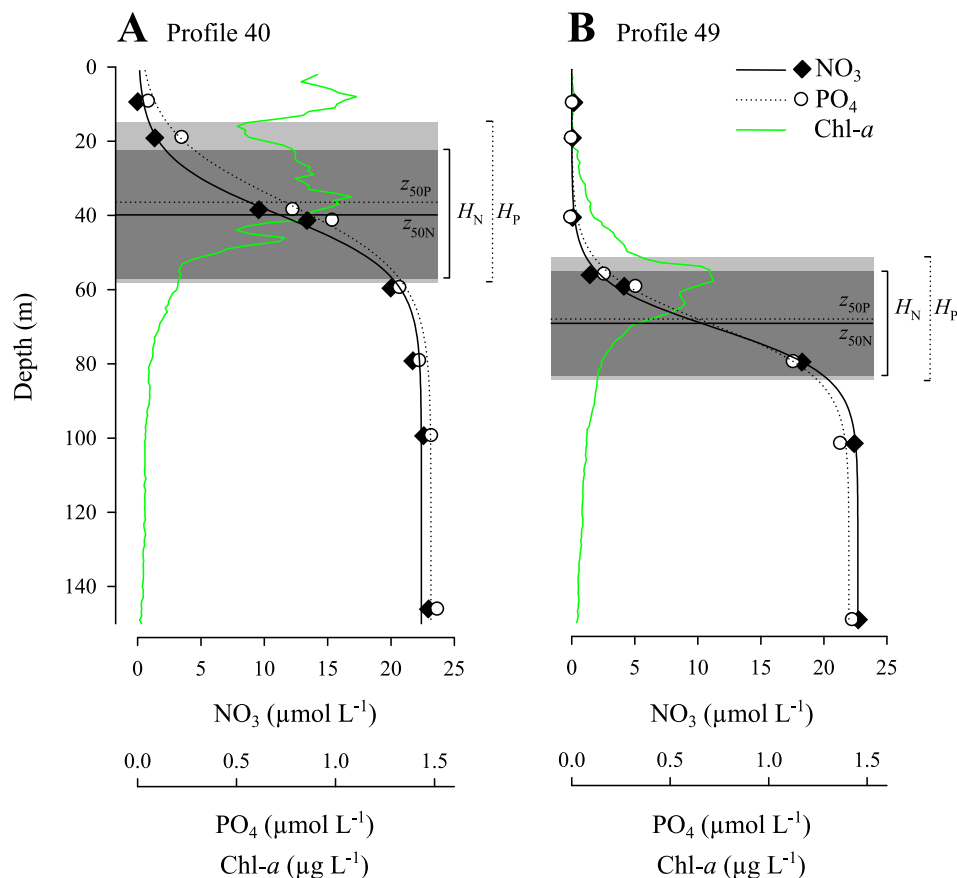


Figure IV.2: Two nutrient and chl-*a* profiles from M83-1 (fall 2010) on the shelf (#40, panel A) and offshore (#49, panel B) to illustrate the estimation of nutricline depth (inflection point of sigmoid functions z_{50} , horizontal lines) and thickness (distance between depths where 10 and 90% of concentration below photic zone is reached, height H of grey boxes). Symbols are measured values. At the three surface depths of #49 concentrations of both NO_3^- and PO_4^{3-} are close to zero, therefore symbols are partly concealed. Continuous chl-*a* profile from CTD is overlaid to indicate phytoplankton distribution. For location of these stations refer to figure IV.1.

IV.3 Results

The spatial distribution of integrated chl-*a* was characterized by high standing stocks on and close to the West African shelf (Fig. IV.3 A), with the exception of one shelf station at $12^\circ 30' \text{N}$ which featured comparatively low chl-*a* concentrations ($< 30 \text{ mg m}^{-2}$). While very low values of less than 20 mg m^{-2} prevailed in most of the offshore area, two centres of slightly higher chl-*a* values were observed, one approximately $07\text{--}09^\circ \text{N}$ and $020\text{--}023^\circ \text{W}$, an area characterized by rough bathymetry (Fig. IV.1) and high diapycnal flux (Banyte et al. in press), and one single station at the western margin of the investigation area (at 09°N , 028°W). The nitracline depth revealed a similar spatial pattern, being shallower than 50 m at the onshore stations and as deep as 80 m offshore (Fig. IV.3 B). Nitracline thickness was quite variable throughout the sampling

area (Fig. IV.3 C). The vertical distance between the nitracline and the phosphacline was largest close to the coastal upwelling, and almost zero in the offshore area (Fig. IV.3 D).

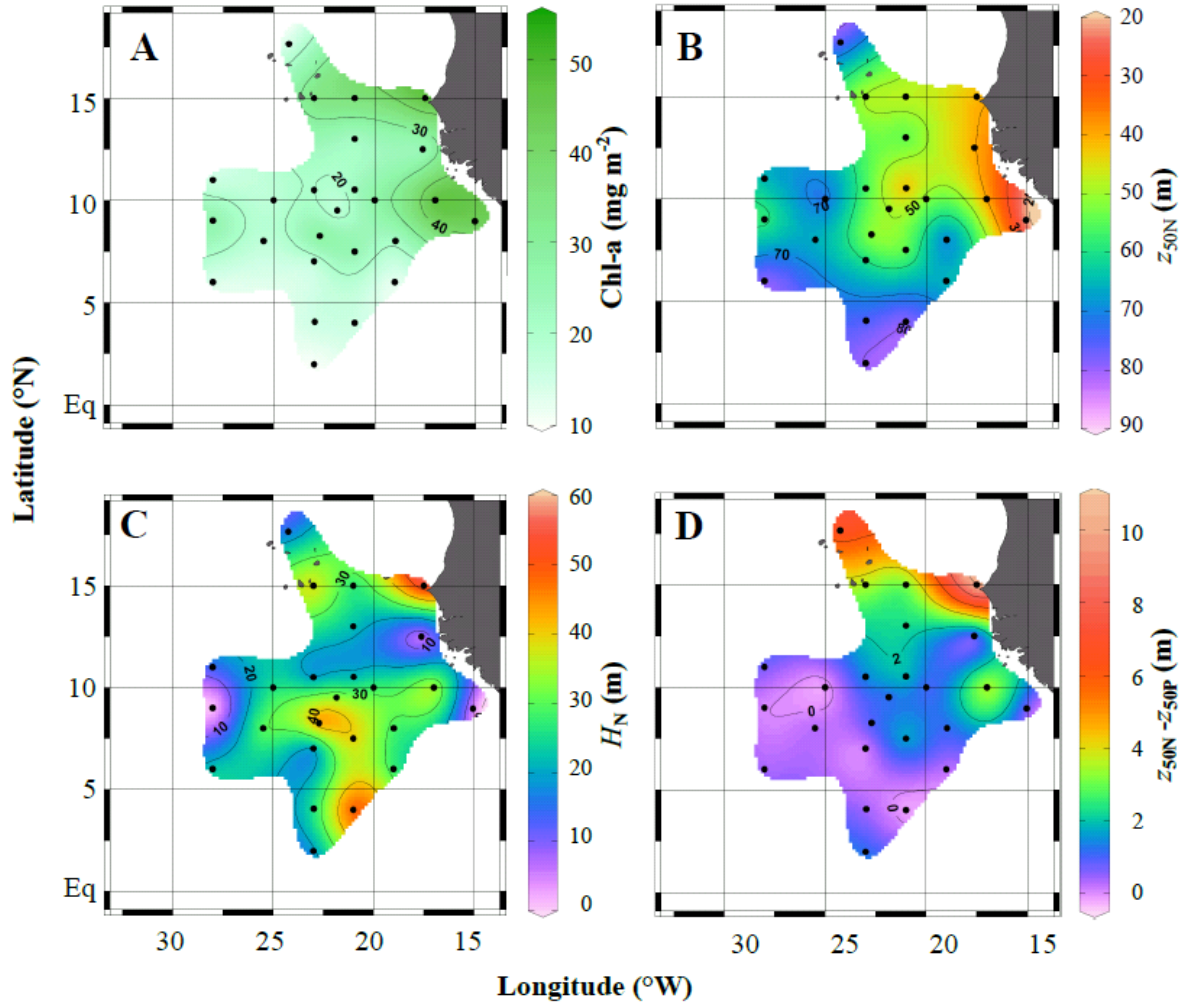


Figure IV.3: Spatial distribution of integrated chlorophyll-*a* (mg m^{-2} , panel A), nitracline depth z_{50N} (m, panel B), nitracline thickness H_N (m, panel C) and the vertical distance between nitracline and phosphacline depth $z_{50N} - z_{50P}$ (m, panel D) as observed in October/November 2010. Contour plots of horizontal distribution were created using OceanDataView 4 (Schlitzer 2009).

The depth of the phosphacline and the depth of the nitracline were strongly related (Fig. IV.4 A, $r^2=0.98$) with a slope of $1.04(\pm 0.03)$. However, an intercept of $-3.87(\pm 1.96)$ indicated that the sharpest nutrient concentration increase was on average almost 4 m shallower for phosphate than for nitrate. Moreover, as indicated by the intercept of the regression of H_P as a function of H_N , the nutricline was consistently thicker for phosphate than for nitrate (Fig. IV.4 B) by $7.58(\pm 3.77)$ m.

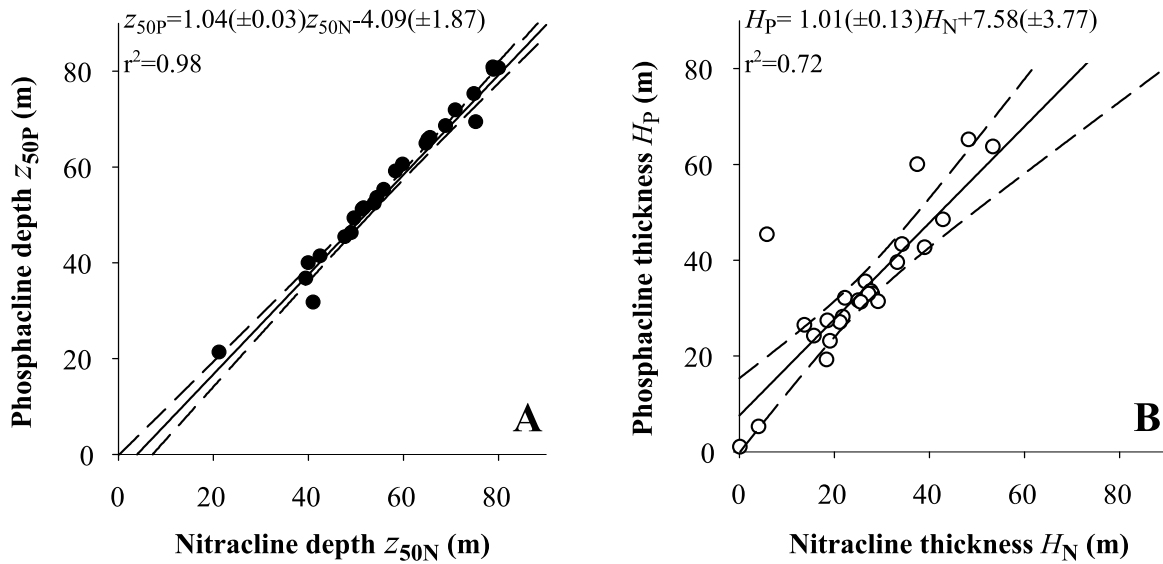


Figure IV.4: Relationship between depth of the phosphacline (m) and the depth of the nitracline (m), defined as the depth of greatest increase z_{50} (panel A), and between phosphacline thickness (m) and nitracline thickness (m), defined as the layer between 10% and 90% of the maximum value reached within the upper 150m (panel B). Solid line denotes linear regressions with 95% confidence interval (dashed).

Integrated chl-*a* was highly correlated with nitracline depth (negative) and thickness (positive). A multiple linear regression with z_{50N} and H_N as independent variables described 72% of the variability in chl-*a* (Fig. IV.5), with all regression parameters being significantly different from zero ($p < 0.05$). In spite of the close relationship between the two nutrient distributions, and while the depth of the phosphacline was also a significant predictor of chl-*a*, its thickness was not ($p = 0.16$).

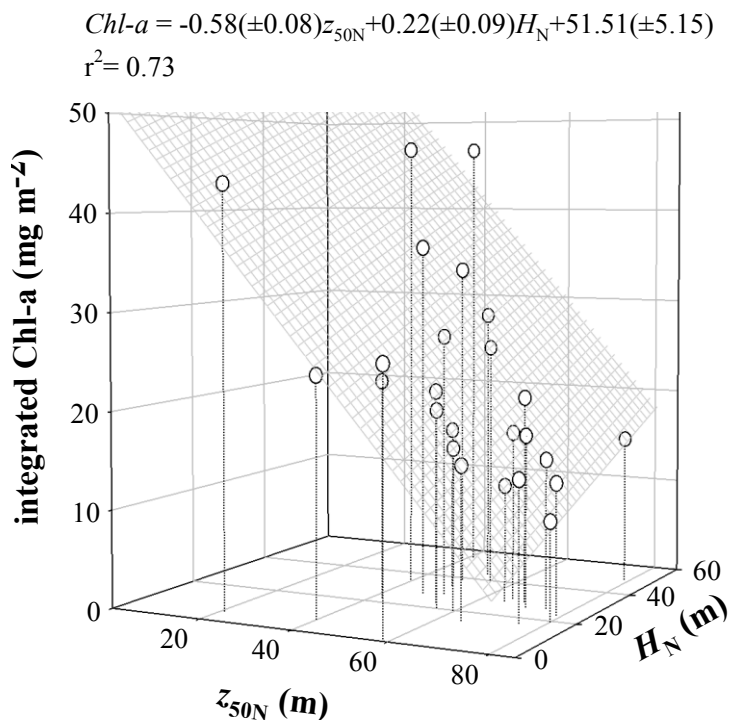


Figure IV.5: Multiple linear regression (grey mesh) and observed values (black circles) of integrated chlorophyll-*a* (mg m^{-2}) depending on the nitracline depth z_{50N} (m) and its thickness H_N (m).

Mean $\delta^{15}\text{N}$ of zooplankton pooled according to their presumed feeding type (carnivore, omnivore, herbivore) sampled on M80-2 (December 2009) was highly variable (Fig. IV.6). Within stations, $\delta^{15}\text{N}$ was enriched according to the presumed trophic levels, with a mean ($\pm\text{SD}$) difference of $1.3(\pm 1.06)\text{‰}$ between herbivores and omnivores and $0.7(\pm 0.5)\text{‰}$ between omnivores and carnivores. Among stations, maximum differences within the carnivore, omnivore and herbivore group were 2.5, 2.1 and 3.9‰ , respectively. $\delta^{15}\text{N}$ decreased from east to west, with generally higher values east of 022°W (Fig. IV.6). $\delta^{15}\text{N}$ from omnivores and carnivores were closely correlated ($r=0.84$, $p<0.05$), however $\delta^{15}\text{N}$ data from pure herbivores were lacking on some stations, and no significant correlation with the other two feeding type groups was found.

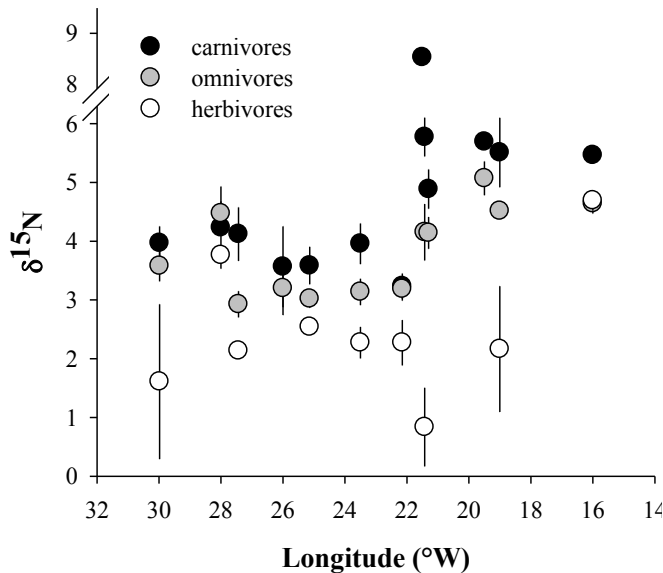


Figure IV.6: Mean $\delta^{15}\text{N}$ of major zooplankton feeding types versus longitude ($^\circ\text{W}$) sampled on M80-2 in December 2009. Values are station means ($\pm\text{SE}$). Pooled as carnivores are larval fish, siphonophores, pteropods (Gymnosomata), *Phronima* sp. (Amphipoda), *Lucifer* sp. (Decapoda), *Tomopteris* sp. (Phyllococida), and *Euchaeta marina*; omnivores include euphausiids, salps, saphirinid and pontellid copepods, *Corycaeus* spp., *Oithona* spp., *Oncaea* spp., *Eucalanus* spp., *Candacia* spp., and *Scolecithrix danae*; herbivores are appendicularians, *Microsetella* spp., *Miracia* spp., and *Undinula vulgaris*.

Mean ($\pm\text{SD}$) $\delta^{15}\text{N}$ values observed in copepods in November 2010 (M83-1) ranged from $2.39(\pm 1.09)$ to $7.33(\pm 0.4)$ in *E. marina*, from $1.77(\pm 0.49)$ to $7.23(\pm 0.19)$ in *S. danae* and from $1.93(\pm 0.33)$ to $6.87(\pm 0.39)$, in *U. vulgaris* (Fig. IV.7, top row). Data from all three species were very closely correlated (Table IV.1). Of the size-fractionated bulk zooplankton, the largest size fraction ($>500\ \mu\text{m}$) agreed least with the single species data (r values ranging from 0.57 to 0.72, Table IV.1), and also with the smaller size fractions. In all species and size fractions, the highest values were observed in the eastern part of the study area and the lowest values occurred on the southernmost stations (Fig. IV.7, top row).

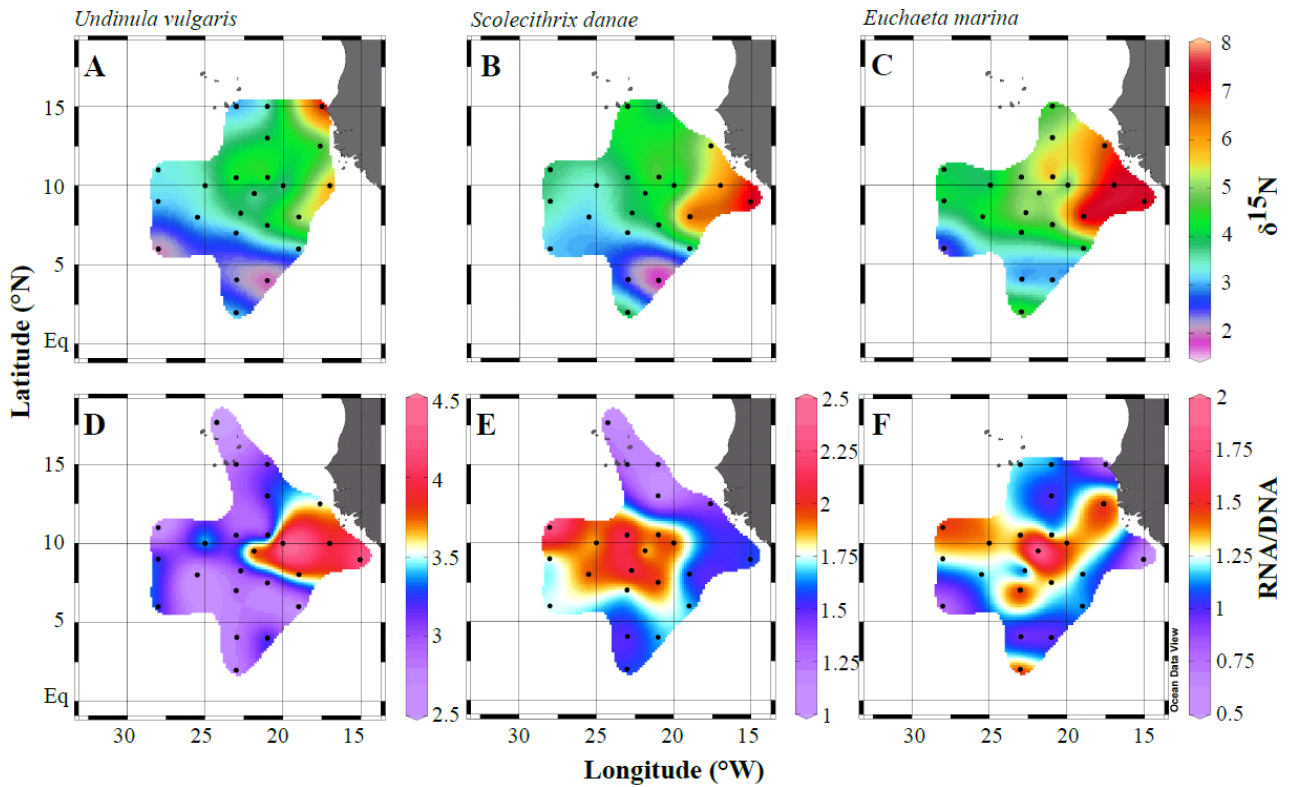


Figure IV.7: Spatial distribution of $\delta^{15}\text{N}$ (top row) and RNA/DNA (bottom row) for the three copepod species *U. vulgaris* (panels A, D), *S. danae* (panels B, E) and *E. marina* (panels C, F) determined in October/November 2010. Contour plots of horizontal distribution were created using OceanDataView 4 (Schlitzer 2009).

Table IV.1: Correlation matrix for $\delta^{15}\text{N}$ determined in three different copepod species and zooplankton size fractions. Shown are r values ($p < 0.05$) for the different combinations.

	<i>U.vulgaris</i>	<i>S.danae</i>	>500 μm	200-500 μm	<200 μm
<i>E.marina</i>	0.95	0.94	0.62	0.83	0.81
<i>U.vulgaris</i>		0.90	0.57	0.85	0.93
<i>S.danae</i>			0.72	0.83	0.95
500 μm				0.79	0.81
200-500 μm					0.94

Table IV.2: Stepwise multiple linear regression results for $\delta^{15}\text{N}$ of three different copepod species and zooplankton size fractions as a function of nitracline depth ($z_{50\text{N}}$), nitracline thickness (H_{N}) and distance between nitracline and phosphacline ($z_{50\text{N}} - z_{50\text{P}}$). Bold letters are parameter estimates for significant in regression; asterisks denote significance level (*** $p < 0.001$, ** $p < 0.01$, * $p < 0.05$).

			intercept		$z_{50\text{N}}$		H_{N}		$z_{50\text{N}} - z_{50\text{P}}$		
	n	total r^2	B	($\pm\text{SE}_B$)	r^2 added	B	($\pm\text{SE}_B$)	r^2 added	B	($\pm\text{SE}_B$)	r^2 added
species											
<i>U.vulgaris</i>	60	0.60	5.58 (± 0.58)**		-0.04 (± 0.01) 0.47***		-0.004 (± 0.009) 0.00		0.27 (± 0.07)		0.13***
<i>S.danae</i>	60	0.64	7.52 (± 0.53)**		-0.05 (± 0.01) 0.60***		-0.027 (± 0.01) 0.03**		0.20 (± 0.12)		0.02
<i>E.marina</i>	59	0.53	8.23 (± 0.66)**		-0.06 (± 0.01) 0.52***		-0.005 (± 0.012) 0.00		0.18 (± 0.16)		0.01
size fraction (μm)											
<200	11	0.82	9.86 (± 1.83)**		-0.10 (± 0.02) 0.48**		-0.028 (± 0.031) 0.04		0.52 (± 0.15)		0.30*
200-500	25	0.81	7.77 (± 0.63)**		-0.07 (± 0.01) 0.69***		0.003 (± 0.012) 0.03		0.22 (± 0.07)		0.10**
>500	25	0.52	10.33 (± 1.38)**		-0.09 (± 0.02) 0.49***		-0.009 (± 0.026) 0.00		0.18 (± 0.15)		0.03

In all species and size fractions, $\delta^{15}\text{N}$ was significantly negatively related to the depth of the nitracline $z_{50\text{N}}$ (Table IV.2), with the proportion of explained variability in the data ranging from 47 to 69%. The intercept of the multiple linear regression ranged from 5.58(± 0.58) in *U. vulgaris* to 10.33(± 1.38) in the largest size fraction (>500 μm). Among the size-fractionated zooplankton, the intercept of the multiple linear regression was lowest in the intermediate size class (200-500 μm). Nitracline thickness H_{N} and the difference between nitracline and phosphacline depth were only in some cases significant predictors of zooplankton $\delta^{15}\text{N}$, with a negative relationship in the former and a positive one in the latter (Table IV.2). Even when significant, the added proportion of explained variability was below 4% for nitracline thickness. The difference between nitracline and phosphacline depth, however, explained between 10 and 30% of additional variability in the model when significant.

Marked differences were found for RNA/DNA values in the different species and regions (Fig. IV.7, bottom row), contrasting the similarity in spatial distribution of stable nitrogen isotope signatures between the species investigated. In *U. vulgaris*, the largest range of RNA/DNA values, with station mean values (\pm standard deviation) ranging from 2.2 (± 0.42) to 4.4 (± 0.68) was observed. In this species, RNA/DNA was correlated to chl-*a* standing stock ($r=0.54$, $p < 0.05$). In contrast, for *S. danae* highest values were recorded in the open ocean between approximately 5° and 12°N and west of 20°W, with lowest values in the Cape Verde region. The range of station mean values (\pm SD) was 1.1(± 0.54) to 2.3(± 0.7). In *E. marina*, the most subtle differences between stations were observed, ranging from 0.6 (± 0.12) to 1.9 (± 0.31), and several stations with higher than average RNA/DNA could be identified both close to the

coast and offshore. Despite the variability among individual females in RNA/DNA, differences between the stations with highest and lowest values were significant for all three species (ANOVA, $p < 0.05$). Neither in *E. marina* nor in *S. danae* was RNA/DNA significantly correlated to chl-*a* standing stock, surface water temperature, or nutricline depth.

Using the intercept of the multiple linear regression as $\delta^{15}\text{N}_{\text{REF}}$ in equation (2) yielded a proportion of N_{D} contribution ranging from close to zero on the Guinea shelf to almost 60% offshore (Fig. IV.8 A). This proportion is positively related to nitracline depth (Fig. IV.8 B, $r^2 = 0.78$, $p < 0.05$). Prior to the cruise, the Saharan dust plume was concentrated mainly north of 10°N (Fig. IV.8 C).

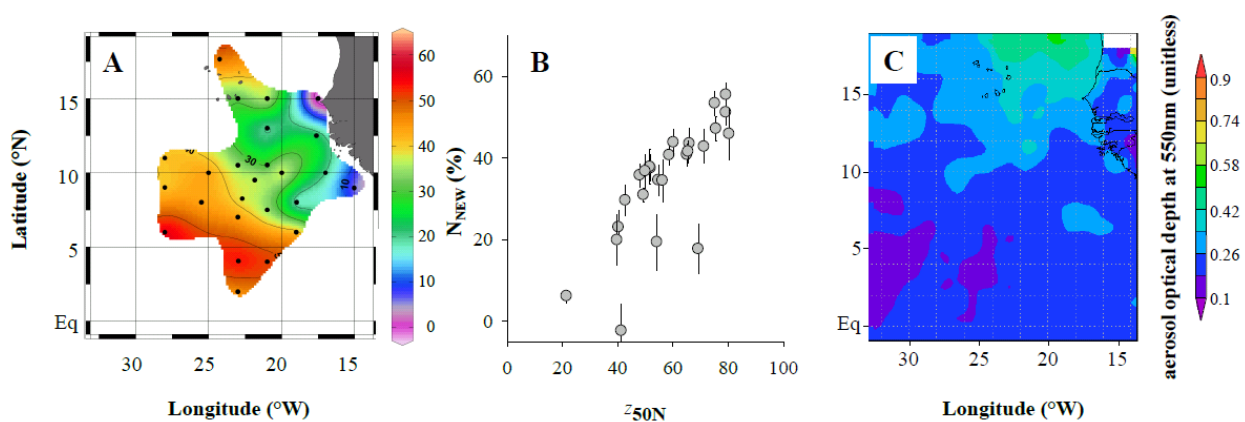


Figure IV.8: Spatial distribution (panel A) and relation to nitracline depth (panel B) of the relative contribution (%) of atmospheric N to epipelagic zooplankton biomass. On panel C, the satellite-based airborne dust (dimensionless) distribution prior M83-1 is displayed; values are the average of three months (Aug-Nov) based on monthly Level-3 MODIS-GOCART aerosol optical depth at 550 nm. Resolution of measurement is 1x1 degree. Visualization was produced with the Giovanni online data system, developed and maintained by the NASA Goddard Earth Sciences Data and Information Services Center (GES DISC).

IV.4 Discussion

The significant, negative correlation between integrated chl-*a* and the depth of the nitracline underpins the importance of diapycnal nutrient supply in the regulation of phytoplankton biomass (Agusti & Duarte 1999). While nitracline depth alone explained 65% of the variability in chl-*a*, adding nitracline thickness as a parameter in a multiple linear regression resulted in 73% explained variability, thus short-term variations in stratification and vertical diffusivity are also a key control of primary productivity. Gradients of all phytoplankton macronutrients are in

general strongly correlated in the highly stratified tropical ocean, therefore phosphocline depth is also highly correlated to chl-*a*. However, the phosphocline was consistently shallower and thicker than the nitracline (Fig. IV.3). The difference in depth was most evident close to the coastal upwelling (Fig. IV.3 D). Here, dissolved N:P below the nutricline is close to Redfield or below (see also Fig. IV.2 A), and surface phytoplankton community is therefore overall N-limited and exploits the supplied nitrogen quicker and more efficient than the supplied phosphate. Offshore, the situation is more complex: although dissolved N:P at depth frequently exceeds 16 (Hansell et al. 2004), and nitrogen fixers in these highly stratified warm surface waters are limited by Fe and P (Mills et al. 2004), the phosphocline is still consistently thicker (all stations) and shallower (all but two stations) than the nitracline. Furthermore, phosphocline thickness was not a significant predictor of total chl-*a*, which indicates that at least non-diazotroph primary productivity remains N-limited in the eastern part of the tropical Atlantic. This is somewhat striking, because the dissolved inorganic N:P ratio below the photic zone tends to be higher in the offshore stations (see also Fig. IV.2 B), often exceeding Redfield. We realize that choosing nitrate rather than total DIN slightly underestimates the N availability in surface waters. We did so as both nitrite and ammonium have a very different vertical distribution and dynamics than upwelled nitrate. Due to direct remineralization within the photic zone, highest nitrite and ammonium values were recorded in or directly above the nutricline. However, only little accumulation was observed, with NO_2^- and NH_4^+ concentration ranging from 0 to 0.65 μmol and 0 to 0.37 μmol , respectively, with the maximum values being recorded at the shelf stations. Nevertheless, the general pattern is not changed when using DIN instead of nitrate only, which is also reflected in the decreasing $\text{DIN}:\text{PO}_4^{3-}$ values in surface waters (Fig. IV.9).

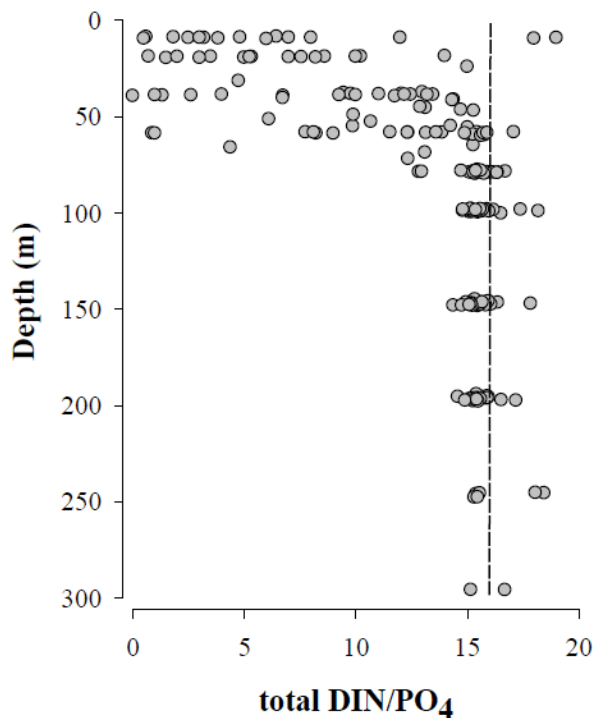


Figure IV.9: Ratio of total dissolved inorganic nitrogen (DIN, $\text{NO}_3^- + \text{NO}_2^- + \text{NH}_4^+$) and phosphorus (PO_4^{3-}) versus depth. Values from all stations of M83-1 are combined.

As we lack simultaneous data on primary (or export) production for the stations investigated, we cannot estimate concomitant rates of vertical nutrient and POM fluxes in this study. Nonetheless, our results demonstrate that atmospheric N input is not entirely “lost”, i.e. exported, from the euphotic zone, forming excess N below the permanent thermocline (Hansell et al. 2004). Rather, a significant amount of it is circulated in the epipelagic food web, as being demonstrated by high plasticity of $\delta^{15}\text{N}$ even in copepod species that are not reported to feed on diazotrophs directly. The three investigated copepod species differ markedly in their feeding preferences. *E. marina* is an exclusive carnivore, while *U. vulgaris* is traditionally considered a herbivore, although it may also feed on heterotrophic protist prey. In *S. danae*, both observations on gut contents as well as mouthpart configuration indicate mixed feeding (Arashkevich 1969), also comprising saprophagy (Ohtsuka et al. 1993). Spatial variations in the RNA/DNA ratio of females demonstrate differences in their habitat and food preferences: *U. vulgaris* appears to take advantage of upwelling conditions, which is in line with observations of this species selectively preying on diatoms and dinoflagellates (Kleppel et al. 1996). Areas with favourable conditions for the other omnivore *S. danae* are apparently located further offshore. This may be due to higher sea surface temperatures and/or different feeding preferences. It has been shown by Yebra et al. (2004) in a study off the Canary Islands and the Mauritanian upwelling that this species is virtually absent under strong upwelling conditions and preferably occupies the upper warm layers in highly stratified waters, although its feeding activity (assessed by gut fluorescence) is positively influenced by ambient chl-*a* concentration in upwelling filaments. Nutritional stress

may affect trophic fractionation in consumers, as in starving animals it has been found that loss of body mass without replacement of metabolized ^{14}N leads to increasing $\delta^{15}\text{N}$ values (Adams & Sterner 2000; Vanderklift & Ponsard 2003). However, the differing spatial patterns of nutritional condition in the three species did not seem to affect their stable isotope signature, since the spatial distribution pattern of $\delta^{15}\text{N}$ is highly correlated between species despite the differences in condition. Stable isotope analyses have become a pivotal technique in ecology to study food web relations in the field, often assuming fixed enrichment in both ^{15}N and ^{13}C with trophic level, with values of about 1‰ and 3.4‰ per trophic level for $\delta^{13}\text{C}$ and $\delta^{15}\text{N}$, respectively (Post 2002). Compared to these values, both the differences between the various feeding types of the copepods analyzed as well as the absolute $\delta^{15}\text{N}$ appear extremely low, given that dominance by small phytoplankton in the oligotrophic ocean is expected to increase the importance of protozoan feeding for copepods, thus leading to a trophic level of 3 (secondary consumer) or higher (Sommer & Sommer 2006). However, while the composition of phytoplankton, protozoan and detrital food in the two omnivorous species may vary depending on its relative abundance in the field, it is unlikely that *E. marina* would switch to a main food source other than crustacean prey, suggesting that trophic fractionation in this system is lower than the average 2.5-3.5‰. The rigidity of trophic enrichment factors and their mechanistic basis has been disputed due to experimental evidence of rather changeable physiology (Adams & Sterner 2000; Aberle & Malzahn 2007). In a meta-analysis of consumer-diet $\delta^{15}\text{N}$ enrichment, Vanderklift & Ponsard (2003) identified several sources of variation in isotopic fractionation. Specifically, lower than average ($\pm\text{SE}$) enrichment of 2.54‰(± 0.11) per trophic level was found in the marine environment (as opposed to freshwater and terrestrial systems), in taxa mainly excreting ammonia (instead of urea or uric acid) and in consumers with high nitrogen use efficiency (i.e. low nitrogen excretion relative to ingestion), all of which is the case for calanoid copepods and the area investigated in this study (e.g. Le Borgne 1982b). Further, significantly lower enrichment was found in consumers feeding on detritus, which may explain the comparatively low values determined in *S. danae*, given that this species is known to feed on heterotrophic and often quite large prey items (Arashkevich 1969). To compare trophic levels among species, the intercept of the multiple linear regression can be used as it represents conditions where the nitracline is at the surface and thus assumes remineralized deep water nitrate as the only N source; again, the lowest $\delta^{15}\text{N}$ is found in *U. vulgaris*. Compared to this value in a mainly herbivorous species, the size fractionated zooplankton all yield higher intercept values due to the mixture of feeding types in the community. As the intermediate size fraction mainly comprises copepodite stages of calanoid copepods, its mean trophic level is lower than that of the smallest

fraction with a large contribution of cyclopoids (mainly *Oithona* and *Oncaea* spp.) that are known to preferably ingest protozoan prey (Turner 2004). The large standard error of the intercept in the large size fraction indicates that the $\delta^{15}\text{N}$ of this size fraction may be particularly affected by its community structure, as it can comprise a vast variety of trophic level signatures, from gelatinous filter feeders to fish eggs, in differing amounts.

Previous studies have suggested that a substantial part of the high standing stock of chl-*a* off the West African coast can be attributed to diazotroph phytoplankton (e.g. Hood et al. 2004), and *Trichodesmium* was frequently found in considerable abundances in surface waters here (Margalef 1973; Vallespinos 1985; Voss et al. 2004). The two possible sources of isotopically light N (N_2 -fixation and mineral dust) can hardly be disentangled, but we can estimate the contribution of new N relative to remineralized N. Based upon the stable nitrogen isotope signatures in zooplankton as well as the nutrient control on total chl-*a*, we conclude that the relative diazotroph contribution to particulate organic nitrogen is rather low in the coastal shelf area, distinctly separating it from the oligotrophic open ocean where the major fraction of organic N must stem from atmospheric sources with a signature $<0\%$. The distribution within our study area revealed relatively high new N contribution well south of Cape Verde, which is contrasting a previous study by Mahaffey et al. (2003) where $\delta^{15}\text{N}$ of POM was rather high south of 20°N . Direct estimates of turbulent diffusive N flux into the upper mixed layer cover several orders of magnitude, ranging from $140 \mu\text{mol m}^{-2} \text{d}^{-1}$ in the open ocean (Lewis et al. 1986) and $1037 \mu\text{mol m}^{-2} \text{d}^{-1}$ off the Mauritanian upwelling to $>10000 \mu\text{mol m}^{-2} \text{d}^{-1}$ on the shelf slope (Schafstall et al. 2010). For comparison, measured N_2 -fixation along 10°N ranged from 3.4 to $255 \mu\text{mol m}^{-2} \text{d}^{-1}$ (Voss et al. 2004), with the highest rates recorded in the eastern part of the transect. This is well in line with modelled estimates that range from 180 to $450 \mu\text{mol m}^{-2} \text{d}^{-1}$ (Hood et al. 2004), with the higher values located closer to the African coast. In a modeling study by Prospero et al. (1996), total inorganic dust N input estimates between the equator and 20°N ranged from 43 to $52 \mu\text{mol m}^{-2} \text{d}^{-1}$ close to the African continent ($10\text{-}20^\circ\text{W}$) and from 17 to $22 \mu\text{mol m}^{-2} \text{d}^{-1}$ in the open ocean ($20\text{-}30^\circ\text{W}$), respectively. This distribution is supported by observational data (Formenti et al. 2003; Peyridieu et al. 2010), and its N flux range appeared to be in line with observations of dry N flux not exceeding $50 \mu\text{mol m}^{-2} \text{d}^{-1}$ off Africa. More recently, however, measurements were three- to fourfold higher (Baker et al. 2007). The spatial distribution of aerosol optical depth reveals that the majority of the Saharan dust plume enters the Atlantic with the NE trade winds north of 10°N during the summer months (April-November, Peyridieu et al. 2010). Thus, it seems unlikely that the highest N_D contribution at about 5°N is entirely due to inorganic N in dust, and this finding agrees well with the N_2 -fixation

hotspot detected in this region with an improved methodology on a meridional transect in fall 2010 (Großkopf et al. submitted) that was attributed largely to non-filamentous diazotrophs, especially DDAs and diazotrophic γ -proteobacteria. Future studies should focus on examining whether the higher dust load close to the equator and in the Gulf of Guinea during the winter months has a direct impact on zooplankton $\delta^{15}\text{N}$.

As zooplankton incorporate organic nitrogen from their prey, stable isotope analysis in zooplankton provides a tool to determine a spatially and temporally integrated estimate of upwelled and fixed nitrogen. The stable isotope analysis of selected zooplankton in a continuous time series with concomitant data on N_2 -fixation and dust input would be an excellent opportunity to disentangle the relative impact of N sources and to assess the time lag between the bloom and the zooplankton signal. Among single species, $\delta^{15}\text{N}$ agreed more closely than for bulk size-fractionated zooplankton, as trophic structure of the sampled community also influences its $\delta^{15}\text{N}$ signature. Thus, using a widely abundant copepod species as an indicator of differing nitrogen sources is a promising approach for future studies.

Acknowledgements

We thank the crew of R/V *Meteor* for excellent support during the cruises, Kerstin Nachtigall and Martina Lohmann for on-board nutrient measurements, and Dr. Rainer Kiko for comments on the manuscript. This work is a contribution of the DFG-supported project SFB754 (www.sfb754.de).

Conclusions and Perspectives

Pacific-Atlantic comparison: Nutrient limitation

Perhaps the most prominent difference between the eastern tropical Pacific and Atlantic is the difference in deposition of aeolian dust. Because of the vicinity of large, arid landmasses upwind, the Atlantic Ocean basin receives high amounts of dust that contributes both macro- (N, P) and micronutrients (e.g. Fe) to the surface water. Because dust N:P tends to exceed Redfield, and because dust input can relieve oceanic diazotrophs from Fe limitation, which in turn represent a N-source, the ETNA is considered ultimately Fe- and P-colimited (Mills et al. 2004). Satellite imagery (Fig. 5 and 6) reveals that the highest dust concentrations (and thus input) can be observed close to the West African coast. While there is some temporal variability in the location of the dust plume according to storm events (compare during cruise M80-2: highest concentrations in the Gulf of Guinea, and during M83-1: highest between Cap-Vert and the Cape Verde islands, Fig. 6), its seasonal distribution generally follows a similar pattern (compare three-monthly mean prior to the two cruises, Fig. 5). Thus, it is remarkable that in spite of the excess N at depth (Hansell et al. 2004) and the high N:P in the Aeolian dust, the response observed in the ETNA mesocosm experiment (chapter II) was so similar to the one in the Pacific (chapter I).

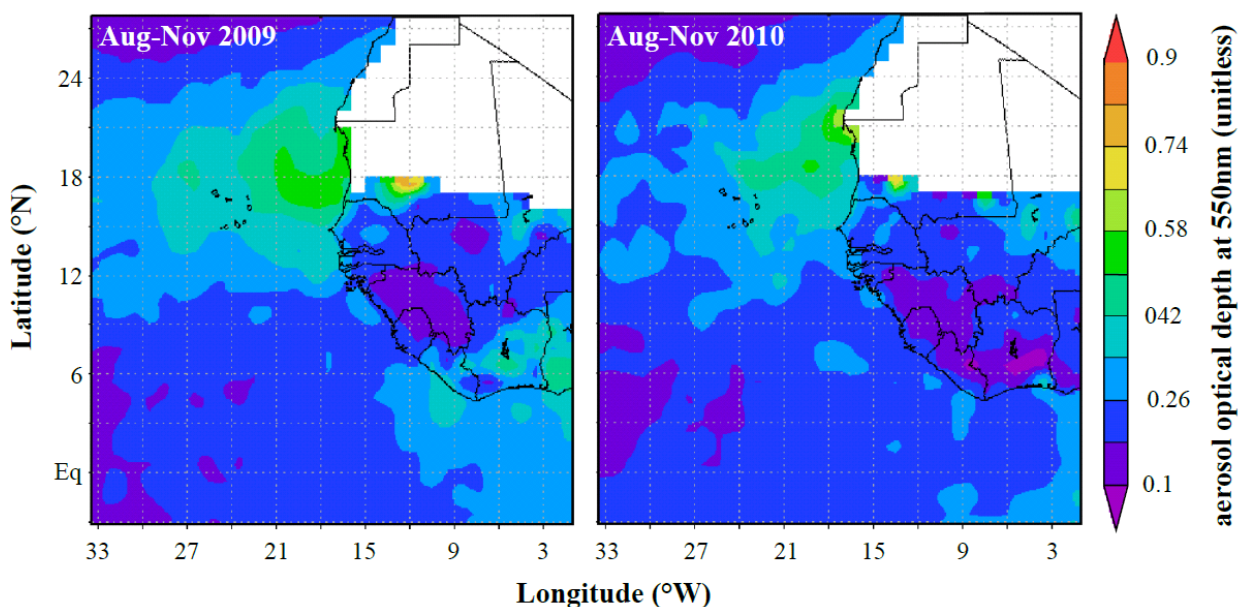


Figure 5: Airborne dust distribution prior to cruises M80-2 (left) and M83-1 (right). Displayed are summed values for the 3rd quarter (Aug-Nov) based on monthly Level-3 MODIS-GOCART aerosol optical depth at 550 nm. Resolution of measurement is 1x1 degree. Visualizations were produced with the Giovanni online data system, developed and maintained by the NASA Goddard Earth Sciences Data and Information Services Center (GES DISC).

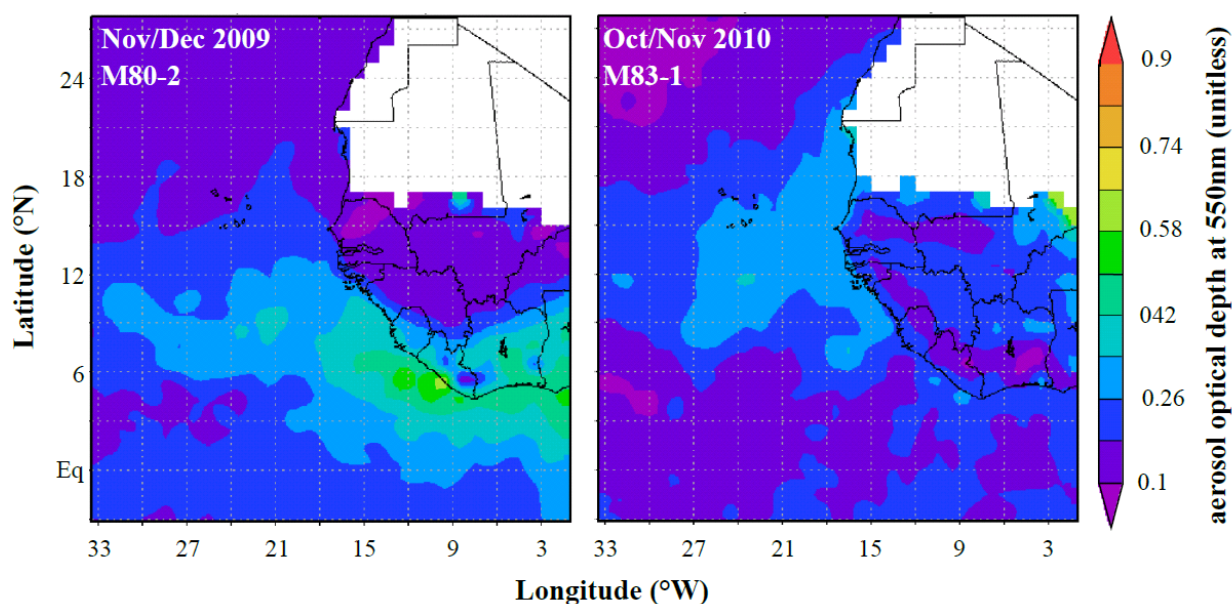


Figure 6: Airborne dust distribution during cruises M80-2 (left) and M83-1 (right). Displayed are monthly Level-3 MODIS-GOCART aerosol optical depth values at 550 nm. Resolution of measurement is 1x1 degree. Visualizations were produced with the Giovanni online data system, developed and maintained by the NASA Goddard Earth Sciences Data and Information Services Center (GES DISC).

Despite the obvious differences in the initial conditions sampled in respect to biomass, water temperature and nutrient load, the manipulation of N and P concentrations resulted in a similar nutrient drawdown pattern and biomass development. For both, the key control was the initial N concentration. At the lowest N:P, where only P was added and no N, the P stock was not depleted until the termination of the experiment (Fig. I.2 and II.1). For both P and silicate, drawdown was faster in the two “high N” than in the two “low N” treatments (Fig. I.2 and II.1). For silicate, this difference was even more pronounced in the Atlantic experiment. Likewise, the total biomass development was controlled by N, regardless of the P concentration, which was evident from microscopic counts (Fig. I.6), flow cytometry (Fig. I.8 and II.3) and particulate organic carbon (Fig. II.2).

In aquatic ecosystems, the nature of nutrient limitation of total primary production has been examined with the aid of a variety of approaches, either by interpretation of observational data of dissolved inorganic nutrient inputs, their concentrations and ratios or by manipulation experiments. Apart from manipulations of entire ecosystems (Elser et al. 1998), bioassay experiments have been widely used to achieve this. These include assays where the response of natural plankton to a variety of nutrient additions (single or in combinations) is evaluated, in containers ranging from small bottles to mesocosms (Howarth 1988). The majority of the bioassay experiments conducted in coastal marine ecosystems have detected a positive effect of

nitrogen addition, but not of phosphorus addition (Ryther & Dunstan 1971; Hassett et al. 1997; Downing et al. 1999). Up to now, the views on the relative importance of these two macronutrients remain controversial.

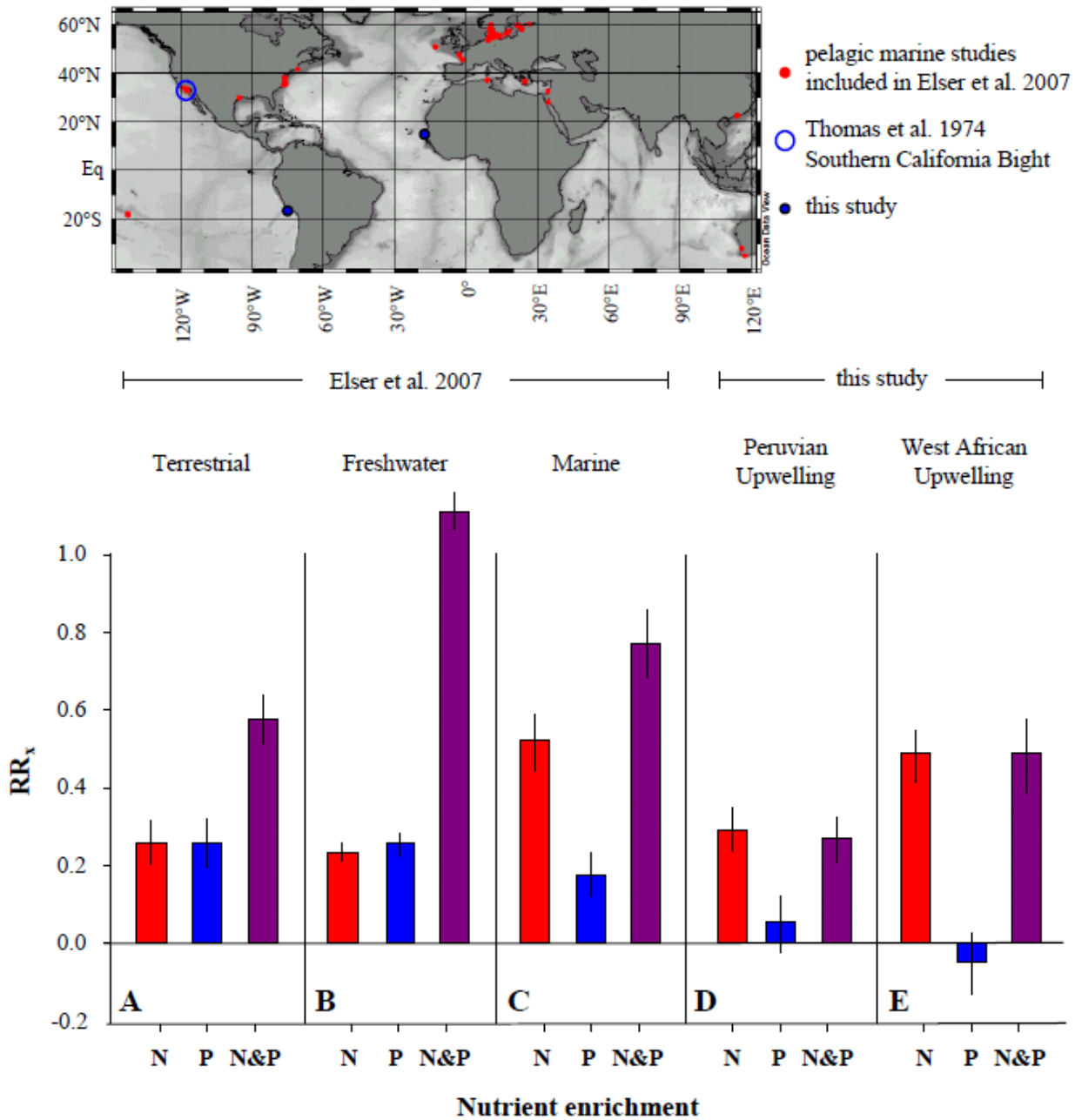


Figure 7: Response Ratio RR_x estimated as $RR_x = \ln(E/C)$, where E is the effect size in the respective nutrient (X) enrichment treatment, and C is the effect size in the unamended control. Data on panel A-C are from the metaanalysis by Elser et al. (2007) available at the National Center for Ecological Analysis and Synthesis (NCEAS # 347.3), values are means (\pm SE). Data on panel D and E are from the present study. Effect sizes in terms of biomass (POC) were calculated for individual mesocosms versus the mean of the unamended control on those three days where the maximum biomass was measured. Values presented are mean (\pm SE).

In a large-scale meta-analysis of nutrient enrichment assays in terrestrial, freshwater and marine ecosystems, Elser et al. (2007) found that, although single addition of P led to a weaker response than single addition of N (Fig. 7 C), simultaneous additions of N and P tended to produce higher responses than single nutrient additions across all systems.

The authors therefore concluded that significant synergistic effects of combined N and P enrichment, and thus growth limitation by N and P are common to all ecosystems. However, this was not the case in both our experiments in the Peruvian upwelling and off West Africa. Here, the clear biomass response to N addition, regardless whether P was added simultaneously or not, does suggest N-limitation of both systems.

Clearly, upwelling systems featuring an intense N-deficit due to redox-dependent changes in N:P stoichiometry may resemble an extreme case among marine ecosystems. From the 23 studies investigating pelagic marine communities that were included in the Elser et al. (2007) analysis (see map within Fig. 7), only one originated from an eastern boundary current system, the Southern California Bight. In this study, Thomas et al. (1974) found that little or no growth relative to the unamended control occurred unless nitrogen was added, and likewise concluded that nitrogen is the primary limiting nutrient. These regional differences have to be taken into account when meaningful comparisons across ecosystems are to be made. In addition, the existing nutrient enrichment assay data are still somewhat biased towards coastal areas of North America and Europe. The metaanalysis conducted by Downing et al. (1999), which was restricted to the evaluation of marine studies, covered a dataset roughly similar to the one from Elser et al. (2007). However, they did not include simultaneous additions of N and P, but even for the single nutrient addition their finding was somewhat contrary to Elser et al. (2007), as they hardly found positive responses to “P only” additions, especially in those coastal areas with anthropogenic nutrient sources.

Tyrell (1999) pointed out that the view of N being the “master limiting nutrient” for phytoplankton productivity in surface waters is often promoted by biologists based on enrichment experiments, like ours. In contrast, the “geochemist’s view” argues that an N-deficit can be topped up by atmospheric sources (N_2 -fixation), while there is no alternative source of P. Thus, the latter must be limiting ocean productivity over longer time scales. In a modeling study comparing these two views, Tyrell (1999) defined the “proximate limiting nutrient” and the “ultimate limiting nutrient”, assuming that, at a steady state, there would be an N-deficit at the surface and a small proportion of the phytoplankton that are diazotrophs. Increased N-addition would increase primary production in the short term, but at the same time cause fewer diazotrophs (due to a diminished ecological niche) and hence reduced new N input. Eventually,

the initial N addition would be compensated by the lacking diazotroph N input, and productivity would reach the same steady state. On the other hand, increased P-addition would initially increase the N-deficit and ultimately cause a steady state with a larger population of diazotrophs, larger total N-input, and increased productivity. This concept, however, is challenged by our finding that, following the initial bloom development of non-diazotrophs, cyanobacterial marker pigments increased to a greater extent in those mesocosms that received a higher initial N-load.

Pacific-Atlantic comparison: N₂-fixation

One of the most striking results, and again very similar in the Pacific and Atlantic mesocosm experiments, was the enhanced increase in concentration of cyanobacterial marker pigments in those mesocosms that had received a higher initial N load. In the M77-3 experiment off Peru (see Chapter I), the only cyanobacterial pigment with this response was aphanizophyll. While aphanizophyll is exclusively found in cyanobacteria, it is not unambiguously diagnostic for diazotrophs. Surprisingly, the aphanizophyll increase did not occur in the mesocosms with low N/high P conditions, where P was still available until the end of the trial (Fig. I.3). Hardly any consistent change in the aphanizophyll signal could be recorded in the lower N:P treatments (5:1 and 2.5:1) during the entire experiment, whereas the cyanobacterial marker pigment responded rather promptly in the treatments with higher N:P (16:1 and 8:1) under complete dissolved N exhaustion after day 4 (Fig. I. 6, panel B). Thus, initial phosphate concentration did not have any significant effects on the development of cyanobacterial marker pigments in both experiments.

In contrast to filamentous species that often reach lengths of 200 µm and form dense colonies, unicellular diazotrophic cyanobacteria with sizes of approximately 1-8 µm are hardly to be found microscopically, neither could they be distinguished from other photoautotrophs by flow cytometry. Only little is known about the pigment composition of N-fixing cyanobacteria such as the lately found “Group A” (Zehr et al. 2001; 2008) or symbiotic forms (e.g. *Richelia* etc.; see e.g. review by Villareal 1992). While nitrogen fixing cyanobacteria may be able to partially compensate the lack of available nitrogen, this appears to happen in a distinct succession rather than a direct response to P availability. Several studies in limnic (Smith 1983; Vrede et al. 2009), brackish (Niemi 1979), and marine (Michaels et al. 1996) environments have reported on cyanobacterial blooms triggered by low inorganic N:P stoichiometry. The ability to fix elemental N by these photoautotrophic prokaryotes is a major advantage as the system becomes N depleted. Thus, it is argued that excess P in the euphotic zone as a result of N losses within the

OMZ in the Tropical Eastern South Pacific could facilitate considerably higher N₂-fixation rates than previously assumed (Deutsch et al. 2007). This is well in line with observations reporting that the role of unicellular cyanobacteria in the nutrient cycle has been underestimated (Zehr et al. 2001; Montoya et al. 2004; Moisaner et al. 2010) compared to the extensive surface blooms of *Trichodesmium* spp. in the oligotrophic ocean. Further studies to investigate this succession pattern are recommended, preferably applying molecular techniques and N₂-fixation rate assays, as it might be an important driver of the onshore-offshore differences in dominating algal functional groups.

This might be accrued to the fact that cyanobacteria are inferior competitors for P than diatoms under conditions of nutrient repletion, when diatoms are feeding their RNA-rich assembly machinery. Hence, the inorganic N stock must be at first severely exploited to limit diatom growth and in turn to facilitate the development of N₂-fixing cyanobacteria by producing access to P. Non-Redfieldian nutrient uptake by non-diazotrophic phytoplankton as proposed by Mills and Arrigo (2010) would then control growth of cyanobacteria. However, this would not explain the lack of response in the +P treatment.

A different mechanism could be an increased iron uptake of the phytoplankton community in those mesocosms receiving “low N”, resulting in iron limitation of cyanobacterial growth later on in the experiment. Sunda & Hunstman (1995) reported that especially coastal diatoms are capable of luxury iron uptake up to 20-30 times of their optimal growth requirements. This Fe acquisition strategy under conditions of Fe repletion and low growth due to N and/or Si limitation would be a key advantage for diatoms to outcompete other autotrophs when the system is provided with ‘new’ N and Si in upwelling areas. Iron uptake kinetics within species would therefore have been modulated by the N and P fertilization treatments to create a scenario featuring “Fe-repletion in high initial N” and “Fe depletion in low initial N”. To compensate for the different biomass, at least a two-fold increase in iron uptake would be required by the N-limited cells. This mechanism of luxury uptake at low growth rates could make sense in the highly variable upwelling environment, so that blooming can commence as soon as sufficient N is supplied. However, to the best of our knowledge, no such process is described in literature, albeit specialized proteins for iron storage have been detected in pennate diatoms (Marchetti et al. 2009).

Limitations to zooplankton production: Food quality or quantity?

A large body of laboratory studies documents that the growth of herbivorous zooplankton is sensitive to the growth status of its microalgal food, with algae in exponential (unlimited) growth phase being of superior quality than those in stationary or senescent (i.e. nutrient-limited) growth phases (e.g. Mitchell et al. 1992 freshwater, *Daphnia magna* as consumer); Diekmann et al. 2009 marine, *Acartia tonsa* as consumer). Whether this is due to a direct mineral limitation of consumers or rather an indirect effect due to changes in the biochemical composition of microalgae has been heavily debated (see e.g. Urabe & Watanabe 1993 and references therein). Some argued that *Daphnia* was actually responding to other determinants of nutritional quality (such as certain essential fatty acids) that covaried with P content, and thus not to P *per se*. (Müller-Navarra 1995; Brett & Müller-Navarra 1997). In favor of direct mineral limitation, however, both Sterner (1993) and Plath & Boersma (2001) found in laboratory experiments that *Daphnia* growth was more closely correlated with algal P content than with cellular content of N, protein, carbohydrate, or several other fractions.

It has to be noted that the majority of the studies examining the direct and indirect effects of mineral limitation and transfer efficiency to zooplankton production is based on freshwater laboratory experiments, and here mostly using *Daphnia* spp. as model organisms and monoalgal cultures with different P-quotas as food. In the marine realm, primary production is most frequently N-limited, however hardly reaching the extremely low cell quotas observed for P-limited freshwater phytoplankton. The lack of observed correlations between food N or P content and zooplankton production, and the frequently observed correlations between primary production (or primary producer standing stock in terms of C or energy) and zooplankton growth led to the general perception that food quantity most frequently limits zooplankton in the ocean.

Nevertheless, some evidence from experimental studies exists suggesting that zooplankton growth can be limited by food N (or rather protein) content. Both Checkley (1980) and Kiørboe (1989) observed that copepod egg production rate was a constant fraction of N ingestion when copepods were supplied with food covering a wide range in C content. However, studies addressing the propagation of nutrient limitation from primary producers in the field or in mixed assemblages are still scarce (Olsen et al. 2011). In contrast, the fatty acid composition of the prey field available to zooplankton has been shown to significantly contribute to their somatic growth and egg production in the field (Jónasdóttir et al. 1995). The abundance of individual essential fatty acids in the food web can also affect the transfer to higher trophic levels such as marine larval fish in the field, as documented by Paulsen et al. (submitted) for larval Baltic herring,

where RNA/DNA was positively related to DHA content of larvae. Similarly, we found that the RNA/DNA ratio of zooplanktivorous copepods in the ETNA was positively related to their PUFA content (Fig. 8).

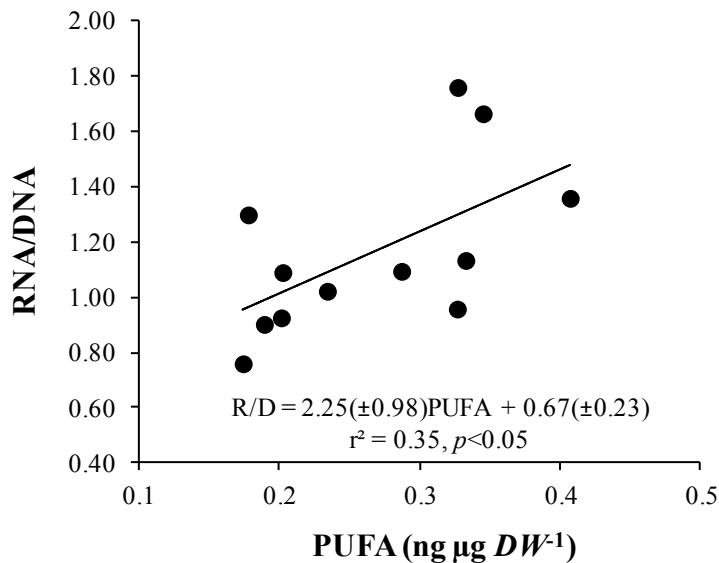


Figure 8: RNA/DNA of individual copepods (*Euchaeta marina*) sampled in the eastern tropical Atlantic (Nov/Dec 2009) in relation to dry weight-specific PUFA content (ng µg DW⁻¹).

The factors controlling PUFA content of particulate organic matter in the ocean include the community composition of the phytoplankton (Dalsgaard et al. 2003), the nutrient and light regime (Guschina & Harwood 2009) as well as ambient pCO_2 (Rossoll et al. submitted). Because all these controls are interrelated, it is difficult to derive causal links to zooplankton growth by field observations.

The haptophyte genus *Phaeocystis* is a common primary producer in the global ocean, with a distribution ranging from the tropics/temperate coastal ecosystems to the boreal Atlantic/Pacific and the Southern Ocean, with *P. globosa*, *P. pouchetii* and *P. antarctica* being the three respective predominant bloom-forming species (Schoemann et al. 2005). *Phaeocystis globosa* is considered a harmful alga in coastal waters, dominating the phytoplankton community over extended time periods and forming massive blooms that can become a nuisance to fisheries and tourism. *P. globosa* exhibits two strikingly different life forms, alternating between single cells (approximately 2-8 µm in diameter) and gelatinous colonies (several mm), which makes it difficult to assess the efficiency of grazing. Size mismatch between colonies and potential grazers as well as mechanical obstruction by the polysaccharidic matrix are certainly contributing to the reported resistance to grazing. However, in the single cell stage it is readily consumed by copepods. It seems that its nutritional value to zooplankton consumers is quite low, as experimental studies using calanoid copepods and a monospecific diet of *Phaeocystis* resulted in low egg production rates (Tang et al. 2001; Turner et al. 2002). In field studies in the English Channel, *Phaeocystis*-dominated plankton assemblages were reported to cause decreases in

copepod fecundity (Bautista et al. 1994), and even a drastic decrease in copepod abundance was observed by Bautista et al. (1992). Based on observations of trends in dissolved N and P loads of riverine discharge and biomass development of *P.globosa* in the southern North Sea, Riegman et al. 1992 concluded that *P.globosa* is a good competitor under low dissolved N:P, which is in line with our observations in the algal assemblage off Peru (Chapter I), where *Phaeocystis*, although never dominating, was clearly profiting from P addition.

Because laboratory experiments focusing on monoalgal diets are always neglecting both changes in phytoplankton community structure and the feeding selectivity of zooplankton, experimentalists should strive to investigate these links in dedicated laboratory studies using mixed diets.

In conclusion, results of the present study indicate that N supply provides a strong control on phytoplankton biomass production in the two eastern boundary current systems investigated. Both N supply and N:P ratio are key controls of phytoplankton community composition, which in turn can effect trophic transfer efficiency to zooplankton consumers. Further, mesozooplankton excretion was related to N:P stoichiometry of particulate matter and the feeding ecology of zooplankton species, providing feedback to the autotroph community within the photic zone.

In the Eastern Tropical North Atlantic, indications of N-limitation of non-diazotroph production are reaching far offshore, thus co-existing with surface N₂-fixation. Due to a highly stratified water column, diazotroph production exists even close to the West African shelf and supplies a substantial fraction of bioavailable N that enters the epipelagic food web.

Future research is recommended addressing

- When conducting observations on excretion and egestion of oceanic zooplankton, food removal (in terms of organic C, N, P) should be estimated concomitantly to be able to sufficiently characterize their role in nutrient cycling *in situ*.
- Laboratory experiments using cultured algae with different C:N:P (by adjusting dilution/growth rate and nutrient N:P) and herbivorous copepods will be helpful to establish both the methodology and the concepts applied in field investigations.
- Fractionation by mesozooplankton of ¹⁵N in the different pools (biomass, excretion, fecal pellets) should be assessed in order to include these components into global models of $\delta^{15}\text{N}$ distribution.
- Finally, in order to estimate the contribution of zooplankton to export flux and surface recirculation of N and P, biomass and stoichiometry of the available prey field should be taken into account along with zooplankton biomass and size distribution as well as environmental conditions (T, $p\text{O}_2$, $p\text{CO}_2$).

References

- Aberle N, Malzahn AM (2007) Interspecific and nutrient-dependent variations in stable isotope fractionation: experimental studies simulating pelagic multitrophic systems. *Oecologia* 154: 291-303
- Aberle N, Hansen T, Boettger-Schnack R, Burmeister A, Post AF, Sommer U (2010) Differential routing of 'new' nitrogen toward higher trophic levels within the marine food web of the Gulf of Aqaba, Northern Red Sea. *Mar Biol* 157: 157-169
- Adams TS, Sterner RW (2000) The effect of dietary nitrogen content on trophic level ^{15}N enrichment. *Limnol Oceanogr*: 601-607
- Agusti S, Duarte CM (1999) Phytoplankton chlorophyll *a* distribution and water column stability in the central Atlantic Ocean. *Oceanologica acta* 22: 193-203
- Agusti S, Duarte CM, Vaqué D, Hein M, Gasol JM, Vidal M (2001) Food-web structure and elemental (C, N and P) fluxes in the eastern tropical North Atlantic. *Deep-Sea Res II* 48: 2295-2321
- Alheit J, Niquen M (2004) Regime shifts in the Humboldt Current ecosystem. *Progress in Oceanography* 60: 201-222
- Al-Mutairi H, Landry MR (2001) Active export of carbon and nitrogen at Station ALOHA by diel migrant zooplankton. *Deep-Sea Res II* 48: 2083-2103
- Ambler JW, Miller CB (1987) Vertical habitat-partitioning by copepodites and adults of subtropical oceanic copepods. *Mar Biol* 94: 561-577
- Andersen T, Hessen DO (1991) Carbon, nitrogen, and phosphorus content of freshwater zooplankton. *Limnol Oceanogr* 36(4): 807-814
- Anderson TR, Hessen DO (1995) Carbon or nitrogen limitation in marine copepods? *J Plankton Res* 17: 317-331
- Arashkevich YG (1969) The food and feeding of copepods in the northwestern Pacific. *Oceanology* 9: 5-709
- Arrigo KR, Robinson DH, Worthen DL, Dunbar RB, DiTullio GR, VanWoert M, Lizotte MP (1999) Phytoplankton community structure and the drawdown of nutrients and CO_2 in the Southern Ocean. *Science* 283: 365
- Arrigo KR, DiTullio GR, Dunbar RB, Robinson DH, VanWoert M, Worthen DL, Lizotte MP (2000) Phytoplankton taxonomic variability in nutrient utilization and primary production in the Ross Sea. *J Geophys Res* 105: 8827-8846
- Arrigo KR (2005) Marine microorganisms and global nutrient cycles. *Nature* 437: 349-355
- Atienza D, Calbet A, Saiz E, Alcaraz M, Trepát I (2006) Trophic impact, metabolism, and biogeochemical role of the marine cladoceran *Penilia avirostris* and the co-dominant copepod *Oithona nana* in NW Mediterranean coastal waters. *Mar Biol* 150: 221-235
- Atienza D, Calbet A, Saiz E, Lopes RM (2007) Ecological success of the cladoceran *Penilia avirostris* in the marine environment: feeding performance, gross growth efficiencies and life history. *Mar Biol* 151: 1385-1396
- Baker AR, Kelly SD, Biswas KF, Witt M, Jickells TD (2003) Atmospheric deposition of nutrients to the Atlantic Ocean. *Geophys Res Lett* 30, 2296
- Baker AR, Weston K, Kelly SD, Voss M, Streu P, Cape JN (2007) Dry and wet deposition of nutrients from the tropical Atlantic atmosphere: Links to primary productivity and nitrogen fixation. *Deep Sea Research Part I: Oceanographic Research Papers* 54: 1704-1720

References

- Bakun A, Weeks SJ (2008) The marine ecosystem off Peru: What are the secrets of its fishery productivity and what might its future hold? *Progress in Oceanography* 79: 290-299
- Bautista B, Harris RP, Tranter PRG, Harbour D (1992) In situ copepod feeding and grazing rates during a spring bloom dominated by *Phaeocystis* sp. in the English Channel. *J Plankton Res* 14: 691
- Bautista B, Harris RP, Rodriguez V, Guerrero F (1994) Temporal variability in copepod fecundity during two different spring bloom periods in coastal waters off Plymouth (SW England). *J Plankton Res* 16: 1367-1377
- Balseiro EG, Modenutti BE, Queimaliños CP (1997) Nutrient recycling and shifts in N:P ratio by different zooplankton structures in a South Andes lake. *J Plankton Res* 19: 805-817
- Banyte D, Tanhua T, Visbeck M, Wallace DWR, Karstensen J, Krahnemann G, Schneider A, Stramma L (in press) Diapycnal diffusivity at the upper boundary of the North Tropical Atlantic oxygen minimum zone. *J Geophys Res*
- Barber RT, Smith RL (1981) Coastal upwelling ecosystems. In: Longhurst A (ed) *Analysis of Marine Ecosystems*. Academic Press, pp 31-68
- Barlow RG, Cummings DG, Gibb SW (1997) Improved resolution of mono- and divinyl chlorophylls a and b and zeaxanthin and lutein in phytoplankton extracts using reverse phase C-8 HPLC. *Mar Ecol Prog Ser* 161: 303-307
- Behrenfeld MJ, Falkowski PG (1997) Photosynthetic rates derived from satellite-based chlorophyll concentration. *Limnol Oceanogr* 42: 1-20
- Bertilsson S, Berglund O, Karl DM, Chisholm SW (2003) Elemental Composition of Marine *Prochlorococcus* and *Synechococcus*: Implications for the Ecological Stoichiometry of the Sea. *Limnol Oceanogr* 48: 1721-1731
- Bertrand A, Ballón M, Chaigneau A (2010) Acoustic observation of living organisms reveals the upper limit of the oxygen minimum zone. *PloS one* 5: e10330
- Bograd SJ, Castro CG, Di Lorenzo E, Palacios DM, Bailey H, Gilly W, Chavez FP (2008) Oxygen declines and the shoaling of the hypoxic boundary in the California Current. *Geophys Res Lett* 35: L12607
- Bopp L, Monfray P, Aumont O, Dufresne JL, Le Treut H, Madec G, Terray L, Orr JC (2001) Potential impact of climate change on marine export production. *Global Biogeochem Cy* 15: 81-100
- Breitbarth E, Oschlies A, LaRoche J (2007) Physiological constraints on the global distribution of *Trichodesmium* - effect of temperature on diazotrophy. *Biogeosciences* 4: 53-61
- Brett MT, Müller-Navarra DC (1997) The role of highly unsaturated fatty acids in aquatic foodweb processes. *Freshw Biol* 38: 483-499
- Bruland KW, Rue EL, Smith GJ, DiTullio GR (2005) Iron, macronutrients and diatom blooms in the Peru upwelling regime: brown and blue waters of Peru. *Mar Chem* 93: 81-103
- Buesseler KO (1998) The decoupling of production and particulate export in the surface ocean. *Global Biogeochem Cy* 12: 297-310
- Calbet A, Saiz E (2005) The ciliate-copepod link in marine ecosystems. *Aquat Microb Ecol* 38: 157-167
- Capone DG, Burns JA, Montoya JP, Subramaniam A, Mahaffey C, Gunderson T, Michaels AF, Carpenter EJ (2005) Nitrogen fixation by *Trichodesmium* spp.: An important source of new nitrogen to the tropical and subtropical North Atlantic Ocean. *Global Biogeochem Cy* 19
- Carpenter EJ, Romans K (1991) Major role of the cyanobacterium *Trichodesmium* in nutrient cycling in the North Atlantic Ocean. *Science* 254: 1356
- Carr ME (2001) Estimation of potential productivity in Eastern Boundary Currents using remote sensing. *Deep Sea Res II* 49: 59-80

-
- Chavez FP, Toggweiler JR (1995) Physical estimates of global new production: The upwelling contribution. In: Summerhayes CP, Emeis KC, Angel MV, Smith RL, Zeitzschel B (eds) *Upwelling in the ocean: Modern processes and ancient records* Wiley, pp 313-320
- Chavez FP, Messié M (2009) A comparison of eastern boundary upwelling ecosystems. *Progr Oceanogr* 83: 80-96
- Checkley Jr DM (1980) The egg production of a marine planktonic copepod in relation to its food supply: Laboratory studies. *Limnol Oceanogr* 25: 430-446
- Checkley DM, Entzeroth LC (1985) Elemental and isotopic fractionation of carbon and nitrogen by marine, planktonic copepods and implications to the marine nitrogen cycle. *J Plankton Res* 7: 553
- Conan P, Søndergaard M, Kragh T, Thingstad F, Pujo-Pay M, le B. Williams PJ, Markager S, Cauwet G, Borch NH, Evans D (2007) Partitioning of organic production in marine plankton communities: The effects of inorganic nutrient ratios and community composition on new dissolved organic matter. *Limnol Oceanogr* 52(2): 753-765
- Cushing DH (1989) A difference in structure between ecosystems in strongly stratified waters and in those that are only weakly stratified. *J Plankton Res* 11: 1-13
- Dalsgaard J, St John M, Kattner G, Müller-Navarra D, Hagen W (2003) Fatty acid trophic markers in the pelagic marine environment. *Adv Mar Biol* 46: 225-340
- Davey M, Tarran GA, Mills MM, Ridame C, Geider RJ, La Roche J (2008) Nutrient limitation of picophytoplankton photosynthesis and growth in the tropical North Atlantic. *Limnol Oceanogr* 53: 1722-1733
- Deutsch C, Gruber N, Key RM, Sarmiento JL, Ganachaud A (2001) Denitrification and N₂ fixation in the Pacific Ocean. *Global Biogeochem Cy* 15: 483-506
- Deutsch C, Sarmiento JL, Sigman DM, Gruber N, Dunne JP (2007) Spatial coupling of nitrogen inputs and losses in the ocean. *Nature* 445: 163-167
- Deutsch C, Brix H, Ito T, Frenzel H, Thompson L (2011) Climate-Forced Variability of Ocean Hypoxia. *Science* 333: 336-339
- Diekmann ABS, Peck MA, Holste L, St John MA, Campbell RW (2009) Variation in diatom biochemical composition during a simulated bloom and its effect on copepod production. *J Plankton Res* 31: 1391
- DiTullio GR, Geesey ME, Maucher JM, Alm MB, Riseman SF, Bruland KW (2005) Influence of iron on algal community composition and physiological status in the Peru upwelling system. *Limnol Oceanogr*: 1887-1907
- Downing JA, Osenberg CW, Sarnelle O (1999) Meta-analysis of marine nutrient-enrichment experiments: variation in the magnitude of nutrient limitation. *Ecology* 80: 1157-1167
- Dugdale R (1985) The effects of varying nutrient concentrations on biological production in upwelling regions. *CalCOFI Reports* 26: 93-96
- Dunstan GA, Volkman JK, Barrett SM, Garland CD (1993) Changes in the lipid composition and maximisation of the polyunsaturated fatty acid content of three microalgae grown in mass culture. *J Appl Phycol* 5: 71-83
- Elser JJ, Hassett RP (1994) A stoichiometric analysis of the zooplankton-phytoplankton interaction in marine and freshwater ecosystems. *Nature* 370: 211-213
- Elser JJ, Chrzanowski TH, Sterner RW, Mills KH (1998) Stoichiometric constraints on food-web dynamics: a whole-lake experiment on the Canadian Shield. *Ecosystems* 1: 120-136
- Elser JJ, Urabe J (1999) The stoichiometry of consumer-driven nutrient recycling: theory, observations, and consequences. *Ecology* 80: 735-751
- Elser JJ, Bracken MES, Cleland EE, Gruner DS, Harpole WS, Hillebrand H, Ngai JT, Seabloom EW, Shurin JB, Smith JE (2007) Global analysis of nitrogen and phosphorus limitation of primary producers in freshwater, marine and terrestrial ecosystems. *Ecol Lett* 10: 1135-1142

References

- Eppley RW, Renger EH, Venrick EL, Mullin MM (1973) A study of plankton dynamics and nutrient cycling in the central gyre of the North Pacific Ocean. *Limnol Oceanogr* 18: 534-551
- Eppley RW, Peterson BJ (1979) Particulate organic matter flux and planktonic new production in the deep ocean. *Nature* 282: 677-680
- Escribano R, Hidalgo P, Krautz C (2009) Zooplankton associated with the oxygen minimum zone system in the northern upwelling region of Chile during March 2000. *Deep-Sea Res II* 56: 1083-1094
- Fawcett SE, Ward BB (2011) Phytoplankton succession and nitrogen utilization during the development of an upwelling bloom. *Mar Ecol Prog Ser* 428: 13-31
- Fernández C, Fariás L, Alcaman ME (2009) Primary production and nitrogen regeneration processes in surface waters of the Peruvian upwelling system. *Progress in Oceanography* 83: 159-168
- Fiedler PC, Talley LD (2006) Hydrography of the eastern tropical Pacific: A review. *Progress in Oceanography* 69: 143-180
- Flint MV, Drits AV, Pasternak AF (1991) Characteristic features of body composition and metabolism in some interzonal copepods. *Mar Biol* 111: 199-205
- Formenti P, Elbert W, Maenhaut W, Haywood J, Andreae MO (2003) Chemical composition of mineral dust aerosol during the Saharan Dust Experiment (SHADE) airborne campaign in the Cape Verde region, September 2000. *J Geophys Res* 108: 8576
- Foster RA, Subramaniam A, Mahaffey C, Carpenter EJ, Capone DG, Zehr JP (2007) Influence of the Amazon River plume on distributions of free-living and symbiotic cyanobacteria in the western tropical north Atlantic Ocean. *Limnol Oceanogr* 52: 517-532
- Foster RA, Subramaniam A, Zehr JP (2009) Distribution and activity of diazotrophs in the Eastern Equatorial Atlantic. *Environmental Microbiology* 11: 741-750
- Franz JMS, Krahnemann G, Lavik G, Grasse P, Dittmar P, Riebesell U (2012) Dynamics and stoichiometry of nutrients and phytoplankton in waters influenced by the oxygen minimum zone in the tropical eastern Pacific. *Deep-Sea Res I* 62: 20-31
- Geider RJ, Roche JL (2002) Redfield revisited: variability of C: N: P in marine microalgae and its biochemical basis. *Eur J Phycol* 37: 1-17
- Gervais F, Riebesell U (2001) Effect of phosphorus limitation on elemental composition and stable carbon isotope fractionation in a marine diatom growing under different CO₂ concentrations. *Limnol Oceanogr* 46: 497-504
- Goebel NL, Turk KA, Achilles KM, Paerl R, Hewson I, Morrison AE, Montoya JP, Edwards CA, Zehr JP (2010) Abundance and distribution of major groups of diazotrophic cyanobacteria and their potential contribution to N₂ fixation in the tropical Atlantic Ocean. *Environ Microbiol* 12: 3272-3289
- Granéli E, Hansen PJ (2006) Allelopathy in harmful algae: a mechanism to compete for resources? In: Granéli E, Turner JT (eds) *Ecology of harmful algae*, pp 189-201
- Großkopf T, Mohr W, Baustian T, Schunck H, Gill D, Kuypers MMM, Lavik G, Schmitz RA, Wallace DWR, LaRoche J (submitted) Closing the gap – Doubling global rates of marine pelagic N₂ fixation.
- Grover JP (1997) *Resource Competition*. Chapman & Hall, London
- Gruber N, Sarmiento JL (1997) Global patterns of marine nitrogen fixation and denitrification. *Global Biogeochem Cy* 11: 235-266
- Gulati R, DeMott W (1997) The role of food quality for zooplankton: remarks on the state-of-the-art, perspectives and priorities. *Freshw Biol* 38: 753-768

- Guschina IA, Harwood JL (2009) Algal lipids and effect of the environment on their biochemistry. In: Arts MT, Brett MT, Kainz MJ (eds) Lipids in aquatic ecosystems, pp 1-24
- Hall RI, Leavitt PR, Dixit AS, Quinlan R, Smol JP (1999) Limnological succession in reservoirs: a paleolimnological comparison of two methods of reservoir formation. *Can J Fish Aquat Sci* 56: 1109-1121
- Hamersley MR, Lavik G, Woebken D, Rattray JE, Lam P, Hopmans EC, Damsté JSS, Krüger S, Graco M, Gutiérrez D, Kuypers MMM (2007) Anaerobic ammonium oxidation in the Peruvian oxygen minimum zone. *Limnol Oceanogr* 52: 923-933
- Hansen HP, Koroleff F (2007) Determination of nutrients. In: Grasshoff K, Klaus Kremling K, Ehrhardt M (eds) Methods of seawater analysis. Wiley-VCH Verlag GmbH, Weinheim, Germany, pp 159-228
- Hannides C, Landry MR, Benitez-Nelson CR, Styles RM, Montoya JP, Karl DM (2009) Export stoichiometry and migrant-mediated flux of phosphorus in the North Pacific Subtropical Gyre. *Deep-Sea Res I* 56: 73-88
- Hansell DA, Bates NR, Olson DB (2004) Excess nitrate and nitrogen fixation in the North Atlantic Ocean. *Mar Chem* 84: 243-265
- Hansen T, Sommer U (2007) Increasing the sensitivity of ^{13}C and ^{15}N abundance measurements by a high sensitivity elemental analyzer connected to an isotope ratio mass spectrometer. *Rapid Commun Mass Spectrom* 21: 314-318
- Harris RP, Malej A (1986) Diel patterns of ammonium excretion and grazing rhythms in *Calanus helgolandicus* in surface stratified waters. *Mar Ecol Prog Ser* 31: 75-85
- Hassett RP, Cardinale B, Stabler LB, Elser JJ (1997) Ecological stoichiometry of N and P in pelagic ecosystems: comparison of lakes and oceans with emphasis on the zooplankton-phytoplankton interaction. *Limnol Oceanogr* 42(4): 648-662
- Hayward TL (1980) Spatial and temporal feeding patterns of copepods from the North Pacific central gyre. *Mar Biol* 58: 295-309
- Hecky RE, Kilham P (1988) Nutrient limitation of phytoplankton in freshwater and marine environments: A review of recent evidence on the effects of enrichment. *Limnol Oceanogr* 33(4): 796-822
- Herrera L, Escobedo R (2006) Factors structuring the phytoplankton community in the upwelling site off El Loa River in northern Chile. *J Mar Sys* 61: 13-38
- Hertzberg S, Jensen SL (1966) The carotenoids of blue-green algae II: The carotenoids of *Aphanizomenon flos-aquae*. *Phytochemistry* 5: 565-570
- Hessen DO (1992) Nutrient element limitation of zooplankton production. *Am Nat* 140(5): 799-814
- Hillebrand H, Dürselen CD, Kirschtel D, Pollinger U, Zohary T (1999) Biovolume calculation for pelagic and benthic microalgae. *J Phycol* 35: 403-424
- Hoepffner N, Sturm B, Finenko Z, Larkin D (1999) Depth-integrated primary production in the eastern tropical and subtropical North Atlantic basin from ocean colour imagery. *Int J Remote Sens* 20: 1435-1456
- Holl CM, Montoya JP (2005) Interactions between nitrate uptake and nitrogen fixation in continuous cultures of the marine diazotroph *Trichodesmium* (Cyanobacteria). *J Phycol* 41: 1178-1183
- Holmes RM, Aminot A, Kérouel R, Hooker BA, Peterson BJ (1999) A simple and precise method for measuring ammonium in marine and freshwater ecosystems. *Can J Fish Aquat Sci* 56: 1801-1808
- Hood RR, Coles VJ, Capone DG (2004) Modeling the distribution of *Trichodesmium* and nitrogen fixation in the Atlantic Ocean. *J Geophys Res* 109: C06006
- Howarth RW (1988) Nutrient limitation of net primary production in marine ecosystems. *Annu Rev Ecol Syst* 19: 89-110

References

- Hutchins DA, Hare CE, Weaver RS, Zhang Y, Firme GF, DiTullio GR, Alm MB, Riseman SF, Maucher JM, Geesey ME (2002) Phytoplankton iron limitation in the Humboldt Current and Peru Upwelling. *Limnol Oceanogr* 47: 997-1011
- Hutchins DA, Pustizzi F, Hare CE, DiTullio GR (2003) A shipboard natural community continuous culture system for ecologically relevant low-level nutrient enrichment experiments. *Limnol Oceanogr: Methods* 1: 82-91
- Ianora A, Miralto A, Poulet SA, Carotenuto Y, Buttino I, Romano G, Casotti R, Pohnert G, Wichard T, Colucci-D'Amato L (2004) Aldehyde suppression of copepod recruitment in blooms of a ubiquitous planktonic diatom. *Nature* 429: 403-407
- Ikeda T (1985) Metabolic rates of epipelagic marine zooplankton as a function of body mass and temperature. *Mar Biol* 85: 1-11
- Ikeda T, Kanno Y, Ozaki K, Shinada A (2001) Metabolic rates of epipelagic marine copepods as a function of body mass and temperature. *Mar Biol* 139: 587-596
- Ingall E, Jahnke R (1994) Evidence for enhanced phosphorus regeneration from marine sediments overlain by oxygen depleted waters. *Geochimica et Cosmochimica Acta* 58: 2571-2575
- Isla JA, Ceballos S, Anadón R (2004a) Mesozooplankton metabolism and feeding in the NW Iberian upwelling. *Estuarine, Coastal and Shelf Science* 61: 151-160
- Isla JA, Llope M, Anadon R (2004b) Size-fractionated mesozooplankton biomass, metabolism and grazing along a 50° N-30° S transect of the Atlantic Ocean. *J Plankton Res* 26: 1301-1313
- Jaeschke A, Abbas B, Zabel M, Hopmans EC, Schouten S, Damste JSS (2010) Molecular evidence for anaerobic ammonium-oxidizing (anammox) bacteria in continental shelf and slope sediments off northwest Africa. *Limnol Oceanogr* 55: 365-376
- Johns DG, Edwards M, Greve W, John AWG (2005) Increasing prevalence of the marine cladoceran *Penilia avirostris* (Dana, 1852) in the North Sea. *Helgol Mar Res* 59: 214-218
- Jónasdóttir SH, Fields D, Pantoja S (1995) Copepod egg production in Long Island Sound, USA, as a function of the chemical composition of seston. *Mar Ecol Prog Ser* 119: 87-98
- Judkins DC (1980) Vertical distribution of zooplankton in relation to the oxygen minimum off Peru. *Deep-Sea Res* 27: 475-487
- Kainz M, Arts MT, Mazumder A (2004) Essential fatty acids in the planktonic food web and their ecological role for higher trophic levels. *Limnol Oceanogr* 49: 1784-1793
- Karstensen J, Stramma L, Visbeck M (2008) Oxygen minimum zones in the eastern tropical Atlantic and Pacific oceans. *Prog Oceanogr* 77: 331-350
- Katechakis A, Stibor H, Sommer U, Hansen T (2004) Feeding selectivities and food niche separation of *Acartia clausi*, *Penilia avirostris* (Crustacea) and *Doliolum denticulatum* (Thaliacea) in Blanes Bay (Catalan Sea, NW Mediterranean). *J Plankton Res* 26: 589
- Keeling RF, Körtzinger A, Gruber N (2010) Ocean deoxygenation in a warming world. *Annual Review of Marine Science* 2: 199-229
- Kérouel R, Aminot A (1997) Fluorometric determination of ammonia in sea and estuarine waters by direct segmented flow analysis. *Mar Chem* 57: 265-275
- Kimor B, Reid FMH, Jordan JB (1978) An unusual occurrence of *Hemiaulus membranaceus* Cleve (Bacillariophyceae) with *Richelia intracellularis* Schmidt (Cyanophyceae) off the coast of Southern California in October 1976. *Phycologia* 17: 162-166

- Kjørboe T (1989) Phytoplankton growth rate and nitrogen content: implications for feeding and fecundity in a herbivorous copepod. *Mar Ecol Prog Ser* 55: 229-234
- Klausmeier CA, Litchman E, Daufresne T, Levin SA (2004) Optimal nitrogen-to-phosphorus stoichiometry of phytoplankton. *Nature* 429: 171-174
- Klein Breteler WCM, Schogt N, Baas M, Schouten S, Kraay GW (1999) Trophic upgrading of food quality by protozoans enhancing copepod growth: role of essential lipids. *Mar Biol* 135: 191-198
- Klein Breteler WCM, Schogt N, Rampen S (2005) Effect of diatom nutrient limitation on copepod development: role of essential lipids. *Mar Ecol Prog Ser* 291: 125-133
- Kleppel GS (1993) On the diets of calanoid copepods. *Marine Ecology-Progress Series* 99: 183-183
- Kleppel GS, Burkart CA, Carter K, Tomas C (1996) Diets of calanoid copepods on the West Florida continental shelf: relationships between food concentration, food composition and feeding activity. *Mar Biol* 127: 209-217
- Koslow JA, Goericke R, Lara-Lopez A, Watson W (2011) Impact of declining intermediate-water oxygen on deepwater fishes in the California Current. *Mar Ecol Prog Ser* 436: 207-218
- Kudela RM, Dugdale RC (2000) Nutrient regulation of phytoplankton productivity in Monterey Bay, California. *Deep-Sea Res II* 47: 1023-1053
- Kudela R, Cochlan W, Roberts A (2002) Spatial and temporal patterns of *Pseudo-nitzschia* species in central California related to regional oceanography. *Harmful Algae*: 347-349
- Kuypers MMM, Lavik G, Woebken D, Schmid M, Fuchs BM, Amann R, Jørgensen BB, Jetten MSM (2005) Massive nitrogen loss from the Benguela upwelling system through anaerobic ammonium oxidation. *Proceedings of the National Academy of Sciences* 102: 6478-6483
- Landrum JP, Altabet MA, Montoya JP (2011) Basin-scale distributions of stable nitrogen isotopes in the subtropical North Atlantic Ocean: Contribution of diazotroph nitrogen to particulate organic matter and mesozooplankton. *Deep-Sea Res I* 58: 615-625
- Langlois RJ, LaRoche J, Raab PA (2005) Diazotrophic diversity and distribution in the tropical and subtropical Atlantic Ocean. *Appl Environ Microbiol* 71: 7910
- Le Borgne R (1982a) Les facteurs de variation de la respiration et de l'excrétion d'azote et de phosphore du zooplancton de l'Atlantique intertropical oriental: II. Nature des populations zooplanctoniques et facteurs du milieu. *Océanographie Tropicale* 17: 187-201
- Le Borgne R (1982b) Zooplankton production in the eastern tropical Atlantic Ocean: Net growth efficiency and P:B in terms of carbon, nitrogen, and phosphorus. *Limnol Oceanogr* 27: 681-698
- Le Borgne R, Rodier M (1997) Net zooplankton and the biological pump: a comparison between the oligotrophic and mesotrophic equatorial Pacific. *Deep-Sea Res II* 44: 2003-2023
- Lenton TM, Watson AJ (2000) Redfield revisited 1. Regulation of nitrate, phosphate, and oxygen in the ocean. *Global Biogeochem Cy* 14: 225-248
- Lewis MR, Hebert D, Harrison W, Platt T, Oakey NS (1986) Vertical nitrate fluxes in the oligotrophic ocean. *Science* 234: 870
- Lincoln JA, Turner JT, Bates SS, Léger C, Gauthier DA (2001) Feeding, egg production, and egg hatching success of the copepods *Acartia tonsa* and *Temora longicornis* on diets of the toxic diatom *Pseudo-nitzschia multiseries* and the non-toxic diatom *Pseudo-nitzschia pungens*. *Hydrobiologia* 453: 107-120
- Liu S, Wang WX, Huang LM (2006) Phosphorus dietary assimilation and efflux in the marine copepod *Acartia erythraea*. *Mar Ecol Prog Ser* 321: 193-202

References

- Lochhead JH (1954) On the distribution of a marine cladoceran, *Penilia avirostris* Dana (Crustacea, Branchiopoda), with a note on its reported bioluminescence. *The Biological Bulletin* 107: 92-105
- Loladze I, Elser JJ (2011) The origins of the Redfield nitrogen to phosphorus ratio are in a homeostatic protein to rRNA ratio. *Ecol Lett* 14: 244-250
- Longhurst AR, Bedo A, Harrison WG, Head EJH, Horne EP, Irwin B, Morales C (1989) NFLUX: a test of vertical nitrogen flux by diel migrant biota. *Deep-Sea Res I* 36: 1705-1719
- Longhurst A, Sathyendranath S, Platt T, Caverhill C (1995) An estimate of global primary production in the ocean from satellite radiometer data. *J Plankton Res* 17: 1245-1271
- Mahaffey C, Williams RG, Wolff GA, Mahowald N, Anderson W, Woodward M (2003) Biogeochemical signatures of nitrogen fixation in the eastern North Atlantic. *Geophys Res Lett* 30: 1300
- Malzahn AM, Aberle N, Clemmesen C, Boersma M (2007) Nutrient limitation of primary producers affects planktivorous fish condition. *Limnol Oceanogr* 52: 2062-2071
- Malzahn AM, Hantzsche F, Schoo KL, Boersma M, Aberle N (2010) Differential effects of nutrient-limited primary production on primary, secondary or tertiary consumers. *Oecologia* 162: 35-48
- Marazzo A, Valentin JL (2003) *Penilia avirostris* (Crustacea, Ctenopoda) in a tropical bay: variations in density and aspects of reproduction. *Acta Oecol* 24: S251-S257
- Marchetti A, Parker MS, Moccia LP, Lin EO, Arrieta AL, Ribalet F, Murphy MEP, Maldonado MT, Armbrust EV (2008) Ferritin is used for iron storage in bloom-forming marine pennate diatoms. *Nature* 457: 467-470
- Marcus NH (2001) Zooplankton: responses to and consequences of hypoxia. In: Rabalais NN, Turner RE (eds) *The Effects of Hypoxia on Living Resources, with Emphasis on the Northern Gulf of Mexico*. American Geophysical Union, Coastal and Estuarine Series, pp 49-60
- Margalef R (1973) Fitoplancton marino del la region de afloramiento del NW de Africa: II. Composition y distribucion del fitoplancton. *Res. Exp. Cient. B/O Cornide* 2, 65-94
- Margalef R (1978) Life-forms of phytoplankton as survival alternatives in an unstable environment. *Oceanol acta* 1: 493-509
- Mayzaud P, Chanut JP, Ackman RG (1989) Seasonal changes of the biochemical composition of marine particulate matter with special reference to fatty acids and sterols. *Mar Ecol Prog Ser* 56: 189-204
- Menden-Deuer S, Lessard EJ (2000) Carbon to volume relationships for dinoflagellates, diatoms, and other protist plankton. *Limnol Oceanogr*: 569-579
- Michaels AF, Olson D, Sarmiento JL, Ammerman JW, Fanning K, Jahnke R, Knap AH, Lipschultz F, Prospero JM (1996) Inputs, losses and transformations of nitrogen and phosphorus in the pelagic North Atlantic Ocean. *Biogeochemistry* 35: 181-226
- Mills MM, Ridame C, Davey M, La Roche J, Geider RJ (2004) Iron and phosphorus co-limit nitrogen fixation in the eastern tropical North Atlantic. *Nature* 429: 292-294
- Mills MM, Arrigo KR (2010) Magnitude of oceanic nitrogen fixation influenced by the nutrient uptake ratio of phytoplankton. *Nature Geoscience* 3: 412-416
- Mitchell SF, Trainor FR, Rich PH, Goulden CE (1992) Growth of *Daphnia magna* in the laboratory in relation to the nutritional state of its food species, *Chlamydomonas reinhardtii*. *J Plankton Res* 14: 379
- Mohr W, Großkopf T, Wallace DWR, LaRoche J (2010) Methodological underestimation of oceanic nitrogen fixation rates. *PLoS one* 5: e12583

- Moisander PH, Beinart RA, Hewson I, White AE, Johnson KS, Carlson CA, Montoya JP, Zehr JP (2010) Unicellular cyanobacterial distributions broaden the oceanic N₂ fixation domain. *Science* 327: 1512-1514
- Montoya JP, Carpenter EJ, Capone DG (2002) Nitrogen fixation and nitrogen isotope abundances in zooplankton of the oligotrophic North Atlantic. *Limnol Oceanogr* 47: 1617-1628.
- Montoya JP, Holl CM, Zehr JP, Hansen A, Villareal TA, Capone DG (2004) High rates of N₂ fixation by unicellular diazotrophs in the oligotrophic Pacific Ocean. *Nature* 430: 1027-1032
- Montoya JP, Voss M, Capone DG (2007) Spatial variation in N₂-fixation rate and diazotroph activity in the Tropical Atlantic. *Biogeosciences* 4: 369-376
- Montoya JP (2008) Nitrogen stable isotopes in marine environments. In: Capone DG, Carpenter EJ, Mulholland MR, Bronk DA (eds) *Nitrogen in the Marine Environment*. Academic Press, pp 1277-1302
- Müller-Navarra DC (1995) Biochemical versus mineral limitation in *Daphnia*. *Limnol Oceanogr* 40(7): 1209-1214
- Müller-Navarra DC, Brett MT, Liston AM, Goldman CR (2000) A highly unsaturated fatty acid predicts carbon transfer between primary producers and consumers. *Nature* 403: 74-77
- Müller-Navarra DC, Brett MT, Park S, Chandra S, Ballantyne AP, Zorita E, Goldman CR (2004) Unsaturated fatty acid content in seston and tropho-dynamic coupling in lakes. *Nature* 427: 69-72
- Niemi A (1979) Blue-green algal blooms and N: P ratio in the Baltic Sea. *Acta Bot Fenn* 110: 57-61
- Ohtsuka S, Kubo N, Okada M, Gushima K (1993) Attachment and feeding of pelagic copepods on larvacean houses. *Journal of Oceanography* 49: 115-120
- O'Neil JM, Roman MR (1994) Ingestion of the cyanobacterium *Trichodesmium* spp. by pelagic harpacticoid copepods *Macrosetella*, *Miracia* and *Oculosetella*. *Hydrobiologia* 292: 235-240
- Oschlies A, Schulz KG, Riebesell U, Schmittner A (2008) Simulated 21st century's increase in oceanic suboxia by CO₂-enhanced biotic carbon export. *Global Biogeochem Cy* 22 doi:10.1029/2007GB003147
- Parrish CC, Wangersky PJ (1990) Growth and lipid class composition of the marine diatom, *Chaetoceros gracilis*, in laboratory and mass culture turbidostats. *J Plankton Res* 12: 1011
- Patoine A, Graham MD, Leavitt PR (2006) Spatial variation of nitrogen fixation in lakes of the northern Great Plains. *Limnol Oceanogr* 51(4): 1665-1677
- Paulsen M, Clemmesen C, Malzahn AM (submitted) Essential fatty acid (docosahexaenoic acid, DHA) affects RNA:DNA ratio of larval herring in the field
- Pennington JT, Mahoney KL, Kuwahara VS, Kolber DD, Calienes R, Chavez FP (2006) Primary production in the eastern tropical Pacific: A review. *Progress in Oceanography* 69: 285-317
- Peyridieu S, Chédin A, Tanré D, Capelle V, Pierangelo C, Lamquin N, Armante R (2010) Saharan dust infrared optical depth and altitude retrieved from AIRS: a focus over North Atlantic - comparison to MODIS and CALIPSO. *Atmos Chem Phys* 10: 1953-1967
- Pitcher GC, Bolton JJ, Brown PC, Hutchings L (1993) The development of phytoplankton blooms in upwelled waters of the southern Benguela upwelling system as determined by microcosm experiments. *J Exp Mar Biol Ecol* 165: 171-189
- Plath K, Boersma M (2001) Mineral limitation of zooplankton: stoichiometric constraints and optimal foraging. *Ecology* 82(5): 1260-1269
- Pommier J, Frenette J-J, Massicotte P, Lapierre J-F, Glémet H (2012) Seston fatty acid composition and copepod RNA:DNA ratio with respect to the underwater light climate in fluvial Lac Saint-Pierre. *Aquat Sci*, doi 10.1007/s00027-011-0246-z

References

- Post DM (2002) Using stable isotopes to estimate trophic position: models, methods, and assumptions. *Ecology* 83: 703-718
- Poulton AJ, Stinchcombe MC, Quartly GD (2009) High numbers of *Trichodesmium* and diazotrophic diatoms in the southwest Indian Ocean. *Geophys Res Lett* 36: L15610
- Prince ED, Goodyear CP (2006) Hypoxia based habitat compression of tropical pelagic fishes. *Fish Oceanogr* 15: 451-464
- Prince ED, Luo JC, Goodyear P, Hoolihan JP, Snodgrass D, Orbesen ES, Serafy JE, Ortiz M, Schirripa MJ (2010) Ocean scale hypoxia based habitat compression of Atlantic istiophorid billfishes. *Fish Oceanogr* 19: 448-462
- Probyn TA (1985) Nitrogen uptake by size-fractionated phytoplankton populations in the southern Benguela upwelling system. *Mar Ecol Prog Ser* 22: 249-258
- Prospero JM, Barrett K, Church T, Dentener F, Duce RA, Galloway JN, Levy H, Moody J, Quinn P (1996) Atmospheric deposition of nutrients to the North Atlantic Basin. *Biogeochemistry* 35: 27-73
- Redfield AC (1934) On the proportions of organic derivatives in sea water and their relation to the composition of plankton. *James Johnstone Memorial Volume (Liverpool)*: pp. 176-192
- Redfield AC (1958) The biological control of chemical factors in the environment. *Am Sci* 46(3): 205-221
- Řezanka T, Dembitsky VM (2006) Metabolites produced by cyanobacteria belonging to several species of the family Nostocaceae. *Folia Microbiol* 51: 159-182
- Riegman R, Noordeloos AAM, Cadée GC (1992) *Phaeocystis* blooms and eutrophication of the continental coastal zones of the North Sea. *Mar Biol* 112: 479-484
- Rosa R, Seibel BA (2010) Metabolic physiology of the Humboldt squid, *Dosidicus gigas*: Implications for vertical migration in a pronounced oxygen minimum zone. *Progress in Oceanography* 86: 72-80
- Rossoll D, Bermúdez R, Hauss H, Schulz KG, Riebesell U, Sommer U, Winder M (submitted) Ocean acidification-induced food quality deterioration constrains trophic transfer. *PloS one*
- Ryabenko E, Kock A, Bange HW, Altabet MA, Wallace DWR (2011) Contrasting biogeochemistry of nitrogen in the Atlantic and Pacific oxygen minimum zones. *Biogeosciences Discussions* 8: 8001-8039
- Ryther JH, Dunstan WM (1971) Nitrogen, phosphorus, and eutrophication in the coastal marine environment. *Science* 171: 1008
- Saba GK, Steinberg DK, Bronk DA (2009) Effects of diet on release of dissolved organic and inorganic nutrients by the copepod *Acartia tonsa*. *Mar Ecol Prog Ser* 386: 147-161
- Saba GK, Steinberg DK, Bronk DA (2011) The relative importance of sloppy feeding, excretion, and fecal pellet leaching in the release of dissolved carbon and nitrogen by *Acartia tonsa* copepods. *J Exp Mar Biol Ecol* 404: 47-56
- Sargent JR, McEvoy LA, Bell JG (1997) Requirements, presentation and sources of polyunsaturated fatty acids in marine fish larval feeds. *Aquaculture* 155: 117-127
- Sartoris FJ, Thomas DN, Cornils A, Schnack-Schiel SB (2010) Buoyancy and diapause in Antarctic copepods: the role of ammonium accumulation. *Limnol Oceanogr* 55(5): 1860-1864
- Schafstall J, Dengler M, Brandt P, Bange H (2010) Tidal-induced mixing and diapycnal nutrient fluxes in the Mauritanian upwelling region. *J Geophys Res* 115: C10014
- Schlitzer R (2009) OceanDataView. <http://odv.awi.de>.
- Schoemann V, Becquevort S, Stefels J, Rousseau V, Lancelot C (2005) *Phaeocystis* blooms in the global ocean and their controlling mechanisms: a review. *J Sea Res* 53: 43-66

-
- Seeyave S, Probyn TA, Pitcher GC, Lucas MI, Purdie DA (2009) Nitrogen nutrition in assemblages dominated by *Pseudo-nitzschia* spp., *Alexandrium catenella* and *Dinophysis acuminata* off the west coast of South Africa. *Mar Ecol Prog Ser* 379: 91-107
- Séguin F (2010) Zooplankton community near the island of Sao Vicente in the Cape Verde archipelago: insight on pelagic copepod respiration. Diplomarbeit, Universität Bremen, 77pp
- Seibel BA (2011) Critical oxygen levels and metabolic suppression in oceanic oxygen minimum zones. *J Exp Biol* 214: 326-336
- Semenova TN, Timonin AG, Flint MV (1982) Characteristic features of the lateral and vertical distributions of abundant zooplankton species near the Peruvian coast. *Oceanology* 22: 216-220
- Sereda JM, Hudson JJ (2011) Empirical models for predicting the excretion of nutrients (N and P) by aquatic metazoans: taxonomic differences in rates and element ratios. *Freshw Biol* 56: 250-263
- Sharp JH (1974) Improved analysis for "particulate" organic carbon and nitrogen from seawater. *Limnol Oceanogr* 19(6): 984-989
- Sheridan CC, Steinberg DK, Kling GW (2002) The microbial and metazoan community associated with colonies of *Trichodesmium* spp.: a quantitative survey. *J Plankton Res* 24: 913-922
- Sherr E, Sherr B (1988) Role of microbes in pelagic food webs: a revised concept. *Limnol Oceanogr* 33(5): 1225-1227
- Smith SL, Whitledge TE (1977) The role of zooplankton in the regeneration of nitrogen in a coastal upwelling system off northwest Africa. *Deep Sea Research* 24: 49-56
- Smith VH (1983) Low nitrogen to phosphorus ratios favor dominance by blue-green algae in lake phytoplankton. *Science* 221: 669-671
- Soma Y, Imaizumi T, Yagi K, Kasuga S (1993) Estimation of algal succession in lake water using HPLC analysis of pigments. *Can J Fish Aquat Sci* 50: 1142-1146
- Sommer F (2003) A comparison of the impact of major mesozooplankton taxa on marine, brackish and freshwater phytoplankton during summer. Dissertation, CAU Kiel, 91pp
- Sommer U, Hansen T, Stibor H, Vadstein O (2004) Persistence of phytoplankton responses to different Si:N ratios under mesozooplankton grazing pressure: a mesocosm study with NE Atlantic plankton. *Mar Ecol Prog Ser* 278: 67-75
- Sommer U, Sommer F, Feuchtmayr H, Hansen T (2004) The influence of mesozooplankton on phytoplankton nutrient limitation: A mesocosm study with northeast Atlantic phytoplankton. *Protist* 155: 295-304
- Sommer U, Sommer F (2006) Cladocerans versus copepods: the cause of contrasting top-down controls on freshwater and marine phytoplankton. *Oecologia* 147: 183-194
- Sommer F, Hansen T, Sommer U (2006) Transfer of diazotrophic nitrogen to mesozooplankton in Kiel Fjord, Western Baltic Sea: a mesocosm study. *Mar Ecol Prog Ser* 324: 105
- Staal M, te Lintel Hekkert S, Brummer GJ, Veldhuis M, Sikkens C, Persijn S, Stal LJ (2007) Nitrogen fixation along a north-south transect in the eastern Atlantic Ocean. *Limnol Oceanogr* 52(4): 1305-1316
- Steinberg DK, Goldthwait SA, Hansell DA (2002) Zooplankton vertical migration and the active transport of dissolved organic and inorganic nitrogen in the Sargasso Sea. *Deep Sea Res I* 49: 1445-1461
- Sternner RW (1990) The ratio of nitrogen to phosphorus resupplied by herbivores: zooplankton and the algal competitive arena. *Am Nat* 136(2): 209-229

References

- Sterner RW (1993) *Daphnia* growth on varying quality of *Scenedesmus*: mineral limitation of zooplankton. *Ecology* 74(8): 2351-2360
- Sterner RW, Schulz KL (1998) Zooplankton nutrition: recent progress and a reality check. *Aquat Ecol* 32: 261-279
- Sterner RW, Elser JJ (2002) *Ecological stoichiometry: the biology of elements from molecules to the biosphere*. Princeton University Press
- Stoecker DK, Capuzzo JMD (1990) Predation on protozoa: its importance to zooplankton. *J Plankton Res* 12: 891
- Stramma L, Johnson GC, Sprintall J, Mohrholz V (2008) Expanding Oxygen-Minimum Zones in the Tropical Oceans. *Science* 320: 655-658
- Stramma L, Schmidtko S, Levin LA, Johnson GC (2010) Ocean oxygen minima expansions and their biological impacts. *Deep Sea Res I* 57: 587-595
- Sunda WG, Huntsman SA (1995) Iron uptake and growth limitation in oceanic and coastal phytoplankton. *Mar Chem* 50: 189-206
- Tang KW, Jakobsen HH, Visser AW (2001) *Phaeocystis globosa* (Prymnesiophyceae) and the planktonic food web: feeding, growth, and trophic interactions among grazers. *Limnol Oceanogr* 46(8): 1860-1870
- Thomas WH, Seibert DLR, Dodson AN (1974) Phytoplankton enrichment experiments and bioassays in natural coastal sea water and in sewage outfall receiving waters off southern California. *Estuarine and Coastal Marine Science* 2: 191-206
- Turner JT, Ianora A, Esposito F, Carotenuto Y, Miralto A (2002) Zooplankton feeding ecology: does a diet of *Phaeocystis* support good copepod grazing, survival, egg production and egg hatching success? *J Plankton Res* 24: 1185-1195
- Thamdrup B, Dalsgaard T, Jensen MM, Ulloa O, Fariás L, Escribano R (2006) Anaerobic ammonium oxidation in the oxygen-deficient waters off northern Chile. *Limnol Oceanogr* 51(5): 2145-2156
- Thompson PA, Harrison PJ, Whyte JNC (1990) Influence of irradiance on the fatty acid composition of phytoplankton. *J Phycol* 26: 278-288
- Turner JT (2004) The importance of small planktonic copepods and their roles in pelagic marine food webs. *Zool Stud* 43: 255-266
- Tyrrell T (1999) The relative influences of nitrogen and phosphorus on oceanic primary production. *Nature* 400: 525-531
- Tyrrell T, Maranon E, Poulton AJ, Bowie AR, Harbour DS, Woodward EMS (2003) Large-scale latitudinal distribution of *Trichodesmium* spp. in the Atlantic Ocean. *J Plankton Res* 25: 405-416
- Uitz J, Claustre H, Gentili B, Stramski D (2010) Phytoplankton class-specific primary production in the world's oceans: Seasonal and interannual variability from satellite observations. *Global Biogeochem Cy* 24: GB3016
- Urabe J, Watanabe Y (1993) Implications of sestonic elemental ratio in zooplankton ecology: reply to the comment by Brett. *Limnol Oceanogr* 38(6): 1337-1340
- Utermöhl H (1958) Zur Vervollkommnung der quantitativen Phytoplankton Methodik. *Mitteilungen der Internationalen Vereinigung für Theoretische und Angewandte Limnologie* 9: 263-272
- Vallespinós F (1985) Nitrogen fixation by *Trichodesmium thiebautii* in the upwelling region off Northwest Africa. *Int Symp Upw W Afr. Instituto de Investigaciones Pesqueras, Barcelona*, pp 254-251
- Van Cappellen P, Ingall ED (1994) Benthic phosphorus regeneration, net primary production, and ocean anoxia: A model of the coupled marine biogeochemical cycles of carbon and phosphorus. *Paleoceanography* 9: 677-692

-
- Vanderklift MA, Ponsard S (2003) Sources of variation in consumer-diet $\delta^{15}\text{N}$ enrichment: a meta-analysis. *Oecologia* 136: 169-182
- Vaquer-Sunyer R, Duarte CM (2008) Thresholds of hypoxia for marine biodiversity. *Proceedings of the National Academy of Sciences* 105: 15452-15457
- Vargas CA, Escribano R, Poulet S (2006) Phytoplankton food quality determines time windows for successful zooplankton reproductive pulses. *Ecology* 87: 2992-2999
- Vidal J, Whitley TE (1982) Rates of metabolism of planktonic crustaceans as related to body weight and temperature of habitat. *J Plankton Res* 4: 77
- Villareal TA (1992) Marine nitrogen-fixing diatom-cyanobacteria symbioses. In: Carpenter EJ, Capone DG, Rueter JG (eds) *Marine pelagic cyanobacteria: Trichodesmium and other diazotrophs* Kluwer, pp 163-175
- Vrede T, Ballantyne A, Mille Lindblom C, Algesten G, Gudasz C, Lindahl S, Brunberg AK (2009) Effects of N:P loading ratios on phytoplankton community composition, primary production and N fixation in a eutrophic lake. *Freshw Biol* 54: 331-344
- Voss M, Croot P, Lochte K, Mills M, Peeken I (2004) Patterns of nitrogen fixation along 10°N in the tropical Atlantic. *Geophysical Res Lett* 31: L23S09
- Wainman BC, Smith REH, Rai H, Furgal JA (1999) Irradiance and lipid production in natural algal populations. In: Arts MT, Wainman BC (eds) *Lipids in Freshwater Ecosystems*. Springer, Berlin
- Walve J, Larsson U (1999) Carbon, nitrogen and phosphorus stoichiometry of crustacean zooplankton in the Baltic Sea: implications for nutrient recycling. *J Plankton Res* 21: 2309
- Wannicke N, Liskow I, Voss M (2010) Impact of diazotrophy on N stable isotope signatures of nitrate and particulate organic nitrogen: case studies in the north-eastern tropical Atlantic Ocean. *Isotopes in Environmental and Health Studies* 46: 337-354
- Wen YH, Peters RH (1994) Empirical models of phosphorus and nitrogen excretion rates by zooplankton. *Limnol Oceanogr* 39(7): 1669-1679
- Westberry TK, Siegel DA (2006) Spatial and temporal distribution of *Trichodesmium* blooms in the world's oceans. *Global Biogeochem Cy* 20: GB4016
- Wetz MS, Wheeler PA (2003) Production and partitioning of organic matter during simulated phytoplankton blooms. *Limnol Oceanogr* 48(5): 1808-1817
- Whitley TE (1981) Nitrogen recycling and biological populations in upwelling ecosystems. In: Richards FA (ed) *Coastal Upwelling Coastal and Estuarine Sciences* 1. AGU, pp 257-273
- Whitney FA, Freeland HJ, Robert M (2007) Persistently declining oxygen levels in the interior waters of the eastern subarctic Pacific. *Progress in Oceanography* 75: 179-199
- Wyrтки K (1962) The oxygen minima in relation to ocean circulation. *Deep Sea Research* 9: 11-23
- Yebra L, Hernández-León S, Almeida C, Bécognée P, Rodríguez JM (2004) The effect of upwelling filaments and island-induced eddies on indices of feeding, respiration and growth in copepods. *Progress in Oceanography* 62: 151-169
- Zehr JP, Waterbury JB, Turner PJ, Montoya JP, Omoregie E, Steward GF, Hansen A, Karl DM (2001) Unicellular cyanobacteria fix N_2 in the subtropical North Pacific Ocean. *Nature* 412: 635-637
- Zehr JP, Bench SR, Carter BJ, Hewson I, Niazi F, Shi T, Tripp HJ, Affourtit JP (2008) Globally distributed uncultivated oceanic N_2 -fixing cyanobacteria lack oxygenic photosystem II. *Science* 322: 1110

Contributions of authors

The work presented in this thesis was conducted within the SFB 754 subproject B2 entitled “Pelagic community responses to changes in nutrient stoichiometry” coordinated by the principal investigators Prof. Dr. Ulf Riebesell and Prof. Dr. Ulrich Sommer. I worked in close cooperation with Dipl.-Biol. Jasmin Franz, who was supervised by Prof. Ulf Riebesell (UR).

Chapter I: Changes in N:P stoichiometry influence taxonomic composition and nutritional quality of phytoplankton in the Peruvian upwelling

Helena Hauss (HH), Jasmin Franz (JF) and Ulrich Sommer (US)

accepted in Journal of Sea Research

Planning of experiments: HH, JF, UR and US. Conduction of mesocosm experiments: HH, JF and US. Microplankton counts: US. Flow cytometry and fatty acid analysis: HH. Pigment and particulate matter analysis: JF. Nutrient measurements: Peter Fritsche. Data analysis and figures: HH. Writing: HH, with assistance of JF and US.

Chapter II: Impact of changes in dissolved N:P on the functional composition of phytoplankton and its effect on zooplankton in the Eastern Tropical North Atlantic

Helena Hauss (HH), Jasmin Franz (JF) and Ulrich Sommer (US)

Planning of experiments: HH, JF, UR and US. Conduction of mesocosm experiments: HH and JF. Conduction of zooplankton experiments, flow cytometry, zooplankton counts, fatty acid analysis, RNA/DNA analysis: HH. Microplankton counts: HH, Luke Phelps and Philipp Wilfert. Nutrient measurements: Kerstin Nachtigall and Martina Lohmann. Pigment and particulate matter analysis: JF. Data analysis: HH and JF. Writing and figures: HH.

Chapter III: Can tropical marine zooplankton excretion exacerbate dissolved nutrient imbalances?

Planning and conduction of experiments, sampling, data analysis, figures and text: HH. Nutrient measurements: Kerstin Nachtigall and Martina Lohmann. POC/PON measurements: Cordula Meyer. POP measurements: JF

Chapter IV: Relative contribution of upwelled and atmospheric nitrogen to zooplankton production in the eastern tropical North Atlantic: Spatial distribution and relation to dissolved nutrient dynamics

Helena Hauss (HH), Jasmin Franz (JF), Thomas Hansen (TH), Ulrich Struck (USt) and Ulrich Sommer (US)

Re-submitted to Deep Sea Research I: Oceanographic Research Papers

Planning and conduction of field sampling of copepods: HH, on-board sorting: HH (M83-1 and M80-2) and TH (M80-2), chl-*a* sampling/measurements: HH and JF, nutrient sampling/measurements: JF, Kerstin Nachtigall and Martina Lohmann. RNA/DNA analysis: HH. Stable isotope measurements: TH (M80-2) and USt (M83-1). Data analysis: HH. Figures and text: HH, with helpful comments of JF, TH, USt, and US.

Acknowledgements

I am grateful to Uli Sommer for the supervision of this thesis, and for the trust he put into its completion.

Monika Winder kindly stepped into the breach to act as a second reviewer, thank you!

Jasmin Franz is acknowledged as key collaborator here: thank you for all the good and bad times shared, and especially those weeks and months as room- and labmate on the boat: you're the best!

I am also particularly indebted to Thomas Hansen, who supported me with his profound professional knowledge, however never lacking creativity and a healthy dose of humour (including a memorable christmas party in the tropics).

Now the array is getting a little jumbled, and I apologize to those not mentioned in detail:

For great support as well as pleasant company at sea, I would like to thank the *Meteor*-Crew, the various chief scientists (Martin Frank, Doug Wallace and Martin Visbeck), the CTD-Teams (led by Gerd Krahnemann, Lothar Stramma and Rudi Link) and the nutrient people (Peter Fritsche, Kerstin Nachtigall and Martina Lohmann) on the three cruises, as well as the SFB scientists and PhD-students on board, in particular Caro Löscher, Tobi Großkopf, Harald Schunck, Patricia Grasse, Tim Kalvelage and Anna Dammshäuser.

At the institute in Kiel, thanks are due for admin/technical/motivational support to many of those in the EÖ-N department, especially Cordula Meyer, Carmen Arndt, Gaby Barth, Maike Blankartz, Marko Dittmann, Nicole Sollfrank, Ola Lewandowska, Philipp Wilfert, Saskia Audritz and Luke Phelps. Rainer Kiko provided very helpful comments on earlier versions of chapter I and IV. I thank the Danish crowd at DTU Aqua (Thomas Kiørboe, Torkel Nielsen, Marja Koski, Conny Jaspers and others) for always having me over for fun and inspiring seminars and courses. The rest of the IfM gang, i.e. Enno Prigge, Kerstin Maczassek, Livia Roth, Lasse Marohn, Christoph Petereit, Jan Czerny, and others: Thanks for everything else, including all off-topic activities.

My family, for their unconditional love and support.

Holger, not only for taking care of old Dottir when I was gone, for proof-reading and enduring my moods and confusion, but above all because without you this wouldn't have made any sense at all.

Curriculum Vitae

Helena Margareta Hauss

Geburtstag: 02.05.1983 in Münster

Nationalität: deutsch

Bildungsweg

2002 Abitur, Schillergymnasium Münster

2002-2004: Grundstudium Biologie, Christian Albrechts Universität Kiel

2004-2005: Hauptstudium in Biologie, Christian Albrechts Universität Kiel

Hauptfach: Biological Oceanography (BIOCEAN Programm)

Nebenfach (biologisch): Zoologie

Nebenfach (nichtbiologisch): Toxikologie

2006: Hauptstudium in Biologie, (BIOCEAN Programm) Syddansk Universitet, Odense, Dänemark

2008 Diplomarbeit: “Impacts of prey field characteristics on foraging and condition of larval herring (*Clupea harengus*)”

Betreuer: Prof. Dr. Dietrich Schnack (IFM-GEOMAR, Kiel) und

Prof. Dr. Myron A. Peck (IHF, Hamburg, Germany)

seit 2008 Doktorandin in der Abteilung Experimentelle Ökologie am IFM-GEOMAR, Kiel

Publikationen

Hauss HM, Peck MA (2009) Comparing observed and modelled growth of larval herring (*Clupea harengus*): Testing individual-based model parameterisations. *Scientia Marina* 73S1: 37-45.

Rossoll D, Bermúdez R, Hauss HM, Schulz KG, Riebesell U, Sommer U, Winder M (2012) Ocean acidification constrains trophic transfer efficiency. *PloS One* 7(4): e34737

Haslob H, Hauss HM, Hinrichsen HH, Voss R, Böttcher U, Kraus G (2012) Application of the Daily Egg Production Method to Baltic sprat. *Fisheries Research*

Haslob H, Hauss HM, Petereit C, Kraus G, Clemmesen C, Peck MA (2012) Temperature effects on vital rates of different life stages and implications for population growth of Baltic sprat. *Marine Biology*

Franz JMS, Hauss H, Sommer U, Dittmar T and Riebesell U (2012) Production, partitioning and stoichiometry of organic matter under variable nutrient supply during mesocosm experiments in the tropical Pacific and Atlantic Ocean. *Biogeosciences Discussions*

Hauss HM, Franz JMS, Sommer U (accepted) Changes in N:P stoichiometry influence taxonomic composition and nutritional quality of phytoplankton in the Peruvian upwelling. *Journal of Sea Research*

Hauss HM, Franz JMS, Hansen T, Struck U, Sommer U (subm.) Relative contribution of upwelled and atmospheric nitrogen to zooplankton production in the eastern tropical North Atlantic: Spatial distribution and relation to dissolved nutrient dynamics. Re-submitted to *Deep Sea Research I: Oceanographic Research Papers*

Eidesstattliche Erklärung

Hiermit erkläre ich, daß die vorliegende Promotionsarbeit selbständig von mir angefertigt wurde. Die Dissertation ist in Form und Inhalt meine eigene Arbeit, und es wurden keine anderen als die angegebenen Hilfsmittel verwendet. Diese Arbeit wurde weder ganz noch zum Teil einer anderen Stelle im Rahmen eines Prüfungsverfahrens vorgelegt. Teile dieser Arbeit wurden zur Begutachtung in Fachzeitschriften eingereicht. Dies ist mein erstes Promotionsverfahren. Die Promotion soll im Fach Biologische Meereskunde erfolgen. Des weiteren erkläre ich, daß ich Zuhörer bei der Disputation zulasse.

Kiel, den

Helena Hauss